AEDC-TR-13-T-19

Development and Assessment of a Computer-Based Equation of State for Equilibrium Air

E. Stan Powell
Aerospace Testing Alliance

September 2013

Final Report for Period October 2004 – September 2013

ARNOLD ENGINEERING DEVELOPMENT COMPLEX
ARNOLD AIR FORCE BASE, TENNESSEE
AIR FORCE TEST CENTER
UNITED STATES AIR FORCE

NOTICES
When US Government drawings, specifications, or other data are used for any purpose other than a definitely related Government procurement operation, the Government thereby incurs no responsibility nor any obligation whatsoever, and the fact that the Government may have formulated, furnished, or in any way supplied the said drawings, specifications, or other data, is not to be regarded by implication or otherwise, as in any manner licensing the holder or any other person or corporation, or conveying any rights or permission to manufacture, use, or sell any patented invention that may in any way be related thereto.
Qualified users may obtain copies of this report from the Defense Technical Information Center.
References to named commercial products in this report are not to be considered in any sense as an endorsement of the product by the United States Air Force or the Government.

DESTRUCTION NOTICE

For unclassified, limited documents, destroy by any method that will prevent disclosure of contents or reconstruction of the document.

APPROVAL STATEMENT

Prepared by:

E. STAN POWELL
Aerospace Testing Alliance

Reviewed by:

HARRY CLARK
Air Force Project Manager
Capability Integration Branch
Plans and Programs Division

Approved by:

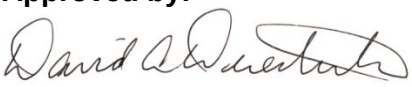

DAVE A. DUESTERHAUS
Technical Director
Test Technology Branch
Test Division

REPORT DOCUMENTATION PAGE

Form Approved
OMB No. 0704-0188

PLEASE DO NOT RETURN YOUR FORM TO THE ABOVE ADDRESS

1. REPORT DATE (DD-MM-YYYY)	**2. REPORT TYPE**	**3. DATES COVERED** *(From – To)*
xx-09-2013	Final Report	October 2004 – September 2013

4. TITLE AND SUBTITLE
Development and Assessment of a Computer-Based Equation of State for Equilibrium Air

5a. CONTRACT NUMBER

5b. GRANT NUMBER

5c. PROGRAM ELEMENT NUMBER

6. AUTHOR(S)
Powell, E. Stan
Aerospace Testing Alliance

5d. PROJECT NUMBER
13373

5e. TASK NUMBER

5f. WORK UNIT NUMBER

7. PERFORMING ORGANIZATION NAME(S) AND ADDRESS(ES)

E. Stan Powell
Facilities and Testing Technology
Aerospace Testing Alliance
MS 4001
676 Second Street
Arnold AFB, TN 37389-4001

8. PERFORMING ORGANIZATION REPORT NO.

AEDC-TR-13-T-19

9. SPONSORING/MONITORING AGENCY NAME(S) AND ADDRESS(ES)
AEDC/XPR
100 Kindle Drive, Suite A-214
Arnold AFB, TN 37389-1214

10. SPONSOR/MONITOR'S ACRONYM(S)

11. SPONSOR/MONITOR'S REPORT NUMBER(S)

12. DISTRIBUTION/AVAILABILITY STATEMENT
Statement A: Approved for public release; distribution is unlimited.

13. SUPPLEMENTARY NOTES
Available in the Defense Technical Information Center (DTIC).

14. ABSTRACT

This report documents development of a computer-based equation of state (EOS) that covers the range of conditions from the air saturation line to beyond lunar reentry conditions. Efforts to ascertain the limits of accuracy of the EOS are also documented. The EOS is largely a computer-based version of the venerable "AEDC Mollier Diagram for equilibrium air," c. 1967. The basis of this EOS is different from its predecessor, but the range of applicability is comparable and the purpose is the same. Efforts have been made to determine the accuracy of the EOS. Transport properties as well as thermodynamic properties are calculated.

The envelope of the EOS will be described in detail in the report, but in general terms it is as follows. The minimum temperature is 27 K or the saturation temperature, whichever is greater for densities less than the critical density. The minimum temperature is 100 K for densities greater than the critical density. The maximum temperature is 5,000 K for densities greater than 100 kg/m^3 and 20,000 K for densities less than 100 kg/m^3. The maximum density is 1,220 kg/m^3 for temperatures less than 5000 K and 100 kg/m^3 for temperatures greater than 100 kg/m^3. The minimum density is 10^{-12} kg/m^3 for temperatures less than 350 K and 10^{-8} kg/m^3 for temperatures greater than 350 K. Some parts of the envelope are of little practical use for the current purposes as will be discussed in the report.

The reference temperature for energy is 0 K, and the reference pressure for entropy is 101,325 Pa.

The AEDC Mollier 2008 EOS has reached a state of development such that it should be used for calculations and predictions. There are no functionally important restrictions for its use at AEDC.

The EOS is a work in progress. This report is an interim report and is expected to be superseded by another report when significant changes are made.

15. Subject Terms
Air, thermodynamic properties, equation of state, chemical equilibrium, real-gas

16. SECURITY CLASSIFICATION OF:			**17. LIMITATION OF ABSTRACT**	**18. NUMBER OF PAGES**	**19A. NAME OF RESPONSIBLE PERSON**
A. REPORT	**B. ABSTRACT**	**C. THIS PAGE**			E. Stan Powell
Unclassified	Unclassified	Unclassified	Same as Report	79	**19B. TELEPHONE NUMBER** *(Include area code)* 931-454-4198

This page is intentionally left blank.

PREFACE

This documentation was prepared by Aerospace Testing Alliance on Project Number 13373. Mr. Harry Clark was the Air Force Project Manager.

The work reported herein is the product of the author's efforts. The work has been accomplished in small increments over a period of about seven years, funded by a series of projects. Discussions with several people were helpful, most notably the continuous dialog with Mr. Fred Shope, recently retired from ATA.

This page is intentionally left blank.

CONTENTS

FIGURES

Figure

EXECUTIVE SUMMARY

The subject of this report is the basic thermodynamics of air at what are normally considered extreme conditions of either density or energy. The subject is a computer-based equation of state (EOS) that covers the range of conditions from the air saturation line to beyond lunar reentry conditions. Air at densities greater than the density of water are included in the EOS. The EOS is largely a computer-based version of the venerable “AEDC Mollier Diagram for equilibrium air,” c. 1967. The basis of this EOS is different from its predecessor, but the range of applicability is comparable. Efforts have been made to determine the accuracy of the EOS. Transport properties as well as thermodynamic properties are calculated.

The AEDC Mollier 2008 EOS has reached a state of development such that it should be used for calculations and predictions. There are no functionally important restrictions for its use at AEDC.

The EOS is a work in progress. This report is an interim report and is expected to be superseded by another report when significant changes are made.

This page is intentionally left blank.

1.0 INTRODUCTION

This report documents two aspects of the development of a new, computer-based, equation of state (EOS), for equilibrium air. The EOS is similar in purpose to what once existed to produce the AEDC Mollier Diagram for equilibrium air.[1] The first aspect is the development of the approach and programming of the EOS. That part is straightforward and does not require a great deal of discussion.

The second part is the evaluation of the accuracy of the developed EOS. There is no single source of data to serve as a standard with which to compare the new EOS. For lack of a standard, the second part is not as straightforward as the first part and as a consequence will receive more attention.

1.1 DEFINITIONS AND TERMINOLOGY

An EOS is a defined relationship among thermodynamic properties. It can take the form of simple algebraic equations, e.g. $P = \rho RT$, $e = constant \times T$, tabulated values (Ref. 1) [largely based on the work of Hilsenrath and Klein] (Ref. 2), graphs, e.g., the classic "AEDC Mollier Diagram for equilibrium air," c. 1967, or computer codes. The simpler formulations are generally more restricted in their range of applicability but easier to use and easier to understand. Accurate thermodynamic properties are essential for accurate calculation of flow phenomena.

Each form has its own advantages and its own limitations. For instance, the simple algebraic equations can lead to simple, closed-form analytic equations to describe many flow scenarios, but the range of applicability of the solutions is limited by the limitations of the underlying EOS. Graphical presentations are superior for visualizing processes and developing understanding but are difficult to use in calculations. Computer codes are excellent for calculations but are more complex in use than simple, closed-form analytic equations, and they obscure the processes, thus hindering the development of understanding.

Finally, some comments about nomenclature are in order. Standard SI units will be used throughout, i.e., kg, m, sec, K, Pa, J, etc. In general, the most common symbols will be used for the thermodynamic properties, i.e., P for pressure, h for enthalpy, etc. Nonstandard usages will be noted.

A related topic is the definition of terms for thermodynamic models, notably "real gas." JANNAF (Joint Army Navy NASA Air Force Interagency Propulsion Committee) has adopted a nomenclature and what is used herein is consistent with that nomenclature. "Thermally perfect" means that the gas is accurately represented by the equation $P = \rho RT$ where P is absolute pressure, ρ is the density, R is the gas constant of the specific gas (or mixture), and T is the absolute temperature. "Calorically perfect" means the internal energy, e, is proportional to the temperature. A gas that is both thermally perfect and calorically perfect is an ideal gas.

[1] The code used to produce the properties depicted in the 1967 Mollier chart existed at the National Bureau of Standards. Computer tapes of the property values were transferred to AEDC. Whether the code which produced the property values was ever transferred to AEDC is unclear at this point. Recollections vary. All personnel directly involved in the original work were gone before this author began work on the subject.

A thermally perfect, calorically imperfect gas is a gas in which the internal energy is a nonlinear function of temperature, i.e., $e = e(T)$, not $e = constant \times T$. Air at moderately elevated temperatures and low densities is an example of a thermally perfect, calorically imperfect gas.

As the temperature is increased further at low or moderate densities, dissociation and ionization will begin to occur. In this case, air is a thermally perfect mixture of thermally perfect species. The effects, varying specific heats, dissociation, and ionization, are properly called high-energy or high-temperature effects.

A real gas is a gas in which the internal energy of the constituent molecules is a function of density as well as temperature, i.e., $e = e(T,\rho)$. The relationship among pressure, temperature, and density is more complicated than the thermally perfect equation for a real gas.

Many people call what are correctly high-temperature effects real-gas effects. For that reason, effects caused by elevated density will be called high-density effects, and effects caused by elevated energy (or elevated temperature) will be called high-energy (high-temperature) effects.

1.2 THERMODYNAMIC BASIS FOR PARAMETERS

If one assumes a simple compressible substance, that is, a substance where the only reversible work mode is pressure-volume work, then given two independent thermodynamic properties, all other thermodynamic properties can be calculated for a simple compressible substance.

All that really exists at the molecular level is the distribution of molecular energies, both kinetic and internal, the number density of molecules (number of molecules per unit volume), and the physical characteristics of the individual molecules (distribution of mass, number of electrons, etc.). Everything else is derived from those three properties or in some cases, e.g. pressure, conjured for our convenience. One can consult any introductory text on statistical thermodynamics for a complete discussion.

From the total energy of a system of molecules and the assumption of equilibrium comes the distribution of energies among and within the molecules. The absolute temperature arises as a parameter in the equilibrium energy distribution. Note that the scale of temperature is an arbitrary choice; the concept and role of temperature is dictated by nature. Strictly speaking, temperature can only be defined for an equilibrium distribution of energy. Any deviation from the equilibrium distribution requires additional constraints to be included in the definition of temperature, cf. the development of the concept of a vibrational temperature.

The concept of entropy as a property definable in terms of other properties arises from the equilibrium distribution. The assumption of the conservation of energy is closely related to the above concept. In the limited case of thermally perfect, calorically perfect behavior, temperature is an acceptable surrogate for energy.

From the concept of the number density of molecules and the physical characteristics of the individual molecules arises the concept of density, either mass density or molar density. The molar density and the mass density are equivalent in the case of fixed composition. The density represents the amount of “stuff” in a unit volume in either case. The reciprocal of the density, the specific volume, is more convenient in some calculations. The assumption of the conservation of mass is closely related to the above concept.

Thus, the nature of the fluid at the molecular level suggests two parameters to characterize the thermodynamic state, to wit, temperature and density. Mass density, rather than molar density, is chosen for reasons that will become obvious later. All other thermodynamic properties can be calculated from those two.

The properties calculated are pressure, enthalpy, and entropy. In addition, certain useful derivatives of those properties and combinations of derivatives of those properties are calculated.

1.3 FORM OF PRESENTATION

The primary form of presentation of the new EOS will be as a Mollier chart. A Mollier chart is a graph showing enthalpy as a function of a second thermodynamic property with lines indicating constant values of other thermodynamic properties. Most conveniently in the case of air, a Mollier diagram is a graph showing enthalpy as a function of entropy with lines of constant temperature, constant density, and constant pressure included. For convenience, the entropy and enthalpy are normally divided by the gas constant for air at a convenient reference condition. Thus, the abscissa, entropy (s), divided by R0 is dimensionless, and the ordinate, enthalpy (h), divided by R0 has dimensions of temperature. A logarithmic scale is used for the ordinate due to the large range of values of enthalpy. A notional Mollier diagram for equilibrium air is shown in Fig. 1 below. The ranges of the parameters and the ranges of the coordinates will be given later.

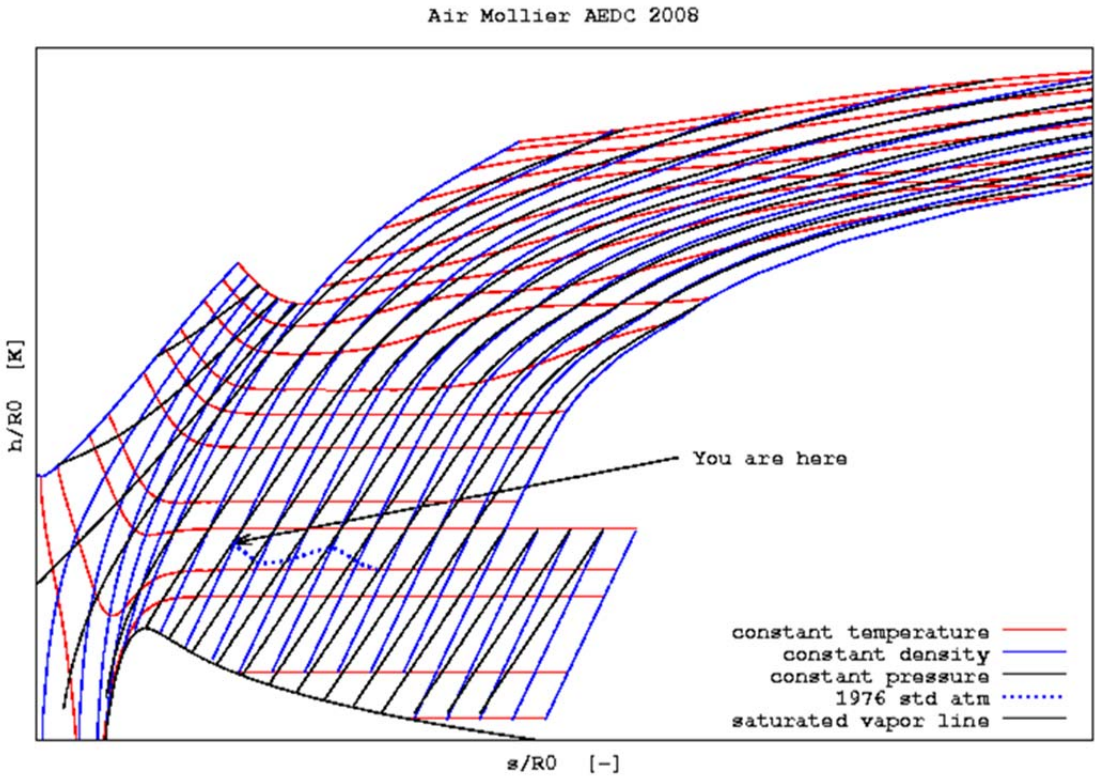

Figure 1. Notional Mollier Diagram for Equilibrium Air, Linear Abscissa, Log Ordinate

The above figure represents the final Mollier diagram produced in this effort. The similarity of Fig. 1 to the ubiquitous "AEDC Mollier Diagram for equilibrium air" is obvious. The "You are here" point represents standard sea-level conditions, based on the 1976 US Standard

Atmosphere, in Mollier coordinates. It is included in most of the figures to serve as a point of reference.

2.0 DEVELOPMENT OF EOS

The process of the development of the EOS, locally known as AEDC Mollier 2008, will now be described.

2.1 IDEAL GAS

The best way to explain the development of the above chart is to begin with the simplest case, e.g., $P = \rho RT$ and $e = constant \times T$. These equations are based on the model of air molecules as point-masses with rotational moments of inertia. The interactions of the molecules are assumed sufficient to maintain equilibrium. The "air" molecules occupy less than 0.1% of the volume and spend less than 1% of their time in the vicinity of another molecule at normal ambient conditions. This means that the assumptions of a dilute, weakly interacting gas on which the ideal-gas model is based are valid.

The lines of constant temperature, constant density, and constant pressure are all straight lines in the chosen format. The Mollier diagram based on the above equations is shown in Fig. 2.

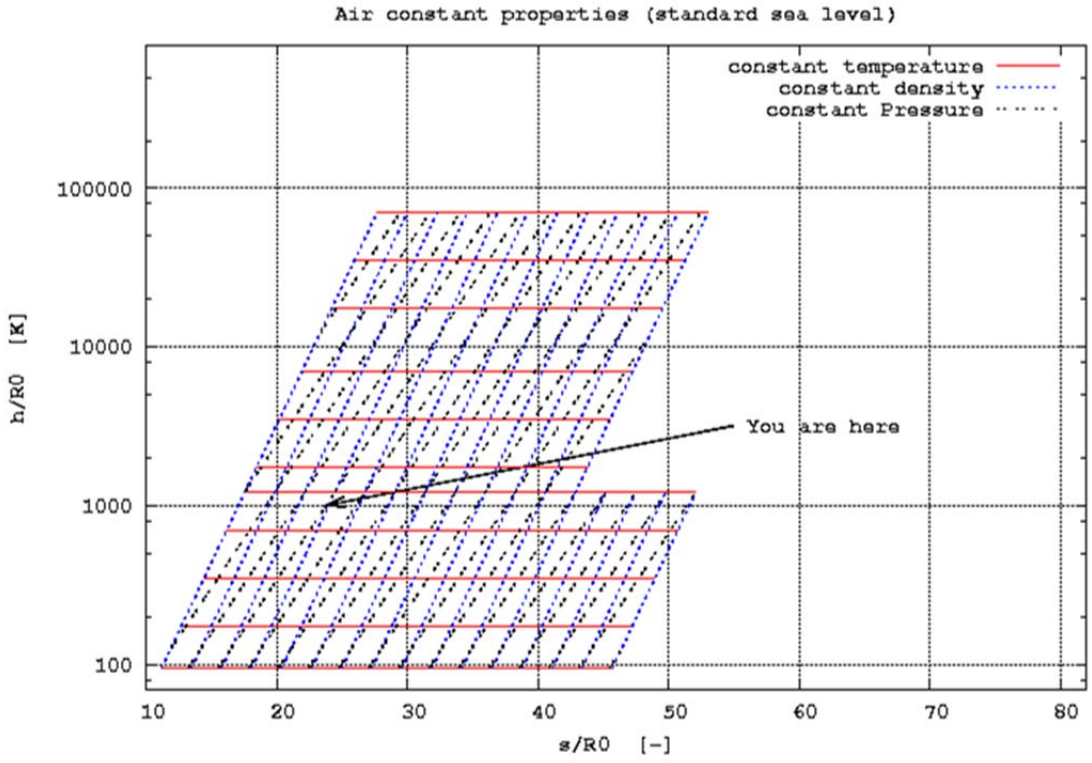

Figure 2. Mollier Diagram Based on Thermally and Calorically Perfect (Ideal) Gas Model

The ideal gas model is appropriate in the vicinity of normal ambient conditions, at lower than ambient densities, (to the right of the indicated point), and at energies somewhat lower and slightly higher (slightly below and slightly above the indicated point).

The thermal imperfections of air become important to the left of the indicated point and are shown by curvature of the constant temperature lines in Fig. 1. The caloric imperfections become important at energies above the ambient and first appear as decreases in the spacing of the constant temperature lines. At still higher energies, dissociation and ionization become important. Those effects are shown by the curvature of the constant temperature lines. Lower densities (higher entropies) exacerbate the high-energy deviations.

The final area of concern is the low-energy, low-entropy region where the constituents of air begin to condense. The ideal gas EOS does not address condensation.

The ideal gas EOS is inappropriate for high densities, for high energies, and for very low energies. However, the ideal gas EOS is appropriate for atmospheric flight at subsonic, transonic, and low supersonic flight speeds. Locally, it is appropriate for the transonic wind tunnels and for vKF Tunnel A. Thus, while limited, the ideal gas EOS is appropriate for a large number of interesting problems. The ideal gas EOS is the basis of the ubiquitous Mach number-γ equations that relate ratios of properties in compressible flows.

The various deviations from ideal gas behavior will be discussed in turn, beginning with high-density effects.

2.2 HIGH-DENSITY EFFECTS

The thermodynamic effects of elevated density will be discussed first.

2.2.1 Introduction

Molecules in a thermally perfect gas interact infrequently, i.e., an individual molecule behaves as if there are no other molecules present most of the time. The volume occupied by the molecules is insignificant in comparison to the total volume, less than 0.1% at sea-level conditions. Such gases are called “dilute” or “weakly interacting.” The molecules in a weakly interacting gas do interact enough to maintain equilibrium and to behave as a continuum, but they do not interact enough to violate the basic assumption. Stated another way, they interact, but they do not interfere.

The portion of the time that any given molecule is being influenced by the presence of nearby molecules increases as the density increases because the distance between neighboring molecules decreases. The volume occupied by the molecules becomes a non-negligible portion of the total volume at some point as density increases. The energy of the gas and the density of the gas determine the nature of the interactions. At low energies and high densities, the force between the molecules is attractive. This is shown in Fig. 1 by the dip in the constant temperature lines at low entropy and low enthalpy. At higher energies or at high enough densities at any energy, the force between molecules becomes repulsive. This is shown by the upturn of the constant temperature lines in the left portion of Fig. 1.

2.2.2 Approaches to High-Density Effects

The theory of dilute gases is well developed (Ref. 3), and the predictions of the theory have been verified. The comparable theory for elevated densities is less well developed. As a consequence, most of the approaches for predicting high-density effects are empirical, with varying degrees of theoretical guidance.

2.2.2.1 Pressure Explicit Equations

There are two general approaches to addressing high-density effects. (See Ref. 4 for an introduction to high-density EOS). The first approach begins with an equation of the form $P = P(T,\rho)$. For convenience, these equations are usually written $P = \rho R_0 T + P_{hd}(T,\rho)$ where the term $P_{\text{hd}}(T,\rho)$ represents the deviation from thermally perfect behavior. Accuracy over large ranges requires complex forms of the term. The term, $P_{\text{hd}}(T,\rho)$ is most often in the form of a power series in densities where the coefficients of the density terms are functions of temperature. The term, $P_{\text{hd}}(T,\rho)$ must approach zero as density approaches zero for all temperatures so that the thermally perfect behavior is recovered.

The effects of high density on all other thermodynamic properties can be calculated from the EOS and appropriate integrals of various partial derivatives of the thermal EOS, for instance

$$e - e_0 = \int_{T_0}^{T} c_{\text{v}}^0 dT + \int_0^{\rho} \frac{1}{\rho^2}\left[P - T\frac{\partial P}{\partial T}_{\rho}\right] d\rho.$$

The primary advantage of the pressure-explicit EOS is its simplicity. The primary disadvantage is that the need to analytically integrate the various partial derivatives limits the analytic forms that can be included in the term $P_{\text{hd}}(T,\rho)$. Note also that for all except the most trivial forms of $P_{\text{hd}}(T,\rho)$, the equation cannot be directly inverted, i.e., given pressure and temperature, finding density requires an iterative approach.

The parameters (constants) in the term $P_{\text{hd}}(T,\rho)$ must be evaluated based on experimental data. This process is complicated because different experimenters use different compositions for "air." For instance, some experiments are done with air in the laboratory, whereas some use a mixture of pure nitrogen and pure oxygen. Others add argon, and still others add argon and carbon dioxide. A few add additional trace species like neon. Evaluation of the experimental data is a critical step in any high-density EOS development.

2.2.2.2 Free Energy Approach

The second approach to calculation of the high-density effects begins with an equation for the Gibbs free-energy or Helmholtz free-energy. The thermodynamic properties of the fluid are calculated from derivatives of the free-energy. Since everything of interest is calculated from derivatives, there are no integrals involved, which eliminates most of the concern of the analytic forms that can be used in the thermally imperfect part of the equation.

This freedom is especially useful in adding terms to improve the accuracy in the vicinity of the critical point,[2] which is very difficult to model. Those terms must only contribute in the immediate vicinity of the critical point, and the mathematical forms typically lead to partial derivatives that cannot be analytically integrated.

[2] The critical point of a pure fluid is the point in thermodynamic space where the distinction between the vapor-phase and the condensed-phase disappears. The location is less straight-forward in the case of a mixture of fluids like air. Most commonly, an "effective" critical point is defined to enhance the overall accuracy of the EOS. Different forms of the EOS will produce different effective critical points although they will produce sensibly identical results away from the critical point.

The primary disadvantages of the free-energy approach are that the function being fitted is not directly measured (it is calculated from measurements) and that the properties are evaluated by derivatives of curve fits, which can amplify uncertainties.

Most recent developments in high-density EOS have used the free-energy approach because the advantages outweigh the disadvantages. Regardless of form, the properties are normally calculated as the sum of a thermally perfect term and a thermally imperfect term. This philosophy will be used again and extended later.

Regardless of the approach, pressure explicit or free-energy, the forms chosen are almost always well behaved on extrapolation to higher temperatures.

2.2.3 Specific Case of AEDC Mollier 2008

The specific high-density EOS used in this effort is an equation of the form $P = \rho R_0 T$ + $P_{\text{hd}}\,(T, \rho)$ where the second term is of the form suggested in Ref. 5. The particular form and the parameters in the equation are taken from Ref. 6. The equation uses a total of 34 parameters, includes a power series through the 6th power of density, and a power series containing odd powers of density, 3rd through the 13th power, in the exponential term. The coefficients of the powers of density are functions of temperature, and none of the coefficients in the density power series contain temperature to a power greater than one. Most include terms in the reciprocal of temperature suggesting that the divergence, if it exists, will be at low temperatures. The low temperature divergence is observed in practice, but at temperatures below those of interest here. The analytic form is well behaved at elevated temperatures.

The form of the Reynolds implementation of the Benedict-Webb-Rubin (BWR) equation (Ref. 5) is

$$\mathrm{P} = \rho \mathrm{R}_0 T \; + \rho^2 \left[A_1 T + A_2 T^{1/2} + \sum_{i=3}^{i=5} A_{\mathrm{i}} T^{3\text{-i}} \right] \; + \; \rho^3 \sum_{i=6}^{i=9} A_{\mathrm{i}} T^{7\text{-i}} \; + \; \rho^4 \sum_{i=10}^{i=12} A_{\mathrm{i}} T^{11\text{-i}}$$

$$+ \; \rho^5 A_{13} \; + \; \rho^6 (A_{14}/T + A_{15}/T^2) \; + \; \rho^7 A_{16}/T \; + \; \rho^8 \left(A_{17}/T + A_{18}/T^2\right) + \; \rho^9 A_{19}/T^2 \; +$$

$$\{\rho^3 \left(A_{20}/T^2 + A_{21}/T^3\right) \; + \; \rho^5 \left(A_{22}/T^2 + A_{23}/T^4\right) \; + \; \rho^7 \left(A_{24}/T^2 + A_{25}/T^3\right) \; +$$
$$\rho^9 \left(A_{26}/T^2 + A_{27}/T^4\right) \; + \; \rho^{11} \left(A_{28}/T^2 + A_{29}/T^3\right) \; + \; \rho^{13} \left(A_{30}/T^2 + A_{31}/T^3 + A_{32}/T^4\right)\} e^{-\beta \rho^2}$$

Note that the density power series which is multiplied by the exponential term contains only odd powers of density. Even powers of density in that power series would create partial derivatives with respect to temperature which cannot be analytically integrated with respect to density. This is an example of the limitations placed on the form of the high-density portion of the pressure equation.

Span suggests that most high-density EOS extrapolate well to higher temperatures (Ref. 4). That means that the contribution of the high-density EOS becomes negligible at high temperatures. That, in fact, is the case with the Ref. 7 high-density EOS. Plots demonstrating this will be given later.

The results from the above equation were compared with the NIST REFPROP 7 (Ref. 7) and the agreement is satisfactory. REFPROP 7 does not treat air as a single species, so the

calculations were made using the mixture rules and the extended principle of corresponding states with an appropriate combination of species. Those approximations increase the inherent uncertainty in the property predictions.

The equation presumes that the air is a fixed composition; it does not account for any changes in chemical composition. Thus, the predictions of the equation are undoubtedly inaccurate at high temperatures where the molecular composition differs from the standard-state composition of air. However, the equation probably would represent the properties of the air at elevated temperatures if the composition were the same as at ambient temperatures. This characteristic will be used later.

2.2.3.1 Thermally Perfect Thermodynamics

The initial implementation of the high-density EOS used the thermally perfect thermodynamic properties based on Ref. 8 as modified locally to represent air as a single species (Ref. 9). This approach was taken because of its simplicity, its range of the representation, and its well-behaved nature under extrapolation to both higher temperatures and lower temperatures. However, this initial approach was abandoned because it cannot be applied to the high-energy portion of the EOS. Consistency of the thermally perfect thermodynamic model was required. Small discrepancies in the overlap region would have been both unavoidable and unacceptable.

The thermally perfect thermodynamic properties are based on the curve fits of Refs. 10 and 11. The Ref. 10 curve fits use a reference temperature of 298.15 K and have a lower limit of 200 K. The reference temperature was shifted to 0 K, and rational extrapolations were made from 200 K to about 10 K for use here. 10 K is well below the minimum temperature needed.

2.2.3.2 Condensation of Air

A separate equation is used to define the saturation curve. The equation used is also taken from Ref. 12. Calculation of properties in the two-phase region would require input beyond temperature and density. Since atmospheric flight does not include this region and since ground-test facilities are designed to avoid this region, two-phase calculations were not included in the EOS.

The equation for the saturation line for air, taken from Ref. 12, is

$log_e(P/P_c) = F_1X + F_2X^2 + F_3\ log_e(T/T_c)$ where $X = \frac{1}{T_c} - \frac{1}{T}$. The parameters $F_1, F_2, \& F_3$ have different values for the dew line and the bubble line.[3]

The Mollier diagram of air according to the Reynolds EOS is shown in Fig. 3.

[3] The dew line (saturated vapor line) is the locus of temperatures and pressures along which the first drop of condensate forms in the vapor phase. Similarly, the bubble line (saturated liquid line) is the locus along which the first bubble of vapor forms in the condensed phase. The pressures at any given temperature would be the same for a pure substance but the pressures are not the same, except the critical temperature, for air because air is a mixture. The dew line and the bubble line are sometimes collectively called the coexistence line since two phases exist at points along the line.

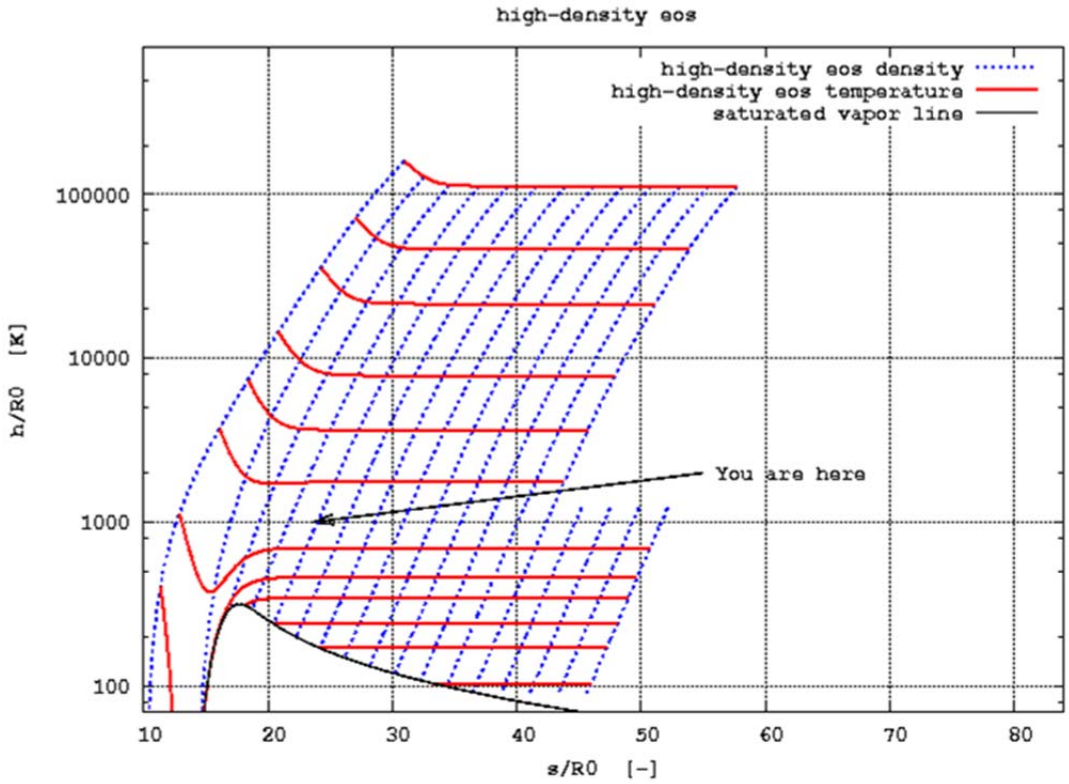

Figure 3. Mollier Diagram of High-Density EOS with Constant Pressure Lines Omitted

The lower limit of density in the "AEDC Mollier Diagram for Equilibrium Air" at temperature below ambient was about $1.29*10^{-10}$ kg/m^3. The limit for current EOS is 10^{-12} kg/m^3. The reduced minimum is more for aesthetic reasons than for practical application. The decrease does not add any useful capability. It preserves the appearance of the final plot and is consistent with the extension in the high-energy portion discussed below.

2.3 HIGH-ENERGY EFFECT

The approach to the effects of elevated energy will be described next.

2.3.1 Phenomenological Description of High-Energy Effects

The high-energy effects are the changes in behavior of air as a result of increases in energy emperature). The first effect observed is the deviation from calorically perfect behavior, i.e., $e = e(T)$, rather than $e = constant \times T$. This occurs when the vibrational degrees of freedom of the polyatomic molecules begin to become excited.[4] Simple well-verified, closed-form equations re available from statistical mechanics for the effects of the vibrational degrees of freedom for low vibrational energies (Ref. 3). As the energy increases, interaction of the vibrational mode and the rotational mode becomes significant. Furthermore, the finite number of vibrational levels and the reduced energy spacing of the levels becomes significant. The simple closed-form equations must be replaced by more general, but more complicated, summations.

[4] For the purposes of this report, it is assumed that the translational and rotational degrees of freedom are fully excited at all times. If lower temperatures cf. 4 K, were considered, then the excitement of the rotational degrees of freedom of air constituents would need to be considered.

This effect on vibrational excitation is easily calculable by a variety of methods. The simplest and fastest approach is through the use of curve fits for the thermodynamic properties with temperature as the independent variable. The advantage of curve fits is that they can quickly produce accurate numbers. The primary disadvantage is that they obscure the physical processes which give rise to the property variations.

The second effect is the change in composition, dissociation, and formation of nonair species. These occur as the energy is increased further. The molecular weight of the mixture decreases, and the specific heats are dominated by the energy required for dissociation (the reaction specific-heat), c_{pe}. The temperature ranges where the major species of air, N_2 and O_2, dissociate are well (but incompletely) separated at low densities. The temperature at which the highest rate of dissociation occurs increases with increasing density. The temperature range over which dissociation occurs also broadens with increased density.

The final effect to be considered is ionization. At still higher energies, the components of the mixture begin to ionize. The composition of the mixture no longer resembles ambient air. Any meaningful calculations must begin with conservation of mass, conservation of energy, conservation of charge, and mechanical and thermodynamic equilibrium. The ionization of an individual molecule is a discrete event, but the ionization of a large collection of molecules is a statistical phenomenon with an ill-defined beginning and an ill-defined end. Furthermore, the ranges of conditions where different molecular species ionize overlap. Higher levels of ionization occur at higher temperatures and increase the complexity of the process.

2.3.2 Equilibrium Calculation

Analysis of the second and third high-energy effects begins with the calculation of the equilibrium composition. The two most common approaches to the calculation of equilibrium composition are the minimization of free energy[6] and the equilibrium constant approach. The two can be shown to be equivalent.

Virtually all codes that are written to calculate chemical equilibrium assume a thermally perfect mixture of thermally perfect gases. This assumption simplifies the calculation because the properties of any individual species are a function of temperature only.

2.3.2.1 Free-Energy Minimization

The industry standard code for chemical equilibrium calculations is the NASA-LeRC (now NASA-GRC) code cea2 (Refs. 11-12). The cea2 code uses the thermodynamic property curve fits from Ref. 10. The code uses the free-energy minimization approach and is very general. The lower limit of its thermodynamic database is 200 K, and the upper limit depends on the specific species, 20,000 K for the air species of interest here. One of the costs of the generality of cea2 is that it is comparatively slow in execution.

The thermodynamic database in Ref. 10 is limited to single ionization for air species. The consequences of this will be discussed later.

[6] The minimization of free energy is easier to understand if it is viewed as the maximization of entropy subject to the other thermodynamic constraints.

2.3.2.2 Equilibrium Constant Approach

An alternative approach was taken to produce the code in Ref. 13. The code presumes that air is always composed of 11 species which can be formed from nitrogen, oxygen, and argon, (including ions and electrons). The code calculated the density-based equilibrium constants based on the thermally perfect thermodynamic properties of the 11 species. The equilibrium constants are then used with the atomic element ratios to combine the equilibrium equations into polynomial equations of a single variable. The order of the equation and the species used to formulate the equation depend on the temperature and density of interest. The specific polynomial is then iteratively solved, and the individual species concentrations are calculated from the constituent equations.

The resultant code is very fast and accurate, but it is not general. The approach itself is general, but the polynomials which are ultimately solved must be rederived each time a new species is considered. The code was written in Fortran-77, and the limit of the thermodynamic properties was 200 to 15,000 K. Several subranges were used to achieve the desired accuracy. The density range was was not explicitly stated in the reference. Figure 1 of the reference suggests a range of 10^{-6} kg/m^3 to 100 kg/m^3. Figure 1 also suggests that the code would converge for extrapolation to lower density and extrapolation to higher temperature. Accuracy under extrapolation cannot be inferred. (See the original reference for more detail and for a code listing.)

2.3.2.3 Implementation of Equilibrium Constant Approach

The code was converted to Fortran-90 and was modified to take advantage of the broader range of thermodynamic properties available from Ref. 10 for use here. The authors of the code presume that air is “air” for temperatures below 350 K for all densities. No extrapolation of the range of the curve fits was required. The reference temperature was shifted to 0 K to be consistent with the high-density EOS.

The range of density used in the composite EOS was

$$10^{-8}\,kg/m^3 \;\leq\; density \;\leq\; 100\,kg/m^3.$$

The lower density limit in the original AEDC Mollier chart was $1.29*10^{-6}$ kg/m^3. Extension of the range to lower densities is of little practical value in terms of test or flight conditions, but it does provide better assurance of convergence in iterative solutions. The final temperature range used in the composite EOS was

$$200K \;\leq\; temperature \;\leq\; 20{,}000K.$$

No convergence problems were ever detected in the equilibrium calculation portion of the final composite EOS.

Increasing the maximum density would have required major reprogramming and would have violated the thermally perfect assumption at low temperatures. The enhancement to the capabilities might have been significant. Increasing the maximum density capability of the code should be considered.

Comparisons were made between the modified special-purpose code and cea2 during the development of the EOS. The differences observed were all within acceptable limits in the range where high-density effects are negligible.

Both cea2 and the equilibrium code used herein are limited to single ionization for air species. Work by Gupta et al. (Ref. 14) indicates that multiple ionization may be important at higher temperatures and the lowest densities. The combination of higher temperatures and low densities corresponds to the upper right portion of the Mollier diagram, the truncated portion of the diagram in Fig. 1.

The single ionization assumption is not a significant limitation for the present purposes, but it might become a limitation if the range of energies were increased. Addition of the multiple ionized species would require major code modifications.

Just as the high-density effects go to zero as density decreases, the high-energy effects go to zero as the temperature approaches ambient temperature. This property facilitates the final calculations as discussed in a subsequent section.

2.3.3 High-Energy Mollier Diagram

The Mollier Diagram of the high-energy EOS is shown in Fig. 4.

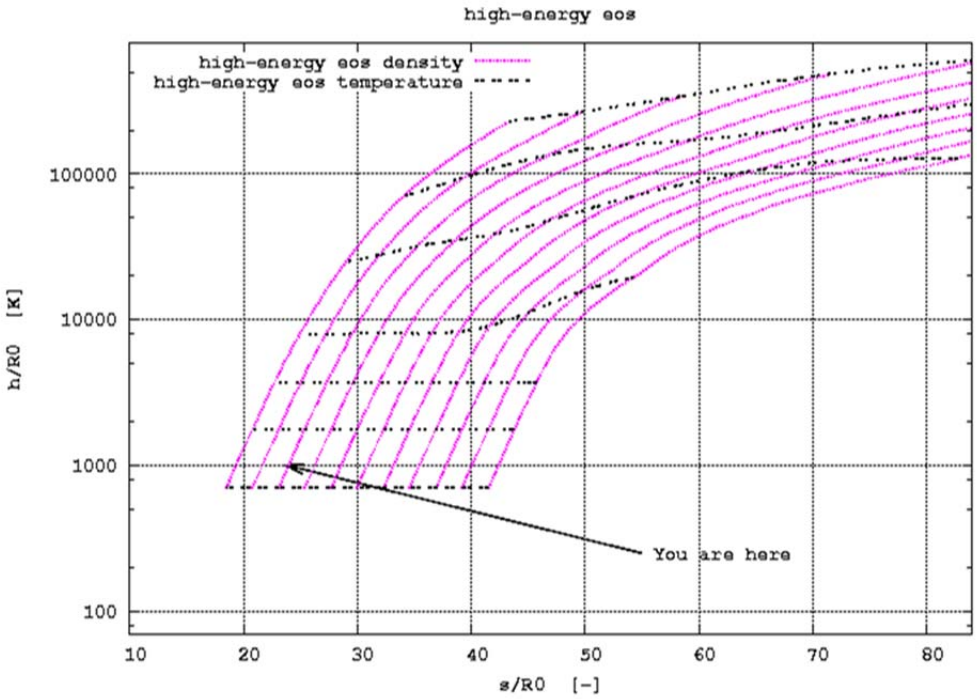

Figure 4. High-Energy EOS in Mollier Coordinates with Constant Pressure Lines Omitted

2.4 COMBINED HIGH-DENSITY AND HIGH-ENERGY EFFECTS

The approach taken to the combination of the high-density EOS and the high-energy EOS will now be discussed.

2.4.1 Combined Effects for Property Calculation

The normal approach in high-density EOS is to calculate the contribution to properties from the thermally perfect EOS and add the contribution to that property due to high-density effects, for instance, $P = \rho R_0 T + P_{hd}(T, \rho)$ where the second term represents the high-density contribution. The same approach is used for other basic properties, energy, entropy, etc. This approach was extended to the high-energy effects, e.g., $P = \rho R_0 T + P_{hd}(T, \rho) + P_{he}(T, \rho)$ where the third term is the contribution to the pressure due to the high-energy effects. The properties that will be calculated are pressure, energy (internal energy and enthalpy), and entropy. The above procedure is consistent with the definitions of those properties. Other properties (involving derivatives) will be discussed later.

Consider an analog of a 2-D Taylor series where the initial point is the thermally perfect, fixed-composition air case, and the two independent variables are the high-density effects and the high-energy effects. The current procedure is similar to retaining only the linear terms in the series expansion. The mixed bi-linear (2nd order) term, the high-density effect on the high-energy contribution, is neglected. This misstates the case slightly, but it is sufficient to illustrate the process.

The data from Figs. 3 and 4 are plotted together in Fig. 5.

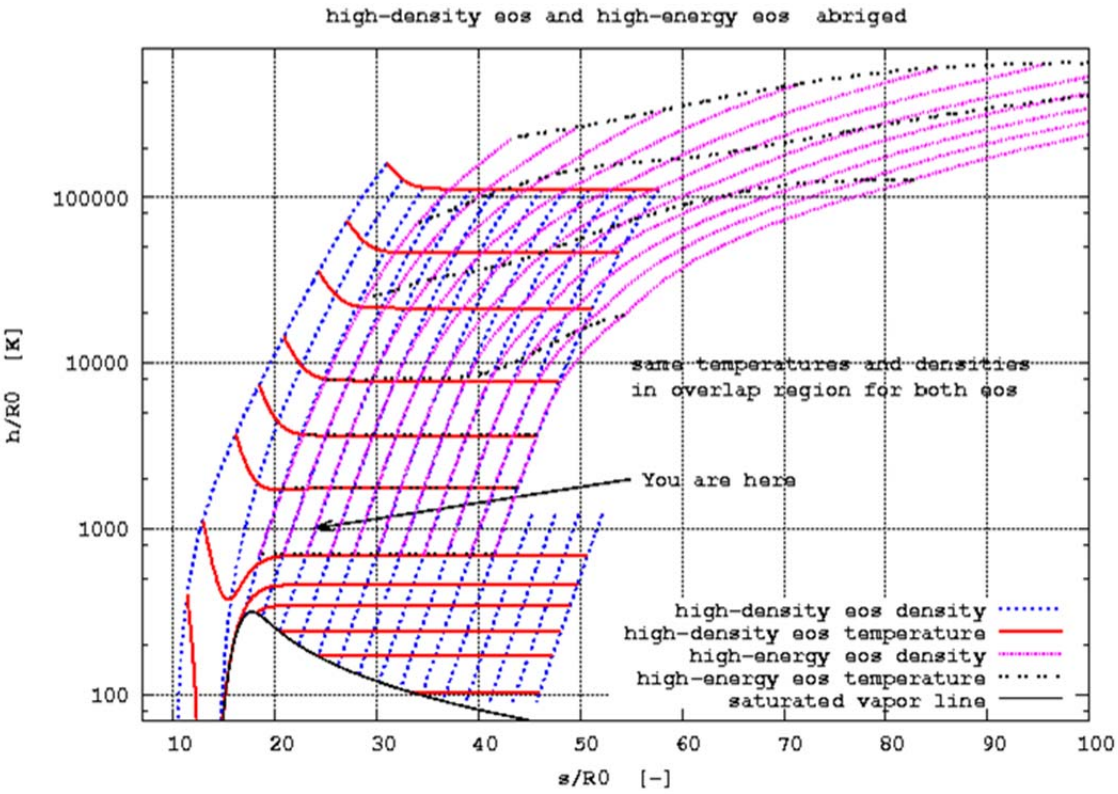

Figure 5. High-Density EOS and High-Energy EOS

The same temperatures and same densities are used in both EOS in the region of overlap. Thus there is a one-to-one correspondence of points in the overlap region. The two separate EOS show good agreement around ambient conditions. This confirms the applicability of the ideal-gas EOS for near-ambient conditions. The discrepancies at high densities and high energies suggests that the effective range of the final EOS should be terminated at about 5,000 K in the high-density portion. The terms neglected in the expansion might become significant above that temperature. The maximum density for the high-density portion of the EOS was 1,220 kg/m^3. The maximum temperature was 5,000 K for densities greater than 100 kg/m^3.

The envelope of the final EOS is shown in Fig. 6 below.

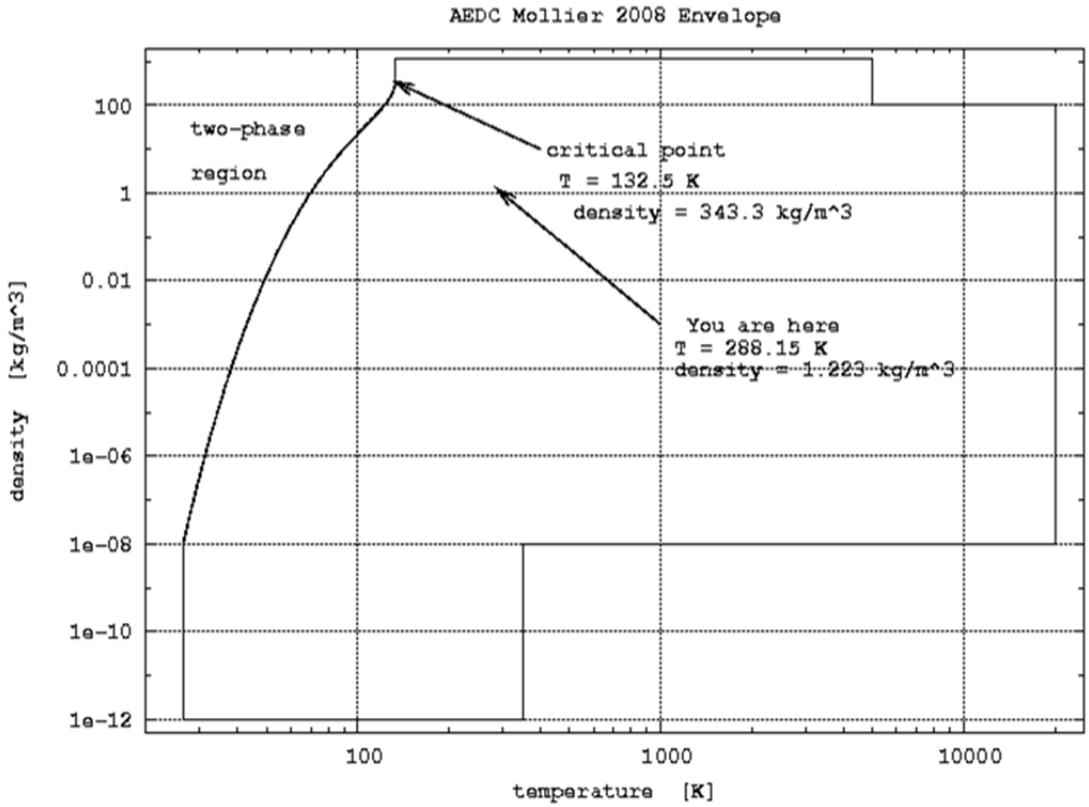

Figure 6. Envelope of the AEDC Mollier 2008 EOS

The envelope of the final combined EOS is shown in Fig. 6. Logarithmic scales are used to show detail over the full range of the EOS. The compressed liquid (temperature less than critical temperature and density greater than critical density) part of the envelope is deleted. Properties in this region can be calculated beginning with temperature and density. The properties cannot be calculated beginning with other pairs of properties because of the difficulties in translating other pairs into temperature and density. Since only partial capability is available in the compressed liquid region, it is not included in the envelope of the EOS. More explanation will be given later.

The Mollier diagram for the final form of the EOS is shown in Fig. 7 and includes the compressed liquid region.

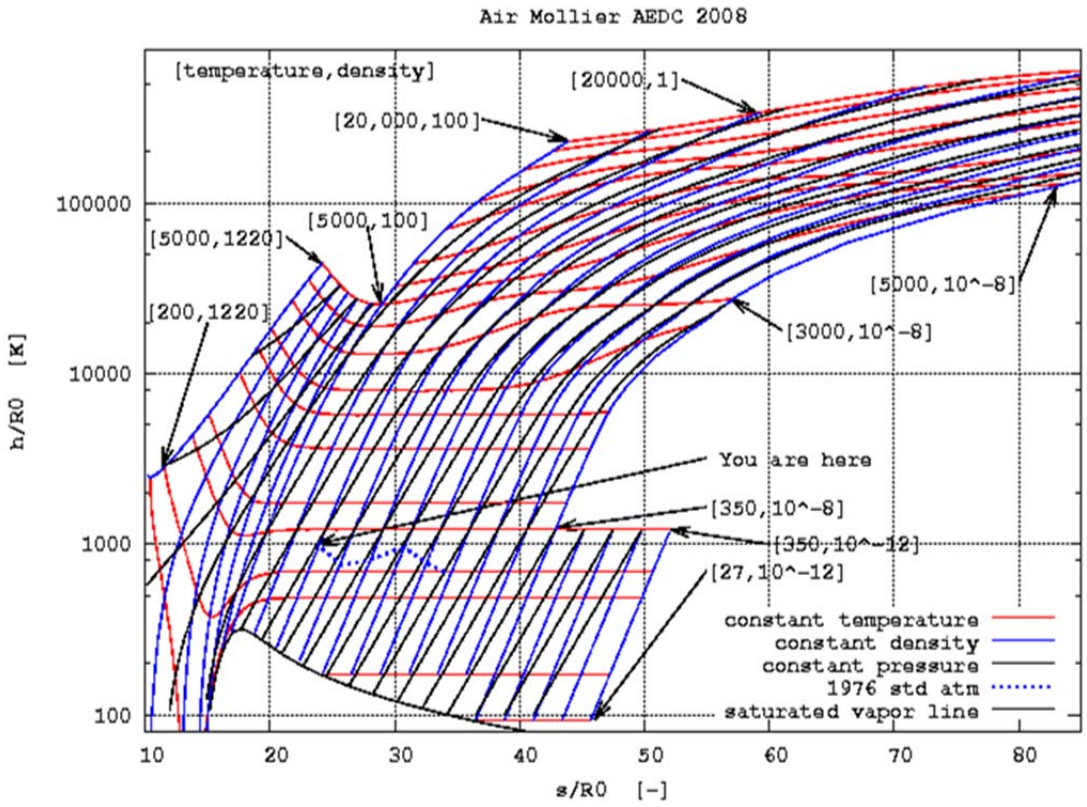

a. Equation of State

Figure 7. AEDC Mollier 2008

Several key points have been identified in the figure. Note that 10^-8 means 10^{-8}, etc. The constant temperatures lines (in degrees Kelvin) reading from bottom to top are 27, 50, 140, 200, 350, 500, 1,000, 1,500, 2,000, 3,000, 4,000, 5,000, 6,000, 75,000, 10,000, 12,000, 15,000, 18,000, and 20,000. The constant density lines (in kg/m3) reading from right to left begin with 10^{-12} and increase by a factor of 10 to a density of 100. The densities to the left of the 100 line are 200, 400, 600, 800, 1,000, and 1,220. The left-most constant pressure is 10^{9} Pa. Each succeeding line moving to the right is a factor of 10 less. The individual lines can be identified on the figure if a large-format figure is made, but space does not permit on this scale.

The abscissa is truncated in Fig. 7a; the highest-temperature, lowest-density portion of the envelope is not represented here. The truncated portion of the Mollier chart represents the conditions where the multiple ionization would occur. Confirmation of this fact will be presented in a later section. This area is of little current interest.

Figure 7a is repeated in Fig. 7b with the addition of the loci of some flow cases of interest. The constant parameter lines shown in Fig. 7b are the same as Fig. 7a. The annotation on Fig. 7a has been omitted on Fig. 7b in the interest of readability.

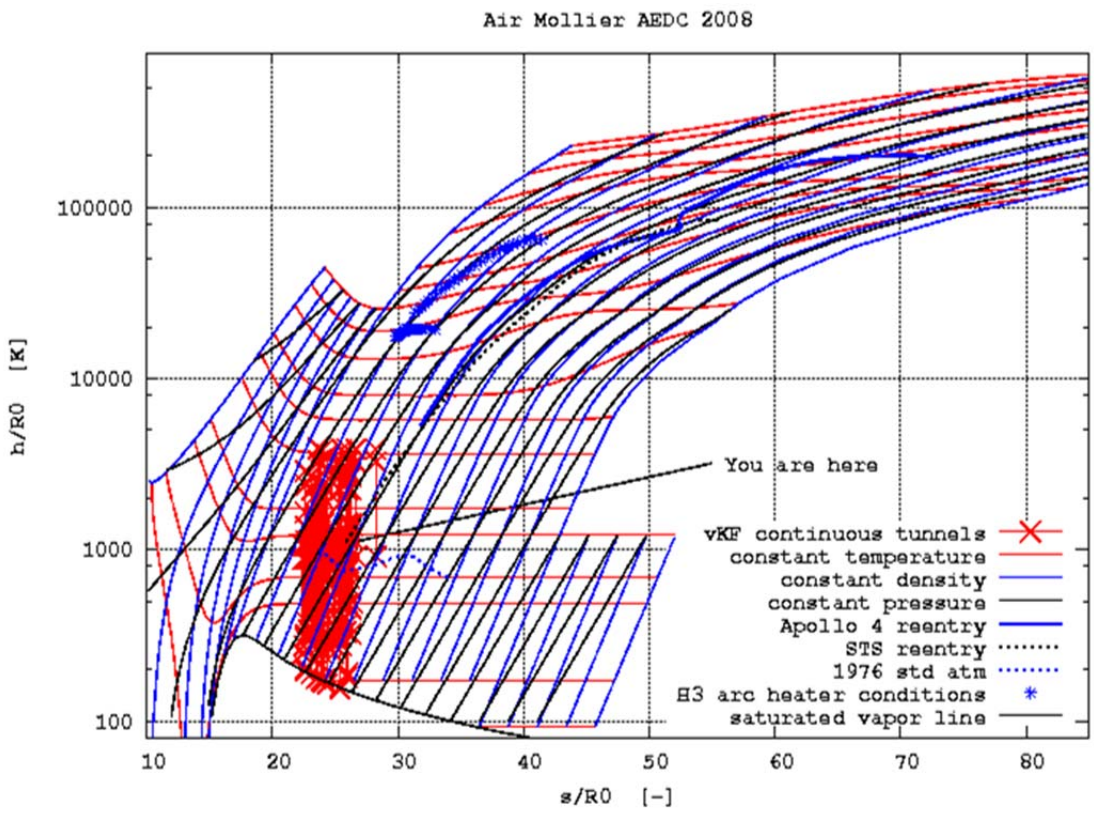

b. With Some Continuous Tunnels and Two Reentry Trajectories Included

Figure 7. Concluded

The VKF (Von Karman Facility) continuous tunnels symbols represent the total, throat, and freestream conditions of the VKF tunnels. Note that many of the expansions terminate at the saturation line. The H3 symbols represent the range of anticipated total conditions for the H3 arc heater.

The two reentry trajectories represent the static conditions behind the normal shock created at the stagnation point of the two reentry vehicles. Each point on the trajectory corresponds to a point in the atmosphere and the speed of the reentry vehicle at that altitude. Note the higher maximum enthalpy, approximately a factor of 2.4, for the Apollo 4 reentry compared to the STS reentry. The Apollo 4 reentry trajectory is typical of all lunar reentry trajectories.[7] The Hayabusa asteroid sample return reentry trajectory (Ref. 15) begins at s/R0 ~ 75 and h/R0 ~ 247,000 K.[8] Return from low earth orbit creates much less extreme conditions than return from lunar orbit. Similarly, return from Mars would create more extreme conditions than return from lunar orbit.

2.4.3 Derivative Properties

The derivatives are a special case and cannot be calculated by summing three contributions as was done for the properties.

[7] Precise details of Stardust reentry trajectory are not known but reasonable estimates of the trajectory suggest that the reentry path would have started at about s/R_0~79 and h/R_0~285,000 K in the coordinates of Fig. 7b. That is about 40% greater enthalpy than the Apollo 4 reentry.

[8] The Hayabusa reentry trajectory is not shown in Fig. 7b because only a partial trajectory was found in the reference.

2.4.3.1 Specific Heats

The various derivatives, c_v, c_p, a, etc. cannot be calculated by adding the thermally perfect, the high-density, and the high-energy contributions. The problem arises because the high-energy contribution cannot be formulated as an analytic expression. Furthermore, taking a derivative of a property while another property is held constant, e.g., $a^2 = \left[\frac{\partial P}{\partial \rho}\right]_s$, is difficult when the property held constant is the sum of contributions from three sources.

The derivative c_v is straightforward because density is one of the independent variables of the EOS. The other derivatives are less so. All of the derivatives can be expressed in multiple mathematically equivalent forms. The forms that were implemented were the forms that could be evaluated in terms of derivatives of properties with respect to temperature and density. Specifically,

$$c_p = \left[\frac{\partial h}{\partial T}\right]_\rho - \frac{\left[\frac{\partial h}{\partial \rho}\right]_T \left[\frac{\partial P}{\partial T}\right]_\rho}{\left[\frac{\partial P}{\partial \rho}\right]_T} \quad \text{and} \quad a = \sqrt{\left[\frac{\partial P}{\partial \rho}\right]_T - \frac{\left[\frac{\partial P}{\partial T}\right]_\rho \left[\frac{\partial s}{\partial \rho}\right]_T}{\left[\frac{\partial s}{\partial T}\right]_\rho}}.$$

All of the derivatives were approximated by 2nd-order accurate finite differences. Central differences were used except at the boundaries where 2nd-order accurate one-sided differences were used. The step sizes used in the finite differences were large enough to minimize the effect of the inherent "noise" in the iterative numerical calculations of the properties and small enough to preserve the local characteristics of the property variations.

Spot checks of the calculated values of c_p were compared with the values from cea2 and the values were sufficiently close. The specific heat is dominated by the "reaction specific heat" in the range where comparisons are valid.

2.4.3.2 Speed of Sound

An independent calculation of the speed of sound was programmed, and the results were compared to the above formula. The pressure was fit as a function of density along a constant entropy path over a small range centered at the point of interest. The form used was a form that blends smoothly into one of the ideal gas forms, to wit,

$$P = b_0 \rho^{b_1} \quad (\text{or } log_e(P) = b_0 + b_1 log_e(\rho))$$

thus, the speed of sound is

$$a = \sqrt{b_1 \frac{P}{\rho}} \quad (\text{or } a^2 = b_1 \frac{P}{\rho})$$

where P and ρ are the properties at the point of interest. The calculated speeds of sound using the two approaches were essentially the same, differing by a few tens of parts per million over the range of the EOS. The parameter b_1 in this formulation is sometimes called the adiabatic index.

The speed of sound was compared with the values calculated using cea2 in selected cases where both should be accurate. The agreement was good although not as good as the

consistency check mentioned above. Insufficient points have been compared to make a statistical assessment.

The properties on which the derivatives are based are smoothly varying and continuous. Deviations in the properties from the anticipated behavior are difficult to observe. The derivatives are much more sensitive to local variations. The sound speed will be used here to demonstrate the behavior.

The variation in the sound speed can be highlighted by rearranging the equation for the sound speed squared and plotting the resulting ratio, $\frac{a^2\rho}{P}$. Following customary practice (Ref. 16), that ratio is plotted for constant pressures in Fig. 8.

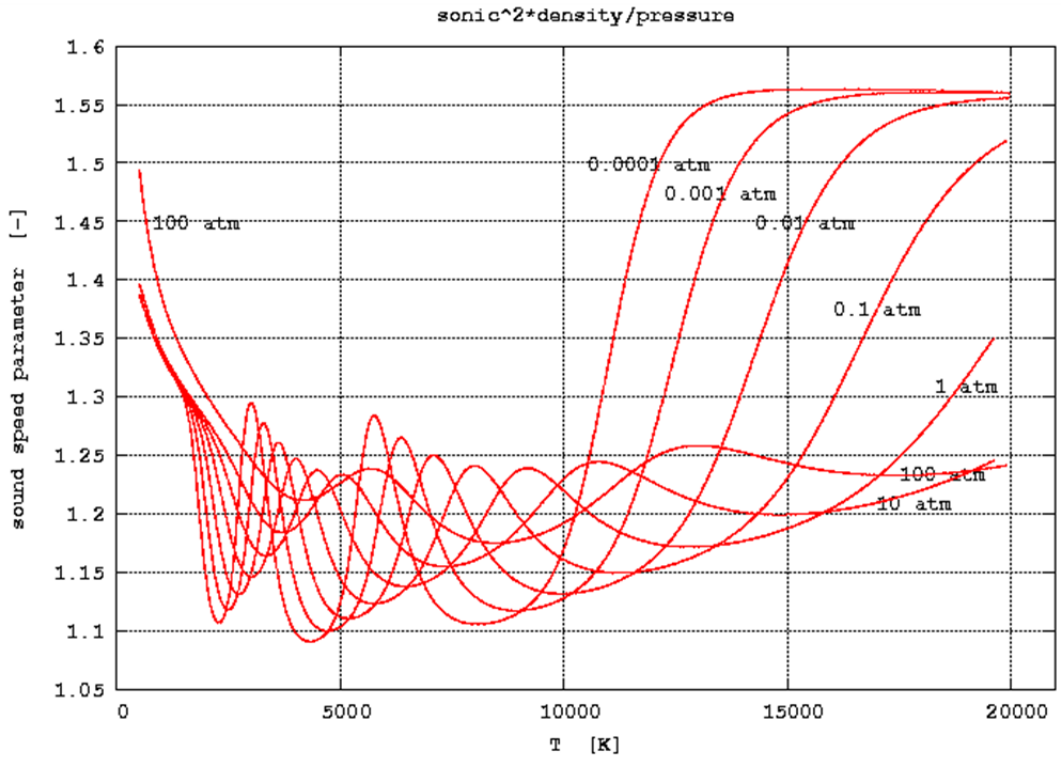

Figure 8. Sound Speed Parameter for Six Pressures

The value of the parameter for air at ambient conditions is about 1.4 as indicated on the plot. The exception for the 100-atm case shows the effect of the elevated density at high pressure and low energy. The initial decrease in each line is a result of the excitation of the vibrational degrees of freedom of the diatomic species. The first maximum, at temperatures of 3,000 to 5,000 K, is a result of the dissociation of O_2, the second maximum at temperatures of 6,000 to 13,000 K represents the dissociation of N_2, and the third maximum represents ionization. The calculated values are consistent with expectations.

2.4.4 High-Density Contributions to Properties

Temperature and density are the independent variables of the EOS. All else is calculated from those two. The primary properties calculated are the pressure, the internal energy, the enthalpy, and the entropy. The high-density portion of the EOS is used to calculate the thermally perfect contribution, to the properties and to calculate the high-density contribution to

the properties. The high-energy portion of the EOS is used to calculate the high-energy contribution which is then added to the other two. This approach presumes that the high-density portion of the EOS produces reasonable results over the entire range. The validity of that assumption is shown in the following figures. The range of independent parameters excludes the highest density, lowest energy region where only the high-density portion of the EOS is used.

The high-density contributions to the properties are divided by the equilibrium properties in all cases so that the difference can be observed.

2.4.4.1 Pressure

The pressure is shown in Fig. 9.

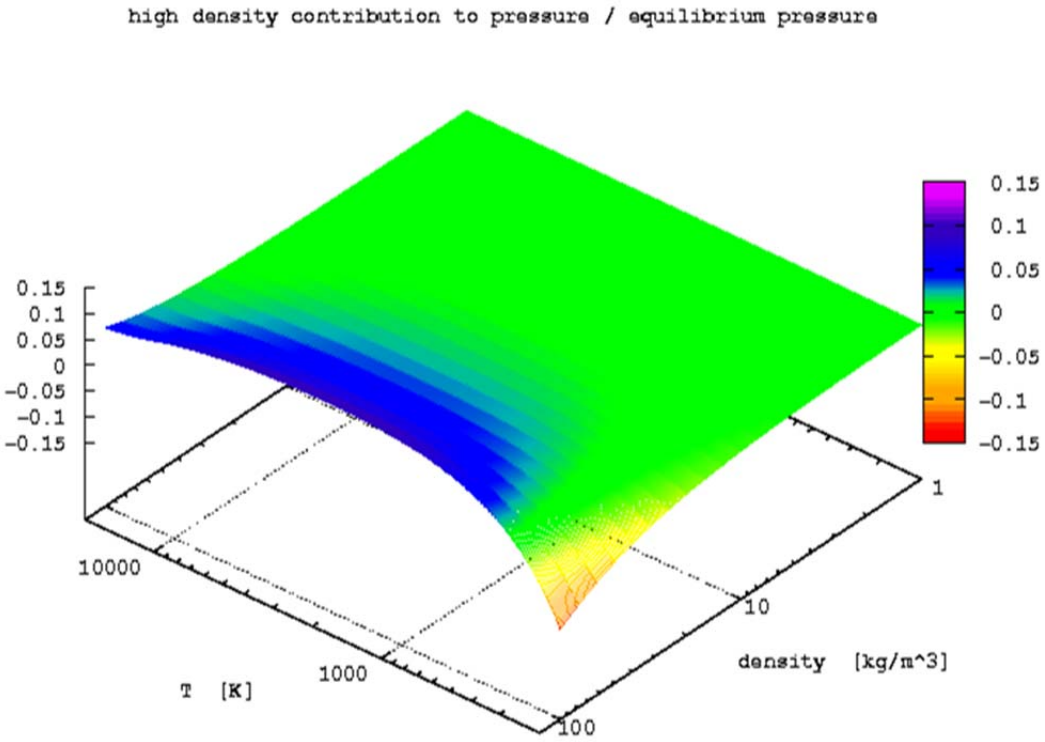

Figure 9. High-Density Contribution to the Pressure Divided by the Equilibrium Pressure

The high-density contribution to the pressure is well behaved over the entire range. The contribution is negligible for all temperatures except at the highest densities. The maximum contribution for temperatures above ambient is less than 11%. The negative contribution at high densities and low temperatures is a result of the attractive force between molecules in that region and is as expected. There is no known source for comparison of high-temperature, high-density effects. The classic "AEDC Mollier Diagram for Equilibrium Air" c. 1967 shows trends consistent with the above, but its provenance is sufficiently ambiguous and its acknowledged limitations in the high-density region are such that it cannot be used as a standard.[9] The largest contributions at elevated energies occur in the highest density where the combined effects are

[9] That is not meant to disparage the 1967 Mollier diagram. It represents a large amount of good work by many talented individuals. It served, and continues to serve, a real need in the aerospace community. However, careful reading of the documentation reveals sufficient gaps, contradictions, approximations, etc., to limit confidence.

the least well understood. Fortunately, this area is of little interest because the conditions are extremely difficult to produce.

2.4.4.2 Enthalpy

The high-density contribution to the enthalpy is shown in Fig. 10.

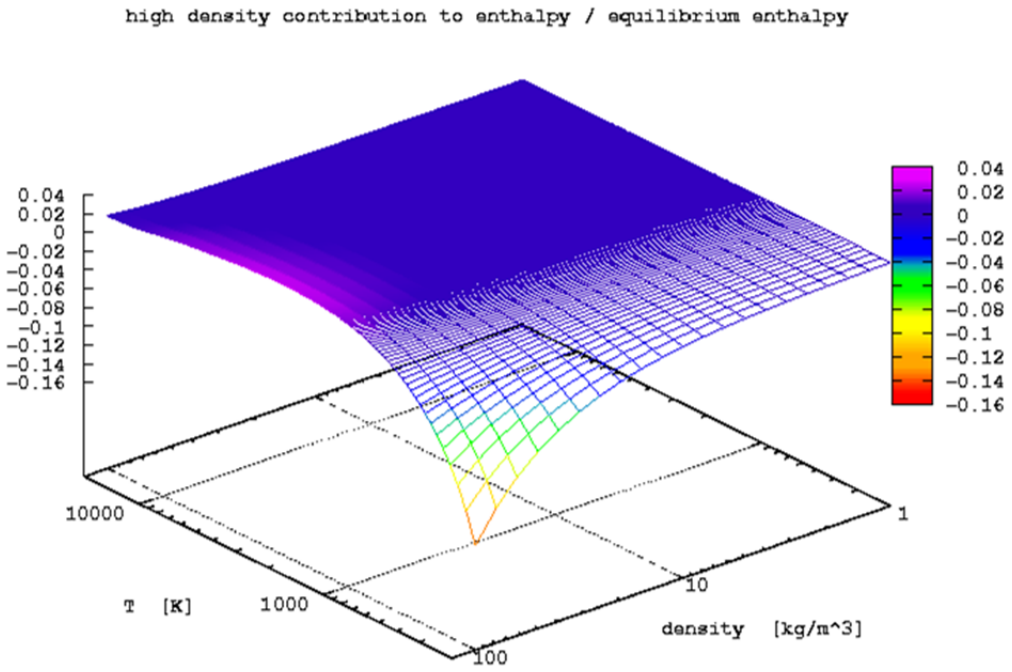

Figure 10. High-Density Contribution to the Enthalpy Divided by the Equilibrium Enthalpy

As with the pressure in Fig. 9, the high-density contribution to the enthalpy is well behaved over the full range. Also like the pressure, the contribution is negligible for all temperatures at all except the highest densities. The maximum contribution at temperatures above ambient is less than 3.5% and occurs at the maximum density, consistent with expectations.

2.4.4.3 Entropy

Finally, the high-density contribution to entropy is shown in Fig. 11.

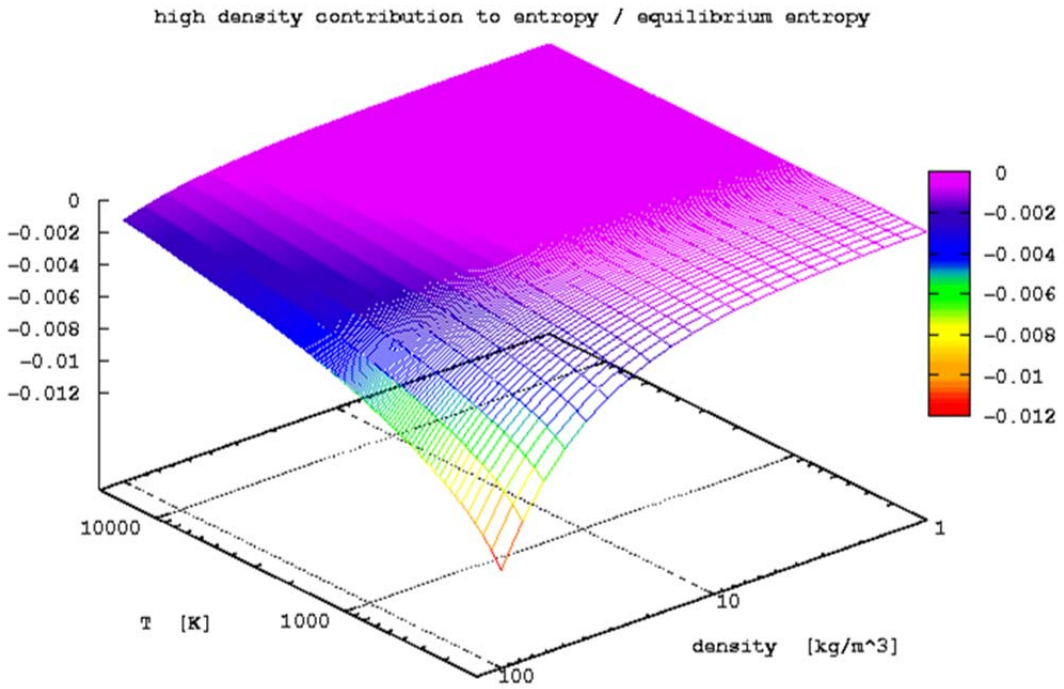

Figure 11. High-Density Contribution to the Entropy Divided by the Equilibrium Entropy

The high-density contribution to the entropy is always negative and approaches zero for all temperatures above ambient. The negative contribution is expected based on the definition of entropy.

The conclusion to be drawn from these plots is that the use of the high-density portion of the EOS as a base to which the high-energy contribution is added is justified.

2.5 ALTERNATIVE APPROACH

The current approach uses a separate EOS for high density and for high energy. The contributions are summed to calculate the property values. This is an essentially linear approach. Another potential approach would be to calculate the thermodynamic properties of the individual species accounting for the high-density effects and to determine the equilibrium composition by a free-energy minimization procedure. This is in some ways analogous to the procedure used to calculate the high-density properties of mixtures of fluids. This approach would require a model and data for the high-density effects at elevated energies, which in general do not exist. Hilsenrath and Klein used this approach (Ref. 2), but the high-density effect was limited to the second virial coefficient. This is analogous to terminating the high-density EOS after the ρ^2 term. This approach limits the accuracy in the high-density portion of the envelope.

Other approaches may exist. All possibilities should be investigated.

2.6 AUXILIARY CALCULATIONS

Three groups of auxiliary subroutines will be briefly discussed. They are, in the order discussed, the transport properties, the alternative independent parameters, and the utility calculations.

2.6.1 Transport Properties

The transport properties, viscosity and thermal conductivity, are not necessarily a part of the EOS. They are required for many of the practical applications of the EOS, e.g., heat transfer, so a procedure was developed to estimate the transport properties over the range of the EOS. Little time and effort was devoted to the transport property calculations relative to the time and effort devoted to the thermodynamic property calculations. The procedure that was developed is adequate, but this aspect of the work should be revised and improved.

The approach taken for the transport property calculation mimics the approach taken for the thermodynamic property calculations. The transport properties of thermally perfect air were calculated, and the additional contributions due to high-energy effects and high density-effects were added.

2.6.1.1 Low-Temperature Viscosity

The viscosity of thermally perfect fixed-composition air was calculated from a locally developed equation of the form

$$\mu = v_1 T^{v_2}(1 + v_3 e^{v_4 T})$$

where the constants $v_1 \rightarrow v_4$ were evaluated by a least-squares fit to a variety of published data. The first term, $v_1 T^{v_2}$, has a sound theoretical basis (Ref. 3) for moderate temperatures. The second term is a well-behaved correction for low temperatures. The form extrapolates well for temperatures outside the range where data are available. The high-density contribution to the viscosity was calculated based on (Ref. 17).

2.6.1.2 Low-Temperature Thermal Conductivity

The thermal conductivity of thermally perfect fixed-composition air was evaluated based on Ref. 18. The high-density contribution to the thermal conductivity was calculated based on Ref. 19.

2.6.1.3 High-Energy Transport Property Addition

The high-energy contribution to the transport properties was calculated using cea2. A 2-D table of transport properties was generated, with temperature and density as the independent variables, and bi-linear interpolation was used to evaluate the properties. The temperatures and densities used in the table were chosen to capture the nature of the variations in the transport properties. Linear interpolation was used to ensure that the interpolated properties would remain realistic in regions of large gradients.

2.6.1.4 Mean Free Path

An estimate of the mean free path at the specified condition can be made. This estimate is essential to determine whether the continuum assumption is valid. If the smallest physical dimension of the flow field is less than about 30 times the mean free path, then the continuum assumption is questionable or invalid and other approaches should be used.

2.6.2 Alternative Independent Parameters

The pair temperature and mass-density are the natural parameters for the EOS, but they are not the most convenient parameters for every calculation. A group of subroutines have been written to "translate" other pairs of independent parameters into temperature and density. The pairs that have been programmed to date are temperature and pressure; entropy and enthalpy; entropy and temperature; entropy and pressure; entropy and mass density; enthalpy and pressure; enthalpy and mass density; pressure and mass density; and internal energy and mass density. Other combinations could be added as needed.

The property pairs involving one of the natural variables are simple and straightforward since they involve a 1-D search in thermodynamic space. The other pairs, the pairs which include neither natural parameter such as entropy and enthalpy, are more challenging since they require a 2-D search in thermodynamic space. A good initial guess and a robust iteration procedure are required for those cases. Discussion of the details of those procedures is beyond the scope of this report.

The enthalpy is a nonmonotone function of density in the compressed liquid region. The derivative of pressure with respect to density at constant temperature is very large and varies by several orders of magnitude in the compressed liquid region. These two facts, and other similar realities, make development of robust translation routines very difficult. The difficulty was judged excessive for the gain, so the compressed liquid region was excluded from the envelope of the EOS.

2.6.3 Unit Problem Calculations

Unit problems are flows in which one physical process dominates to the exclusion of all others. The EOS was developed as a thermodynamic base for engineering calculations. There are some unit problems in engineering analysis that occur often enough to warrant separate, specialized programming, e.g. conditions at the throat of a nozzle given total conditions, shock crossings, etc. More complicated flow scenarios can be constructed as a sequence of unit problems; for instance, calculation of the Pitot pressure in the exit of a nozzle given the total conditions and nozzle geometry.

The following unit problems were individually programmed:

- Thermodynamic and transport properties at a specified condition
- Thermodynamic and flow conditions, given total conditions and isentropic expansion
- Stagnation conditions given flow conditions
- Post-normal shock conditions given flow conditions
- Post-oblique shock conditions given flow conditions, and either flow deflection angle or shock angle
- Flow and total conditions given altitude and Mach number
- Adiabatic free expansion (Joule-Thompson throttling)

- Newtonian pressure distribution on a hemisphere in supersonic flow
- Prandtl_Meyer expansion in supersonic flow
- Flow conditions, given total conditions and mass flux (stilling chamber flows)
- Flow and total conditions, given flight Mach number and dynamic pressure
- Heat-transfer estimation
- Generation of a table of thermodynamic and transport properties

As above, others can be added as needed.

3.0 ACCURACY ASSESSMENT

3.1 INTRODUCTION TO ACCURACY ASSESSMENT

No engineering measurement and no engineering calculation can be considered complete until it includes a realistic assessment of accuracy. Uncertainty analysis is well developed for physical measurements. However, it is less well established for the uncertainty of calculations. Thus, a different approach to accuracy assessment was taken in this case. This approach is described in the succeeding paragraphs.

There is no single source which can serve as a standard for comparison with the developed EOS. This work would not have been necessary and would not have been done if such a source existed. The venerable “AEDC Mollier Diagram for Equilibrium Air” c. 1967 might seem an appropriate standard, but such is not the case. Careful reading of the documentation of its development reveals sufficient gaps, contradictions, etc., to limit confidence. However, it can and did serve as a 1st-order sanity check for the EOS during the development of the EOS.

Two other computer-based EOS could be considered for comparison, the NASA Rgas EOS and the Tannehill curve fits (Refs. 20-21). The NASA Rgas is a database method and can be used for any gas whose thermodynamic properties can be put in the format required by the database. The Tannehill curve fits are curve fits of the thermodynamic properties of equilibrium air as calculated using the NASA Rgas and the appropriate data for equilibrium air. The NASA Rgas EOS does not include high-density effects. Furthermore, the structure of the database method would not be appropriate for the property variations caused by high-density effects. Thus, neither is appropriate for this work.

The calculated properties chosen for the accuracy assessment were pressure, enthalpy, and entropy. Derivative properties, speed of sound, specific heats, et al., were not considered. In general, they represent the sums and products of multiple derivatives. The direct property derivatives would be more sensitive (exhibit greater errors) than the properties, and they are also more likely to highlight local anomalies rather than systematic deviations from the correct value. Furthermore, the property values, not the derivatives, form the basis of the solutions to engineering problems.

The problem of the lack of an adequate standard for comparison arises in the region where both high-density effects and high-energy effects contribute to the final result. This fact suggested the approach taken here to assess the accuracy of the final EOS.

3.2 APPROACH TO ACCURACY ASSESSMENT

The approach taken was to compare the predictions of the EOS with industry standard approaches in the limits where only one effect, high-density or high-energy, made a nontrivial contribution to the final property value. Thist approach was straightforward in the high-density limit. The same approach was used in the high-energy limit, but the application was more involved. Both will be discussed in some detail in the following sections.

Lacking a recognized authority for the region where both high-density effects and high-energy effects contribute to the property values, the approach taken was to demonstrate continuity and consistency between the limits. The procedure used for that evaluation will be discussed also.

3.2.1 High-Density Limit:

The high-density limit, where high-energy effects are negligible, will be addressed first.

3.2.1.1 Industry Standard

NIST-REFPROP is the industry standard for high-density EOS. The latest, version 9, contains the specific parameters for an EOS for air, treated as a pseudo-pure fluid, whereas prior versions did not.[10] A locally programmed version of the NIST-REFPROP-9 EOS for air based on Ref. 22 was used for convenience. The locally programmed version of the NIST EOS used the same high-density approach and same high-density parameters as the NIST version. The thermally perfect property curve fits in the NIST version were adequate for the stated temperature range of the EOS, but they were not accurate for extrapolations to higher temperatures or to lower temperatures. The thermally perfect property curve fits used in the high-energy portion (Ref. 10) of the EOS were used in the high-density portion.

The predictions of the locally programmed air EOS were checked by comparison to the NIST programmed version. The differences were typically a few parts per million, often less. Thus, the locally programmed version of the NIST EOS for air was an adequate standard for assessing the accuracy of the high-density portion of the locally developed EOS with the added benefit of better behavior under extrapolation.

3.2.1.2 Approach

The approach taken was to determine the combinations of temperature and density which would produce a deviation of a preselected magnitude between the property values predicted by the locally developed EOS and the property values predicted by NIST-REFPROP-9. The preselected magnitudes were 0.5, 1, 2, and 5%. The property values as calculated were used in the comparisons for simplicity.

The lowest temperature considered was 140 K. This temperature was selected to avoid the critical region where property prediction is problematic at best. This choice does not materially affect the envelope of the EOS since all points of interest at temperatures below 140 K are also at very low densities where the high-density effects are negligible.

A temperature was then selected. Beginning at a density such that high-density effects were negligible, the density was increased in very small steps at constant temperature until the

[10] If the NIST EOS for air had been available when the current EOS was developed, c. 2008, it would have been used rather than the Reynolds EOS. However, the NIST version first became available in 2011.

preselected relative difference was exceeded. A finite-difference Newton iteration in density at fixed temperature used to determine the density at which the calculated difference matched the preselected level at that temperature.

The procedure was repeated for the other two properties. This established the density at which the selected level of difference was observed for the first temperature.

The temperature was then incremented. The process beginning at a low density was repeated up to the maximum temperature.

3.2.1.3 Specific Case: Enthalpy

The relative difference in enthalpy is shown in Fig. 12 for six temperatures for the full range of density.

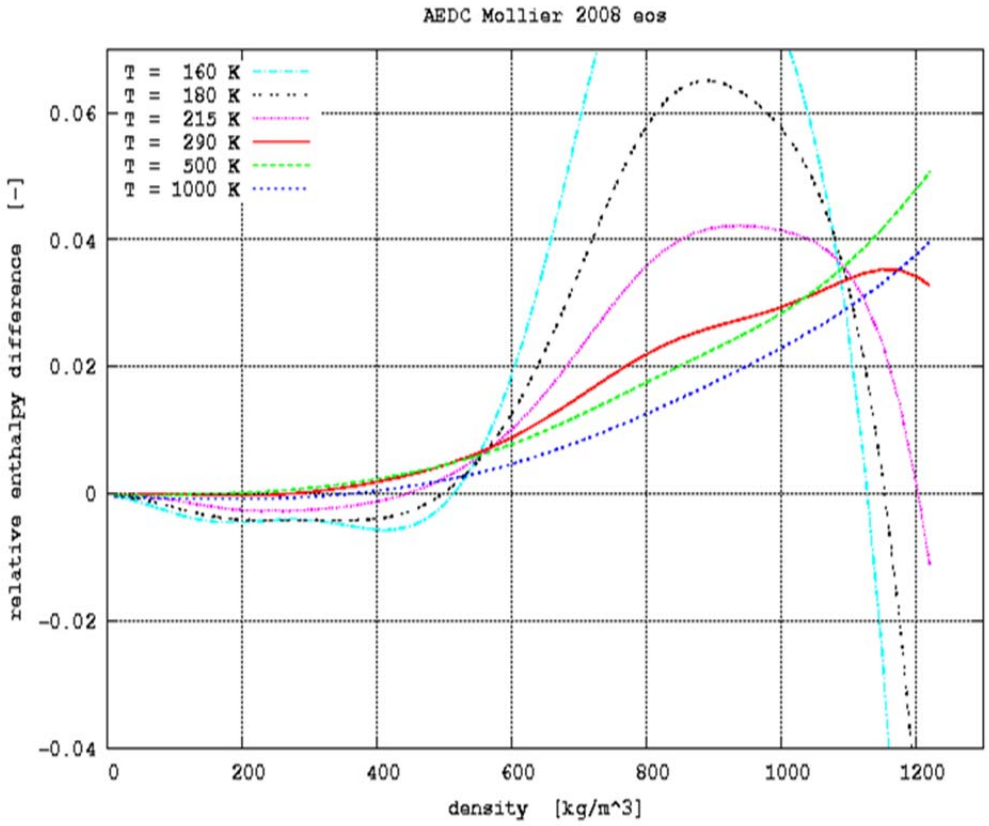

Figure 12. Relative Difference in Calculated Enthalpy for Six Temperatures for Full Range of Density.

Increasing temperatures decreases the difference between the enthalpy calculated by the two EOS. This is consistent with the fact that the high-density effects decrease with increasing temperature. The six temperatures shown in Fig. 12 are representative of all temperatures. Similarly, enthalpy is representative of all three properties.

The relative difference in enthalpy is shown in Fig. 13 for the same six temperatures for the lower range of density.

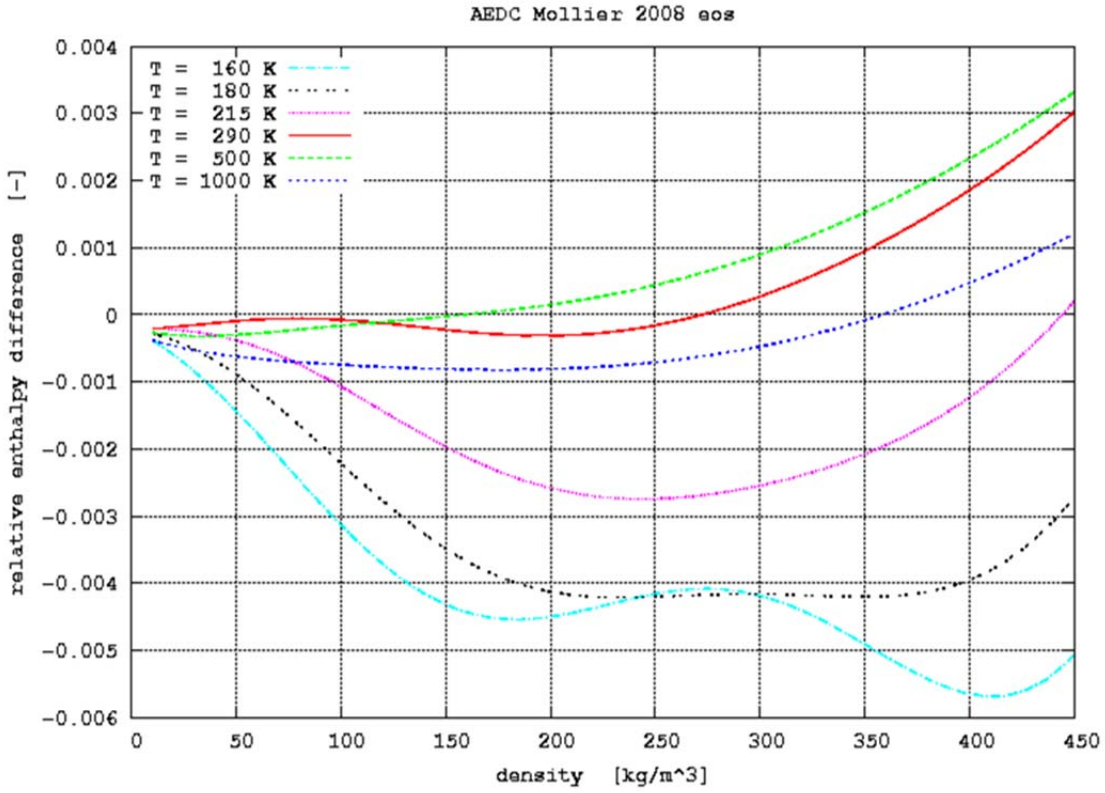

Figure 13. Relative Difference in Calculated Enthalpy for Six Temperatures for Lowest Densities

The nonmonotone variation of the difference is obvious for all six temperatures. The behavior of the enthalpy difference for T = 160 K in the range between 300 kg/m^3 and 450 kg/m^3 suggests a potential problem.

The nature and source of the problem is shown in Fig. 14 where the relative enthalpy difference is shown for four closely spaced temperatures in the density range of 150 kg/m^3 to 450 kg/m^3. The 0.5% relative difference line is also shown.

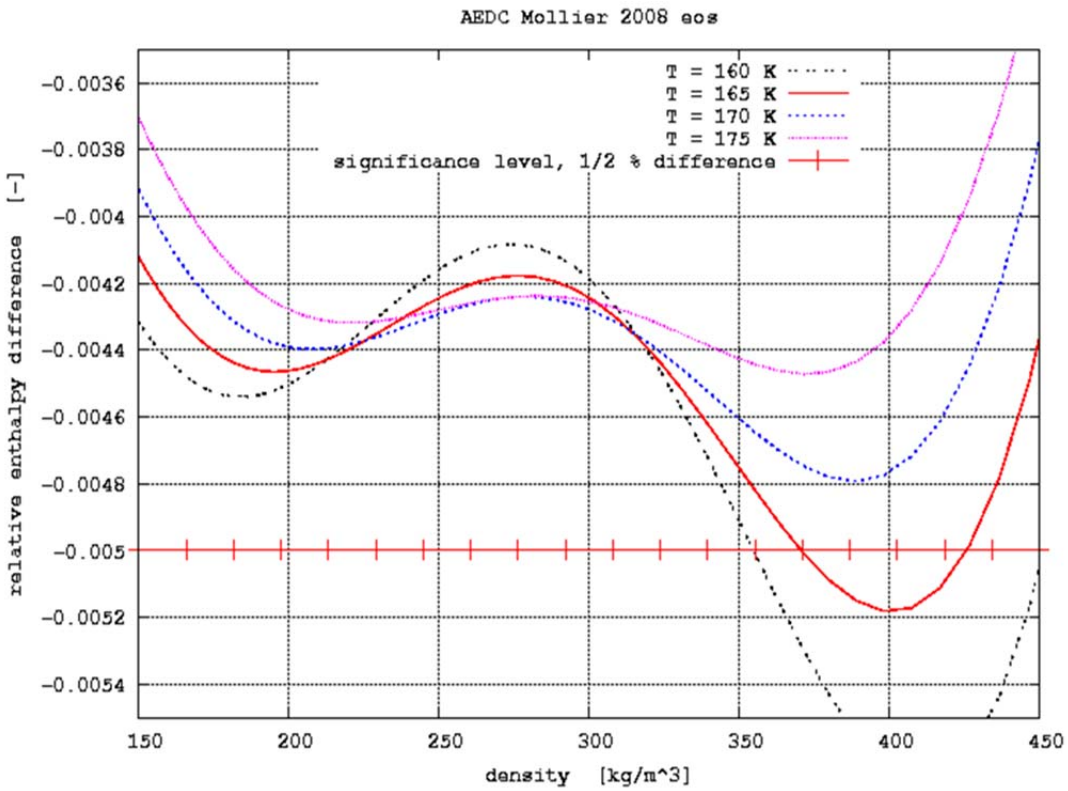

Figure 14. Relative Difference in Calculated Enthalpy for Four Closely Spaced Temperatures

The enthalpy difference reaches 0.5% at a density of about 355 kg/m^3 for a temperature of 160 K and at a density of 371 kg/m^3 for a temperature of 165 K. The error for a temperature of 170 K approaches the 0.5% level in the same region but does not actually reach 0.5% until density reaches 548 kg/m^3. Thus, the plot of density for ½ % enthalpy difference will be discontinuous at that point.

Changing the significance level from 0.5% to 0.475 % would have shifted the discontinuity from between 165 and 170 K to between 170 and 175 K, but any fixed significance level would produce the same result, albeit at a slightly different temperature. Similarly, reducing the temperature increment would have narrowed the range over which the discontinuity occurred, but it would have not eliminated the discontinuity.

The maximum density considered is 1,220 kg/m^3. In some combinations of property and difference level, the maximum density is reached before the difference reaches the selected significance level. These cases appear as gaps in the summary plots.

The stated maximum temperature of the NIST air EOS is 2,000 K. However, the forms of both of the high-density equations suggest that they would be well behaved under extrapolation to higher temperatures. Checks of the property values at temperatures above the stated maximum indicated that, while perhaps not correct, the values were well-behaved and plausible. Based on that observation, the comparisons were continued to higher temperatures.

Not surprisingly, there was a limit beyond which the extrapolation was inappropriate. At the extreme temperatures, there was no density at which the difference between the two high-density EOS was less than the selected level. In other cases, there was no density within the

limit of the EOS at which the difference exceeded the selected level. Neither result is surprising, given that the comparison was between two equations extrapolated well beyond their intended range.

Fortunately, the problems occur in a thermodynamic region that is for all practical purposes inaccessible, i.e., air with ¼ the density of water or more and at temperatures above 2,000 K. The only justification for leaving this region in the envelope of the EOS is to provide a recovery path in case the early steps of an iteration go astray (as they tend to do).

However, there is one one proposed (but not built) facility which is based on much higher densities, albeit at lower temperatures. Laster, Limbaugh, and Jordan (Ref. 23) cite total conditions of 2,000 MPa ($2*10^9$ Pa) and 900 K, which translate to a density of about 1,150 kg/m^3.

3.2.1.4 Three Properties % Disagreement

Bearing in mind the foregoing caveats, explanations, and justifications, the limits of agreement are presented in the following figures. Observe that the range of the ordinate (density) may vary from one plot to the next.

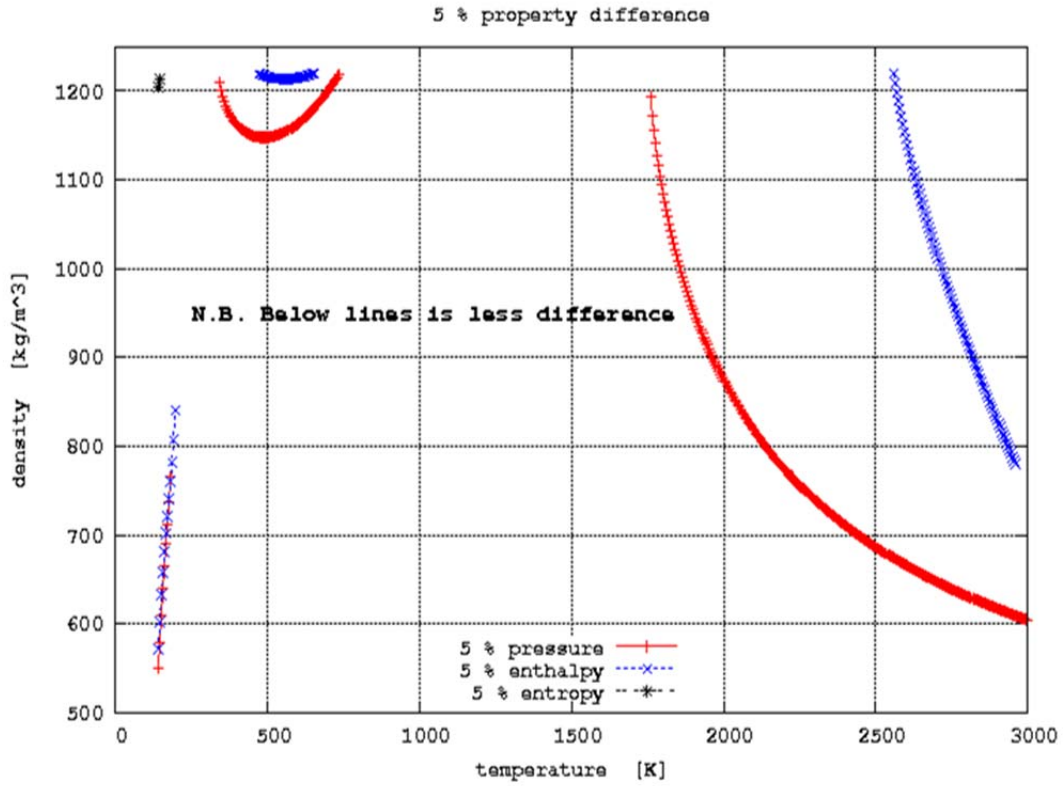

Figure 15. Density as a Function of Temperature for 5% Difference Between NIST and the AEDC EOS

Note that below the lines is less than 5% difference and above the lines is more than 5% difference. Based on Fig. 15, if 5% difference is acceptable, then there is no functionally significant restriction on the envelope of the EOS.

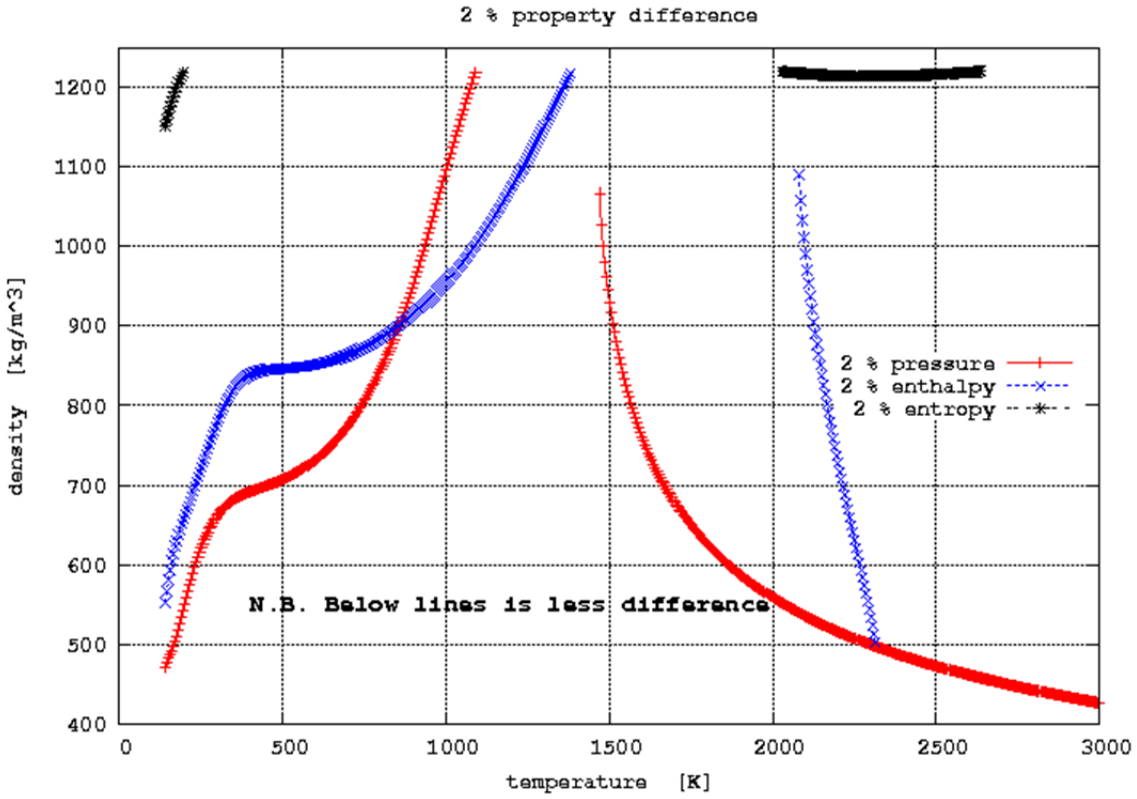

Figure 16. Density as a Function of Temperature for 2% Difference Between NIST and the AEDC EOS

Based on Fig. 16, if 2% difference is acceptable, then there is no functionally significant restriction on the envelope of the EOS. Densities greater than 400 kg/m^3 are acceptable for all temperatures within the envelope of the NIST EOS. The density in the APTU storage tanks at maximum normal pressure and standard temperature is about 300 kg/m^3.

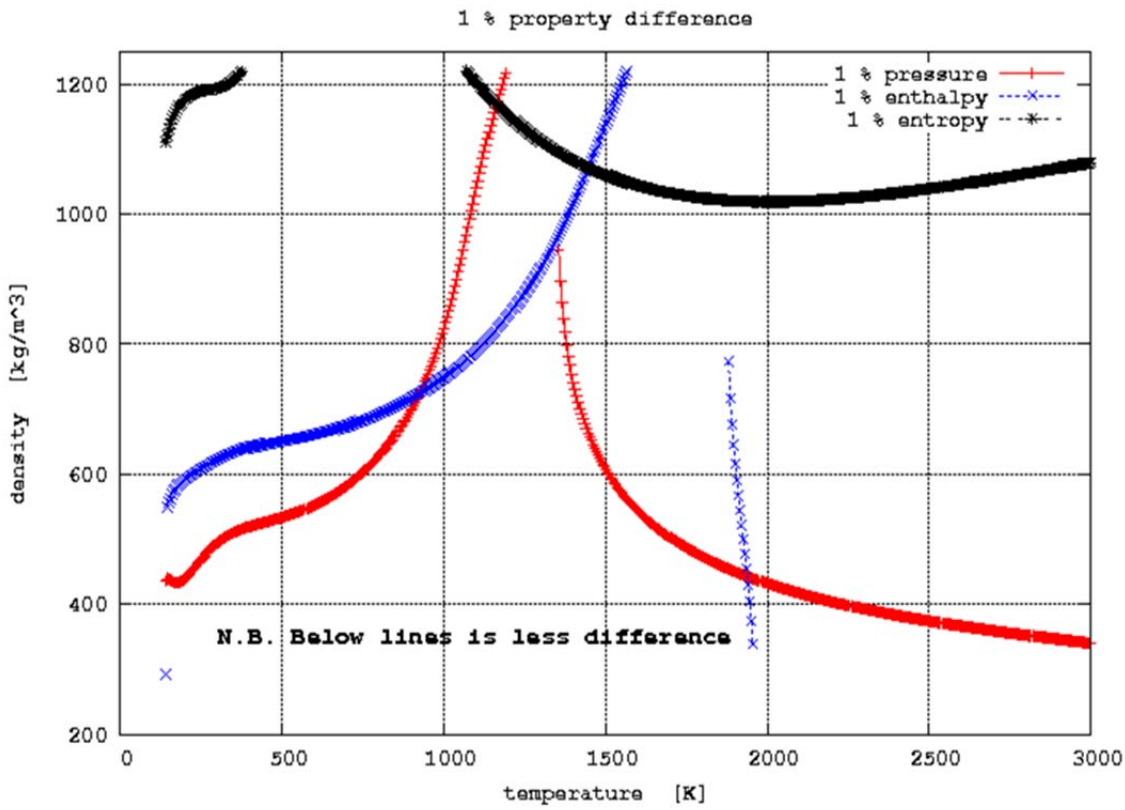

Figure 17. Density as a Function of Temperature for 1% Difference Between NIST and the AEDC EOS

Based on Fig. 17, if 1% difference is acceptable, there is still little restriction to the envelope for conditions likely to be encountered at AEDC.

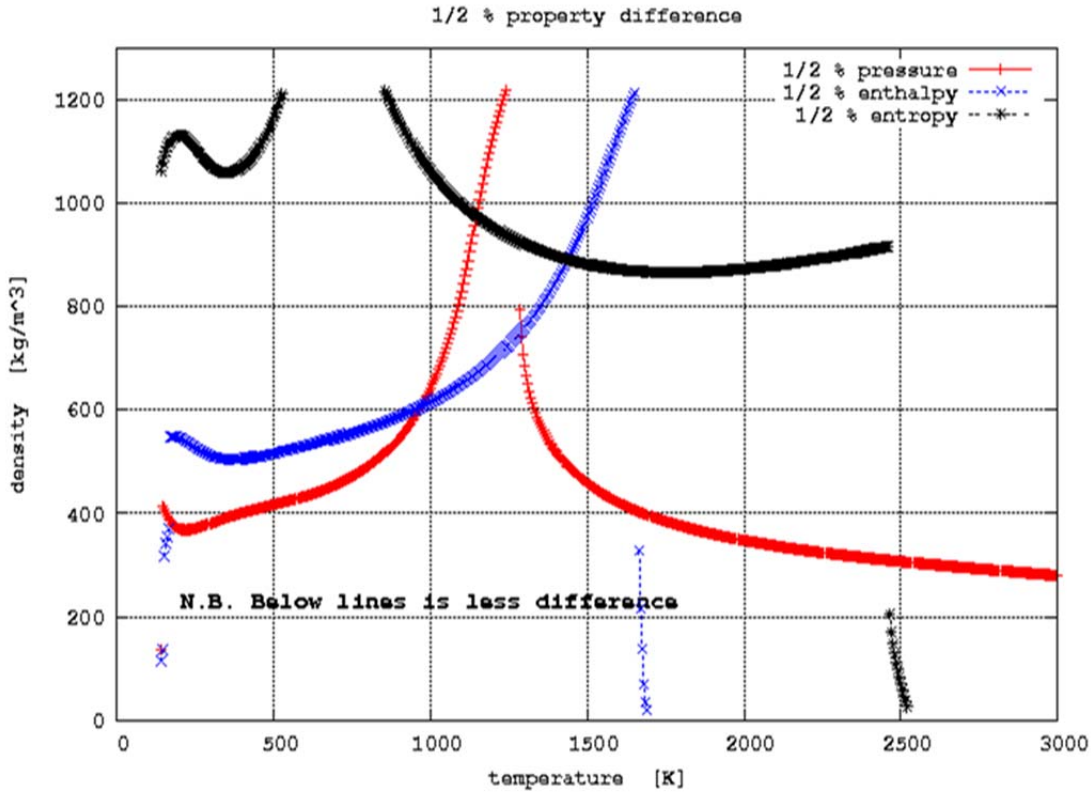

Figure 18. Density as a Function of Temperature for 0.5% Difference Between NIST and the AEDC EOS

Based on Fig. 18, if 0.5% difference is acceptable, there is still little restriction to the envelope for conditions likely to be encountered at AEDC. However, a large portion of the high-density region is compromised.

The next three figures re-present the information from the previous four in a different format.

3.2.1.5 Summary for individual Properties

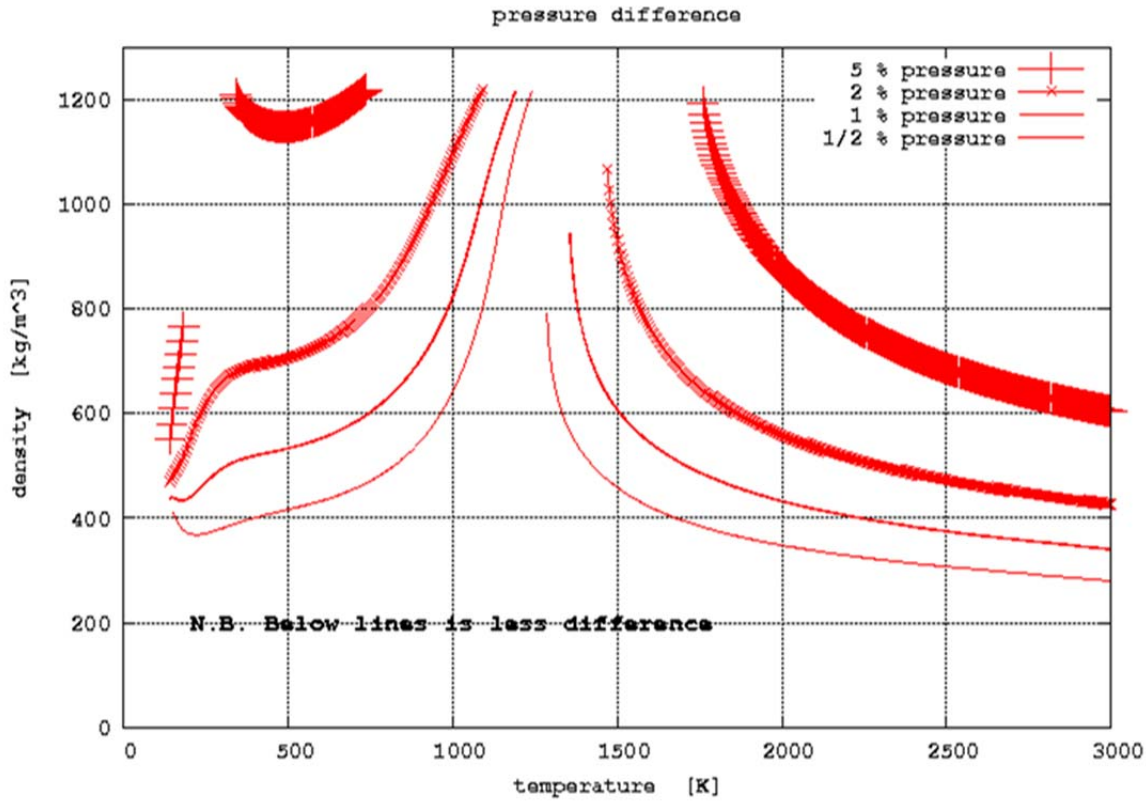

Figure 19. Density as a Function of Temperature for Four Selected Levels of Difference in Pressure

The density difference between the pressure calculated by the local EOS and by the NIST EOS is shown as a function of temperature for four different levels of disagreement in Fig. 19. The shapes of the curves are similar, and the magnitude of the density does not change by more than about a factor of two for an order-of-magnitude change in the level of disagreement. When the two EOS begin to diverge, they diverge rapidly in the case of pressure.

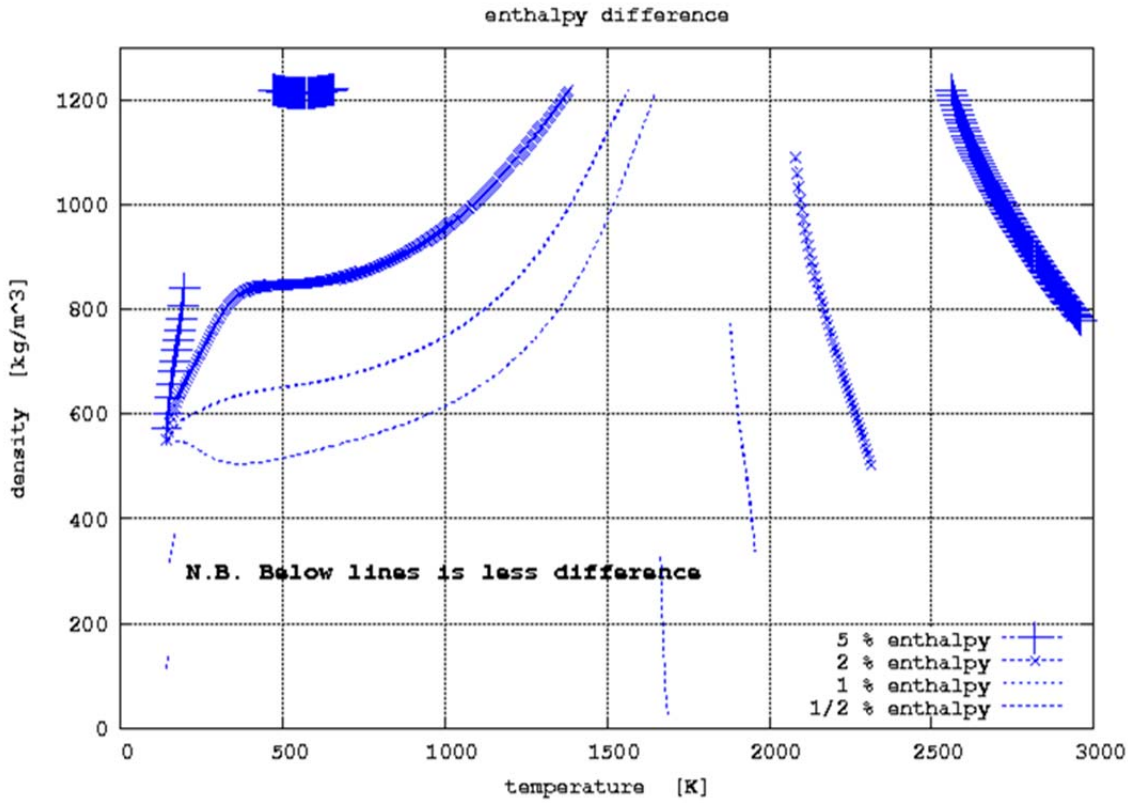

Figure 20. Density as a Function of Temperature for Four Selected Levels of Difference in Enthalpy

The left (low temperature) portion of the plots for enthalpy are similar to the left portion of the plots for pressure. The disagreement between the two EOS is much greater in the high-density, high(er)-temperature region. This is to be expected since there are very little data available in that region.

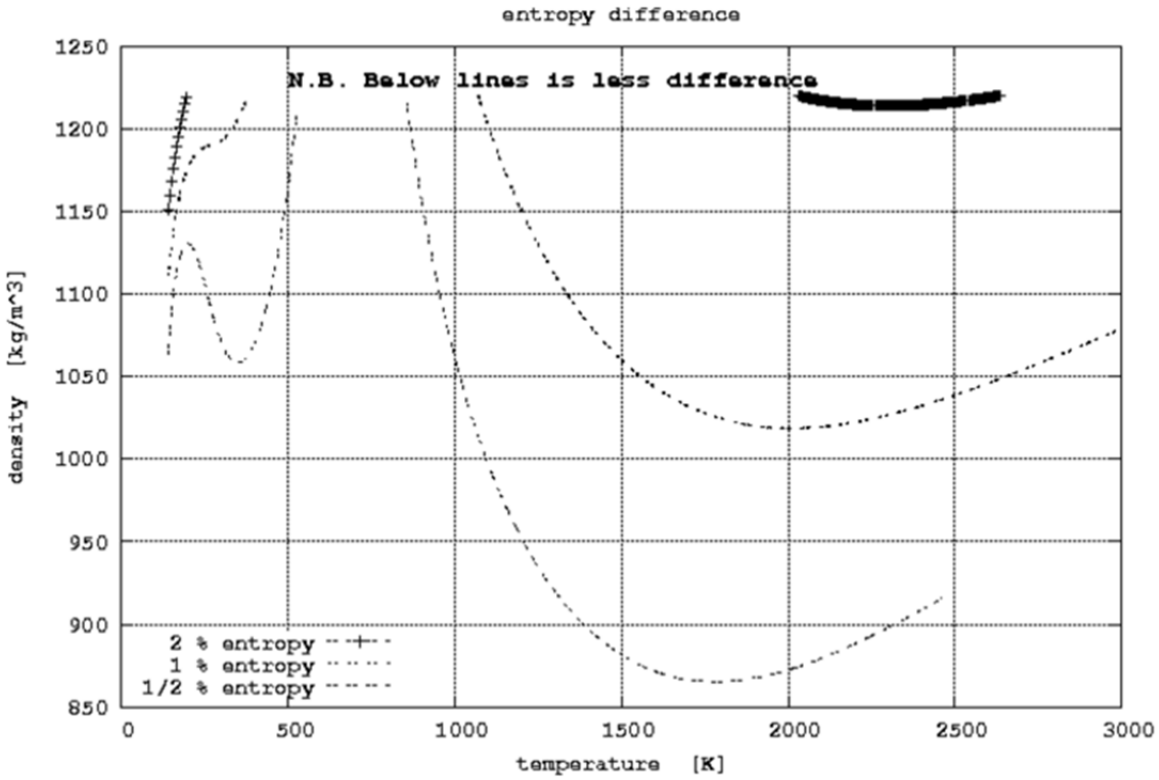

Figure 21. Density as a Function of Temperature for Three Selected Levels of Difference in Entropy

The plots of density required to produce a given level of disagreement in entropy have shapes similar to the preceding two plots. The levels of of the density required are much higher. No combination of temperature and density will produce a 5% difference. Differences in entropy produce no new limitations on the applicability of the Reynolds EOS.

3.2.1.6 Summary of High-Density Accuracy Limits

The temperatures and densities which produce various levels of disagreement between the standard and AEDC Mollier 2008 EOS are shown in the preceding figures. Although the various limits do compromise the high-density range of the EOS, they do not affect regions of normal interest at AEDC. The restrictions could be removed by substituting the locally programmed version of NIST REFPROP 9 for air for the current high-density EOS of Reynolds (Ref. 6).

3.2.2 High-Energy Limit

The differences in properties in the high-energy limit will be due to differences in composition. Specifically, the property differences will arise as a result of the more highly ionized atomic species present at equilibrium but neglected in the AEDC Mollier 2008 EOS.

3.2.2.1 Approach

The philosophy for assessing the accuracy in high-energy limit was the same as the philosophy for the high-density limit. The process was significantly more involved in the high-energy limit. The description of the process follows.

3.2.2.2 Thermodynamics

The ions considered here are not inherently different from other monatomic species in terms of their thermally perfect thermodynamic properties. The variation of the thermodynamic properties with temperature depends on the number and the levels of the excited electronic energy states. The dimensionless sensible enthalpy (subtracting the energy of formation) is similar for all ions. The values for the oxygen ions are shown in the following figure.

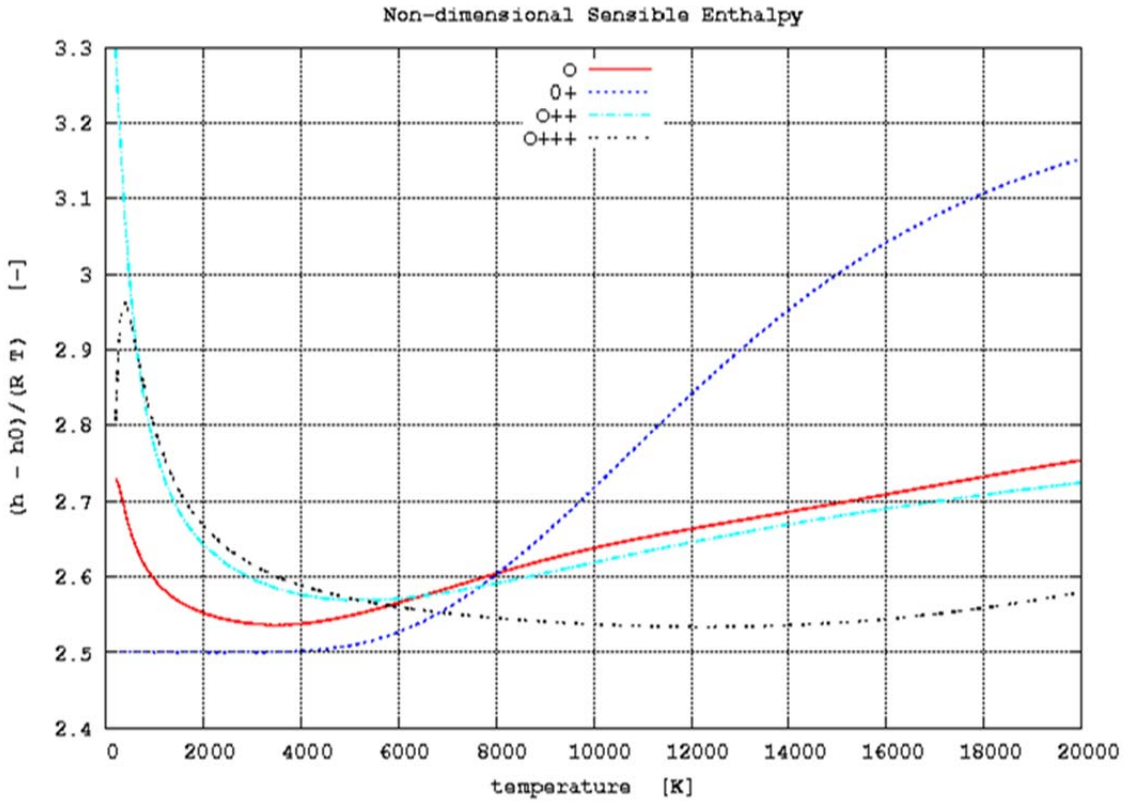

Figure 22. Nondimensional Sensible Enthalpy for Monatomic Oxygen and Its First Three Ions

The primary difference among the ions is the energy of formation. Recall that the energy of formation of the ions is relative to the standard state from which the ion is created, i.e., N_2, Ar, graphite. Removing successive electrons requires increasing energies and the energies are cumulative in the energy of formation. By letting the energy of formation of monatomic oxygen equal 1 in some units, then the energies of formation 0^{+}, O^{++}, and O^{+++} are 6.3, 20, and 41 respectively.

Comparable numbers for Ar^{++}, Ar^{+++}, and Ar^{++++} relative to Ar^{+} are 2.75, 5.3, and 9.1, respectively. Thus, forming successive ions is a highly endothermic process. The number of levels which must be considered is limited by the high positive heats of formation.

3.2.2.3 Equilibrium

Recall that in the high-energy portion of the EOS, the calculation of properties begins with the calculation of the equilibrium composition. cea2, developed by Sanford Gordon and Bonnie McBride at NASA-LeRC (now NASA-GRC), is the industry standard code for calculation of chemical equilibrium (Refs. 11-12). The original purpose of the code was for the prediction of

chemical rocket performance. The code has gone through numerous major upgrades, enhancements, etc. each with a slightly different name. The code is very general and, as a consequence, comparatively slow in execution.

The thermodynamic database (Ref. 10) that cea2 uses is one of the major elements of the code package. The current version contains curve fits for something in excess of 2,000 species, fuels, oxidizers, and products including gaseous, liquid, and solid species. The temperature range of the curve fits varies from species to species. The curve fits for the air species and the products of dissociated and ionized air species all cover the range from 200 to 20,000 K. The curve fits for most other gaseous species cover the range from 200 to 6,000 K.

One of the interesting inconsistencies of the database is that while the curve fits for air species and for the products of the dissociation of air species cover the temperature range to 20,000 K, the database contains only the uni-positive ions of those species, e.g., O^+. The only multiple ionized species included in the database is Be^{++}. Multi-ionized air species, N^{++}, Ar^{++}, O^{++}, et seq., would be expected at low densities for temperatures well below 20,000 K. The reason for this inconsistency in the database is not known although its origin is a logical supposition.

Vestiges of its origin as a code for prediction of rocket performance are still present, particularly in the nomenclature used both within the code and in the description of the code. Another vestige of its origin is that the code, having been initially written when computers were slow and computer memory was expensive, is very tightly written. Several attempts by multiple users to extract a part of the code for use in other codes have produced only frustration. The alternative will be described below.

3.2.2.4 Thermodynamic Data

Part of the flexibility of cea2 is that it has multiple options for determining what species to consider in an equilibrium calculation. The species can be specified by the user or the code can scan its thermodynamic property database to determine which species to include in the equilibrium calculation based on the species present in the input. For instance, if O_2 was one of the input species, the code would include O_2, O_2^-, O, and O^+ as possible product species in the equilibrium. The practical benefit of this flexibility is that if the “missing” species can be included in the database and if the code is instructed to look for them, then they will be included in the equilibrium calculation. Thus the problem of including more highly ionized species in the equilibrium calculation can be reduced to a problem of formulating accurate curve fits in the cea2 format for the desired species.

The problem of forming the curve fits in the cea2 format is straightforward if the requisite data are available. However, such data for multi-ionized species are not readily available. NIST (Ref. 24) maintains a database of current, refereed atomic energy levels for all elements and all ionization levels where sufficient data exist. The NIST database includes the required air-derived species.

To understand how these energy level data are translated into the requisite thermodynamic parameters requires a good understanding of statistical thermodynamics and an introductory level understanding of quantum mechanics. There are some subtleties beyond that which must be considered also. Anyone wanting to delve into the topic further should start with Ref. 25 or Ref. 26.

McBride and Gordon (Ref. 27) have written and made available a Fortran-77 computer program which will produce thermodynamic property curve fits in the format required by the cea2 thermodynamic database. The current version of the code is pac99, which means the 1999 version of the code pac (propertied and coefficients). The latest documentation is Ref. 27 which is seven years older. The differences between the documentation and the distributed code are small, but important. A sufficient number of examples are provided with the code to allow a competent thermodynamicist to make proper use of the code.

One of the several options for input of thermodynamic information is in the form of the atomic energy levels as provided by NIST (Ref. 24). The format provided by NIST is not compatible with pac99, and there are subtle differences in nomenclature, but all the required information is available.

A Fortran-90 code was written to calculate the partition function and the thermodynamic properties using the NIST data as input. The initial intent of the code was to demonstrate to the author that the author understood the data sufficiently well to make proper use of the data. In addition, the code was ultimately useful for investigating the effects of different options including those in pac99 (Ref. 27).

Gordon and McBride (Ref. 26) list the options used to generate the curve fits in the cea2 thermodynamic database. Using these options and the data from NIST, the curve fit parameters and property values were calculated for O^+. Those property values were sufficiently close to the properties calculated from the cea2 thermodynamic database to verify that the approach was replicated.

3.2.2.5 Species and Checks

The basic composition of air was taken from the cea2 thermodynamics database. It consisted of the following mole fractions: N_2 0.78084; O_2 0.209476; Ar 0.00935; and CO_2 0.000319. The composition assumed in the AEDC Mollier 2008 EOS was similar to the above except that the 319 ppm of CO_2 was neglected. The 319 ppm of CO_2 was included here for maximum fidelity. This difference in composition produced slight differences in the properties, on the order of 10^{-4} or less relative difference in the properties, at standard sea-level conditions.

The species potentially present but not included in the thermodynamic database were N^{++}, N^{+++}, N^{++++}, et seq., O^{++}, O^{+++}, O^{++++}, et seq. Ar^{++},

Ar^{+++}, Ar^{++++}, et seq., and C^{++}, C^{+++}, C^{++++}, et seq. Significant effort is required to prepare each new species for inclusion in the database. By comparison, very little effort is required to include the species in the database, so the necessity of each added species was checked as it was added.

The most severe test, the condition that would produce the largest concentration of the most highly ionized species within the envelope of the EOS, is the highest temperature combined with the lowest density. This was a temperature of 20,000 K and a density of 10^{-8} kg/m^3 in the present case. The criterion chosen to terminate the addition of more highly ionized species was that the last species added occur in a concentration of at least two orders of magnitude less than the concentration of the last previously added ion of the same atom. For instance, if the concentration of Ar^{++++} was less than 1% of the concentration of Ar^{+++} at the worst-case condition, then one more Ar ion than necessary had been added, and no more were needed. This is a very conservative criterion, which is appropriate for this effort.

3.2.2.5 Application

The criteria for accuracy of the EOS was based on the calculated pressure, calculated enthalpy, and calculated entropy, not on the composition. For this reason, a four-component model of air is adequate. Trace species, no matter how highly ionized, do not make a significant contribution to the pressure, enthalpy, or entropy. Tighter constraints on property values would justify a more complicated model.

The equilibrium composition was monitored during the species addition phase. Only one unexpected result was observed (orders of magnitude more Ar^{++++} than all other Ar combined), and that result was traced to an anomaly in the pac99 code. Correcting the effect of the anomaly eliminated the unexpected result. This is a check only and depends on the judgment of the observer. That said, it is still encouraging.

The main program of cea2 was rewritten as a subroutine which could be called from a special purpose code. The code calculated the properties using the locally developed EOS and cea2, with proper accounting for the difference in reference state of the two. From that point, the procedure was similar to that used for the high-density effects. The deviation of the two predictions was monotone in density in the range of interest at any temperature, which simplified the programming and the interpretation of the final results.

One of the output options for cea2 includes a list of all species considered in the equilibrium calculation. The final condition, where the difference in property predictions matched the chosen level, was checked with that option selected to make sure that the code had considered all the possible species, that is, to make sure that the augmented thermodynamic database had not been corrupted.

The steps in the procedure are as follows: 1) Select a temperature 2) Select an initial density at that temperature where multiply ionized species are not expected 3) Calculate the composition and the properties at that point 4) Decrease the density, holding the temperature constant, and repeat the calculation 5) Continue the density decrement until the minimum density, 10^{-8} kg/m^3, is reached 6) Select the two densities which bracket the desired level of difference 7) Iterate, using a finite difference Newton iteration, to find the density which produces the desired level of difference 8) Increment the temperature and repeat the series of steps to find the density which produces the desired level of disagreement 9) Continue incrementing the temperature until the loci of points which defines the differences in the three properties is determined.

3.2.2.5.1 Initial Results

The observed property differences are shown in the following figures as a function of density for four fixed temperatures. The first temperature is 2,000 K, which was chosen as the minimum temperature because the dissociation would be negligible at that temperature. Nothing of significance was expected and nothing was found.

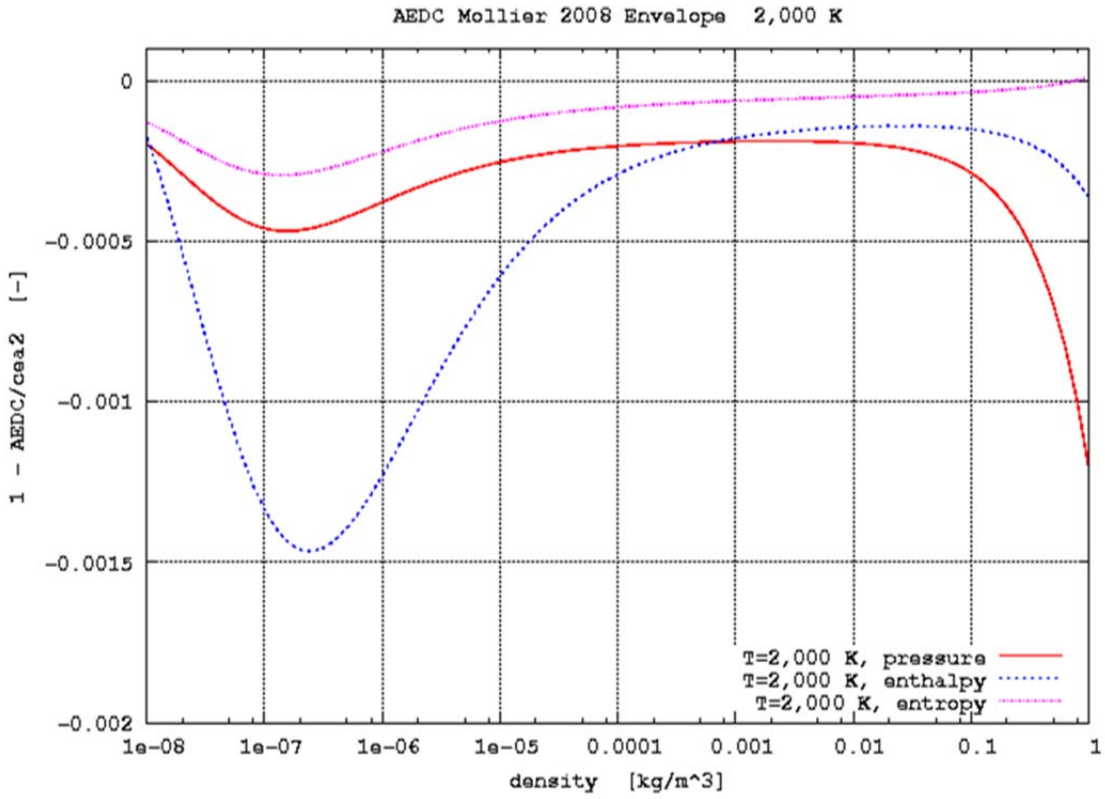

a. As a Function of Density for a Temperature of 2,000 K

Figure 23. Relative Differences in Pressure, Enthalpy, and Entropy

The relative differences shown in Fig. 23a are all negative and are all less than $1.5*10^{-4}$. The differences are primarily the effect of the slight difference in the assumed compositions for the "air."

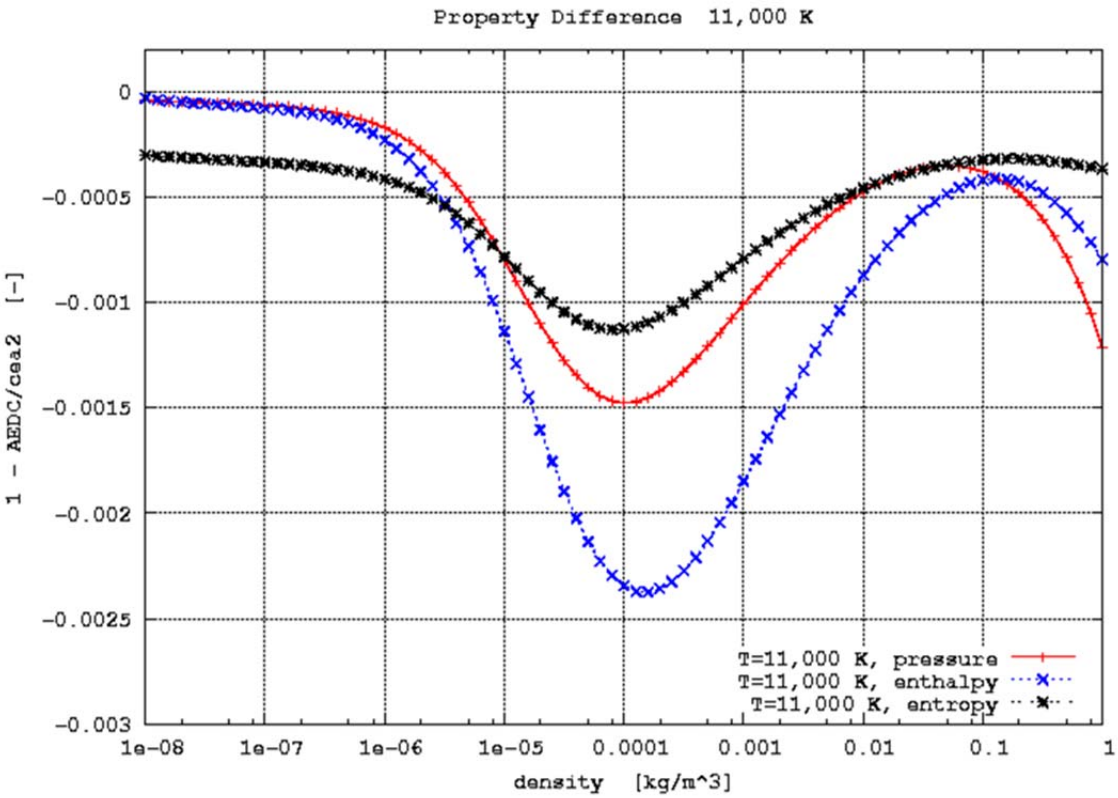

b. As a Function of Density for a Temperature of 11,000 K

Figure 23. Continued

The relative differences in Fig. 23b are all negative and are all less than $2.5*10^{-4}$. The differences are the effect of the slight difference in the assumed compositions for the "air." The temperature was selected because it is just below the temperature where the differences begin to grow rapidly.

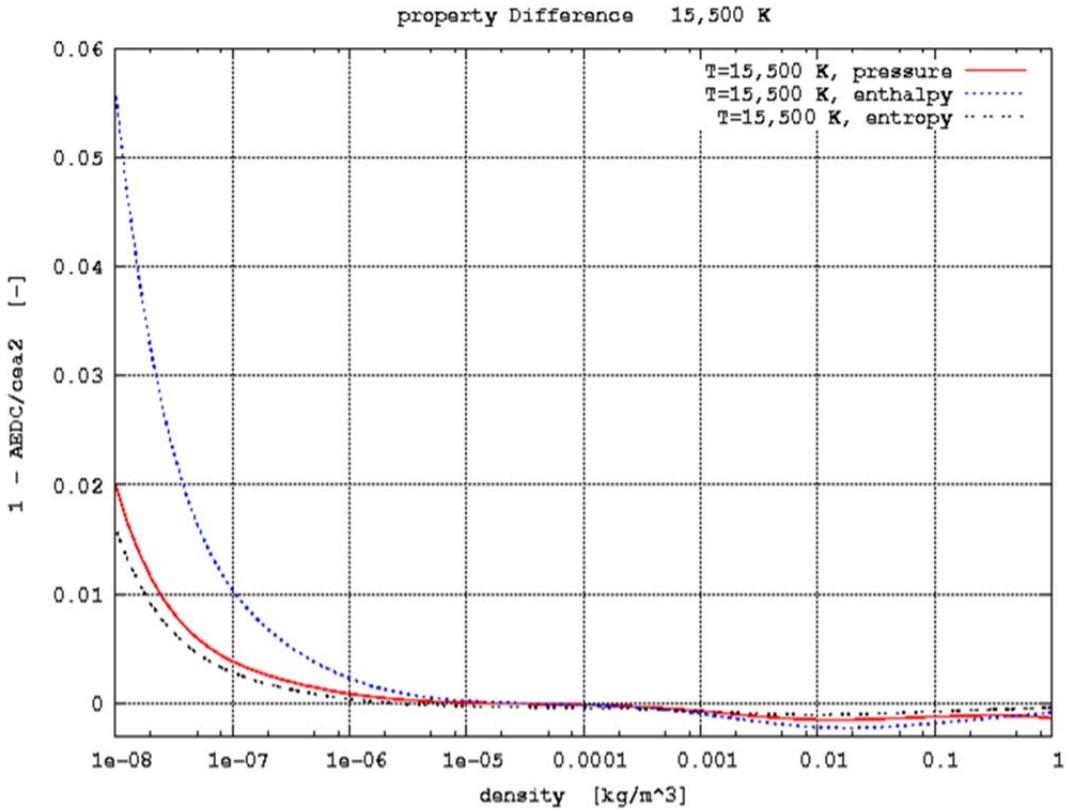

c. As a Function of Density for a Temperature of 15,500 K

Figure 23. Continued

The relative differences in Fig. 23c are all initially negative but then become positive, reaching magnitudes of 1.5, 2, and 5.5% for entropy, pressure, and enthalpy, respectively. The increased differences are the effect of the small concentrations of multi-ionized species from the dissociation of the air. The temperature was selected because it is representative of all temperatures where dissociation has an effect.

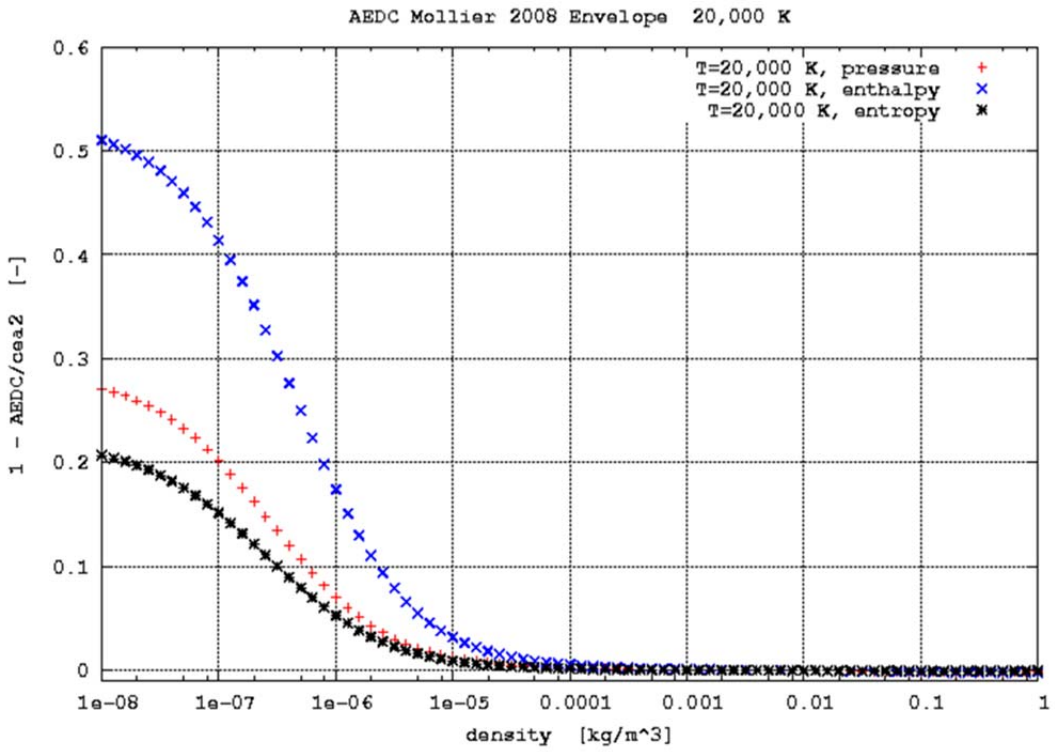

d. As a Function of Density for a Temperature of 20,000 K

Figure 23. Concluded

The relative differences are all initially negative but then become positive, reaching magnitudes of 20, 27, and 51% for entropy, pressure, and enthalpy. The increased differences are the effect of the small concentrations of multi-ionized species of the dissociation of the air. The temperature was selected because it is the maximum temperature of the EOS. The conditions at the left edge of the figure represent the most severe conditions in terms of dissociation and ionization.

The final figure in this group is a composite of the previous three.

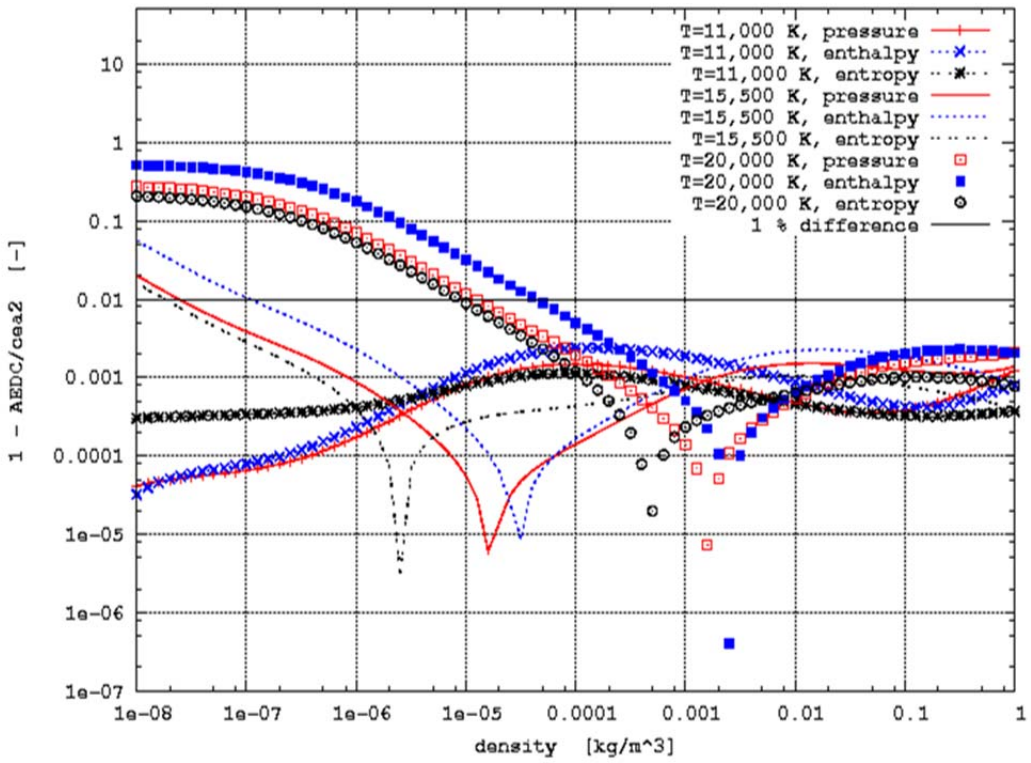

Figure 24. Relative Differences in Pressure, Enthalpy, and Entropy as a Function of Density for Temperatures of 11,000, 15,500, and 20,000 K

The relative differences in pressure, enthalpy, and entropy for constant temperatures of 11,000, 15,500, and 20,000 K are shown in Fig. 24. The magnitudes of the differences are plotted on a log scale so that the details of all three temperatures can be seen. The symbols used in the preceding three figures are carried over for clarity. The 1% difference line is also shown. The figure shows that all three parameters reach the 1% difference line within a fairly narrow range of density, approximately one order of magnitude, for the two temperatures where the difference reaches 1%. The figure also suggests that the differences are a strong function of temperature.

3.2.2.5.2 Molecular Weight

The property differences will arise as a result of the more highly ionized atomic species present at equilibrium, but they are neglected in the AEDC Mollier 2008 EOS.

The molecular weight is a sensitive indicator of the increased ionization, hence the difference in composition, e.g., Ar^{+} -> Ar^{++} + e^{-}, increases the number of moles, but does not change the mass, thus decreasing the molecular weight. The difference in molecular weight, AEDC Mollier 2008 – cea2, is shown in Fig. 25 as a function of temperature and mass density.

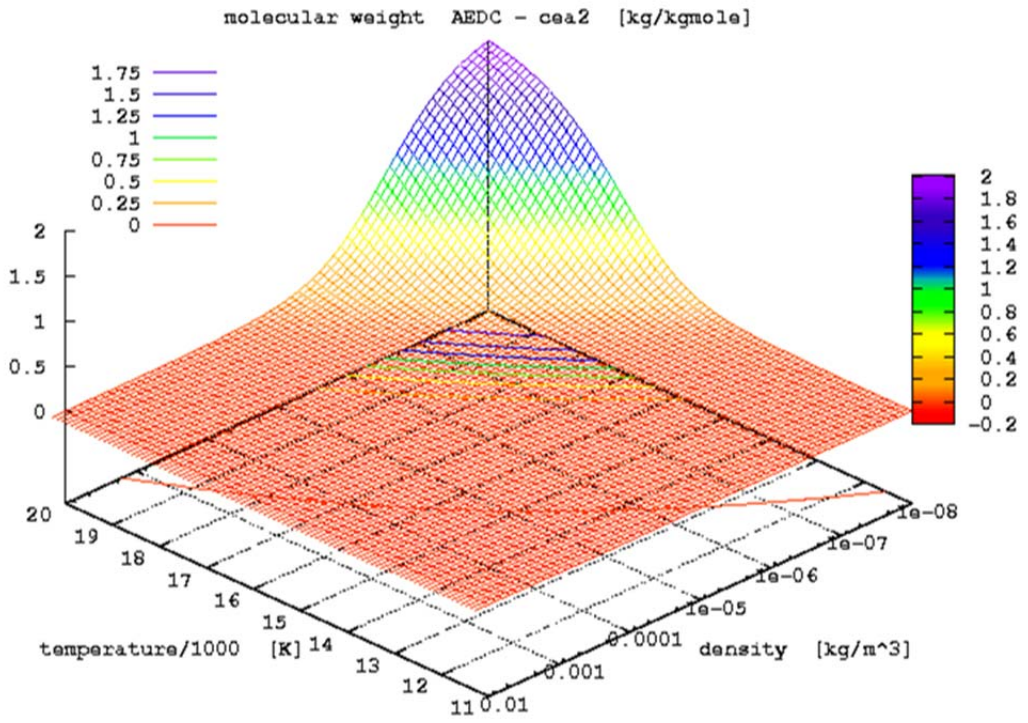

Figure 25. Difference in Predicted Molecular Weight as a Function of Temperature and Mass Density on Expanded Scale

The small, functionally negligible difference over most of the envelope is a result of the different basic compositions assumed for the two calculations, the 319 ppm of CO_2. The difference, never greater than two kg/kgmole, is smoothly varying as a function of temperature and density. Only the region where the difference is non-negligible is shown in Fig. 25.

The differences show the expected trends.

The differences in calculated properties are produced by the differences in composition. The extent to which the difference in molecular weight correlates to the relative difference in properties is shown in Fig. 26.

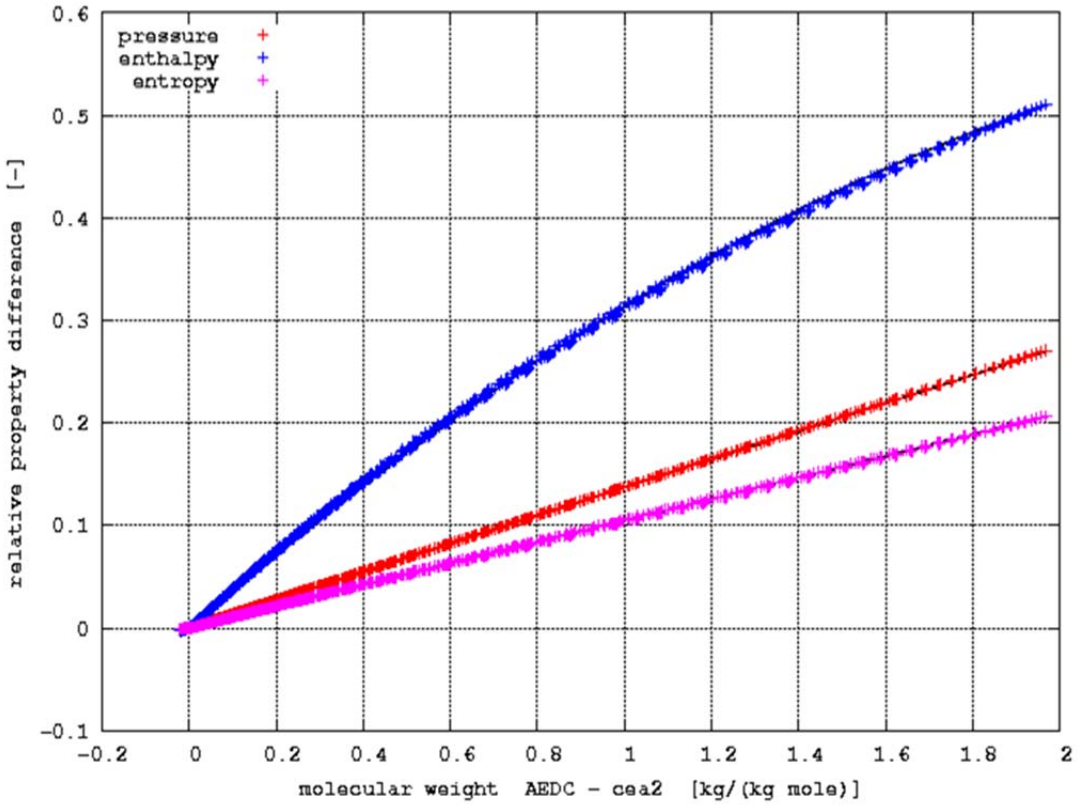

a. As a Function of Difference in Molecular Weight

Figure 26. Difference in Predicted Properties

Barely visible behind each set of points is a line drawn from an analytic expression representing the difference, a crude curve fit. The expressions are linear in the case of pressure and entropy and quadratic in the case of enthalpy. These simple relationships may seem like a useful shortcut in calculating the limits of applicability of the AEDC Mollier 2008 EOS. However, the difference in molecular weight can only be calculated from the equilibrium compositions, and the properties are defined by the compositions, so there is no net simplification. In short, once you have all you need to calculate the result, you can calculate it two ways and get equivalent results. The smooth, well-behaved variations are an indication that the code is internally consistent.

The region of interest here, relative differences on the order of 1%, is shown in more detail in Fig. 26b.

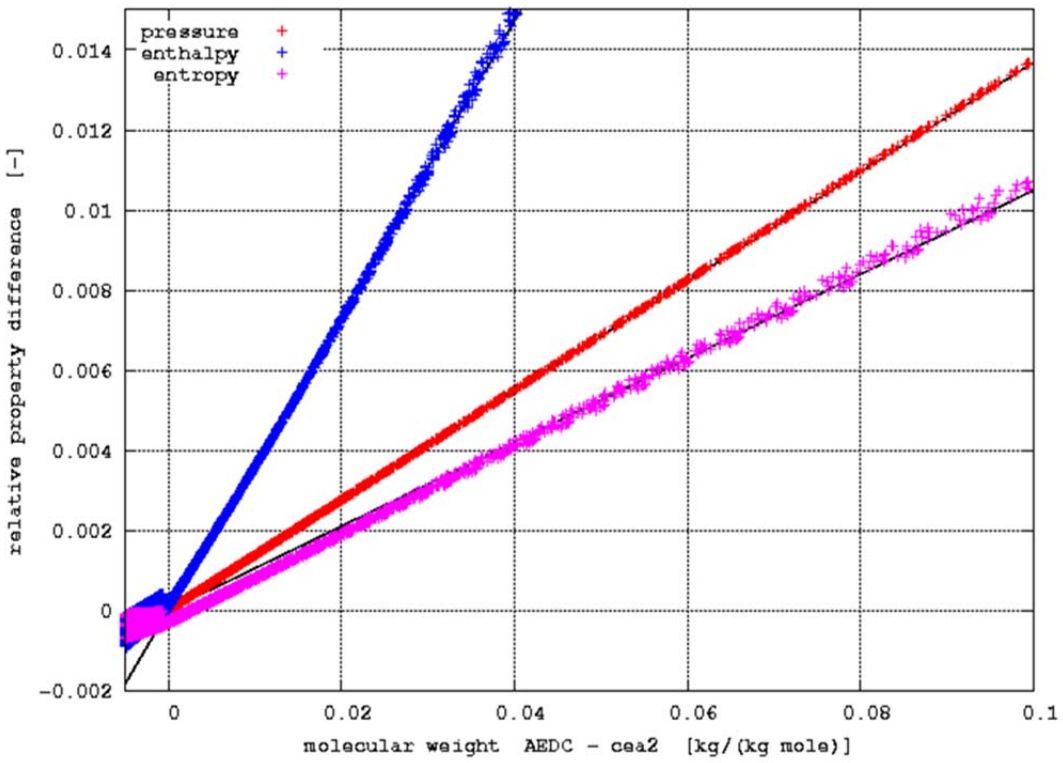

b. As a Function of Difference in Molecular Weight on an Expanded Scale

Figure 26. Concluded

The background lines are more obvious in Fig. 26b. Also more obvious is the slight offset near zero which is a result of the slightly different assumed initial compositions. Over the range shown, all three functions appear linear.

3.2.2.6 Individual Property Differences

The differences in the calculated properties will be discussed in this section. The pressure, enthalpy, and entropy will be discussed separately.

The relative differences in the calculated pressure are shown in Fig. 27 as a function of temperature and density. Note the similarity to Fig. 25.

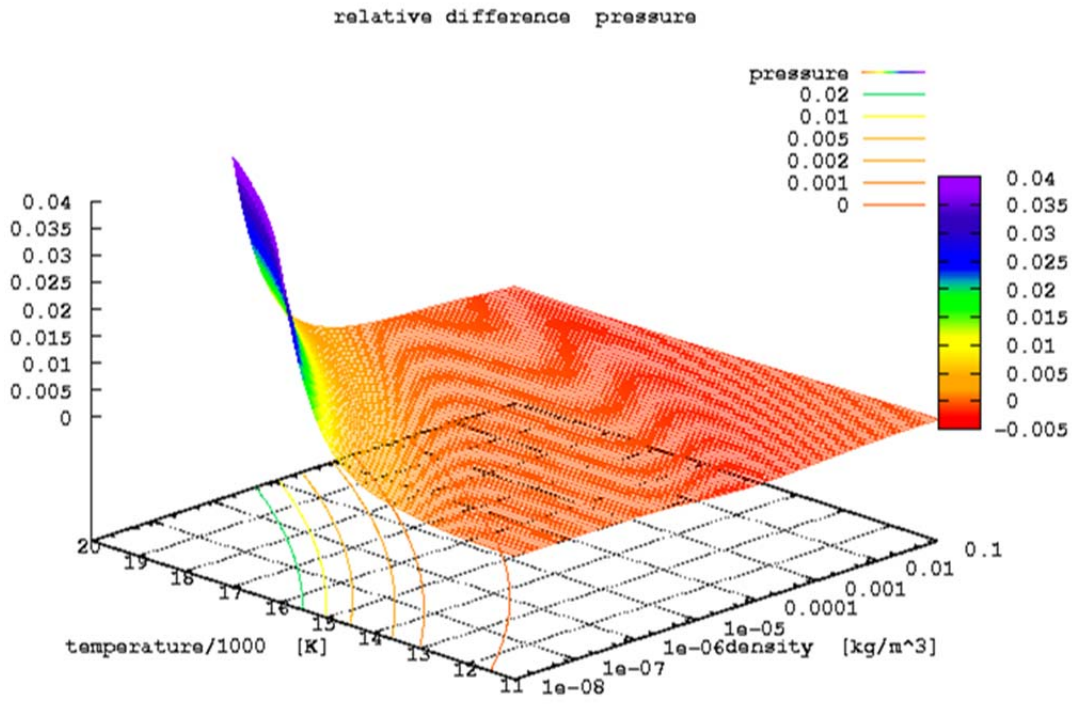

Figure 27. Relative Difference in Predicted Pressure as a Function of Temperature and Mass Density on an Expanded Scale

The plot is terminated at 4% difference so that detail in the range of interest, ~1%, is observable. This also emphasizes how rapidly the pressures diverge once the divergence begins. The contour lines on the base of the plot correspond to relative differences of 0, 0.001, 0.002, 0.05, 0.01, and 0.02. The close spacing of the last four also indicate the rapid rate of divergence.

The relative differences in the calculated enthalpies are shown in Fig. 28 as a function of temperature and density. Note the similarity to Fig. 27.

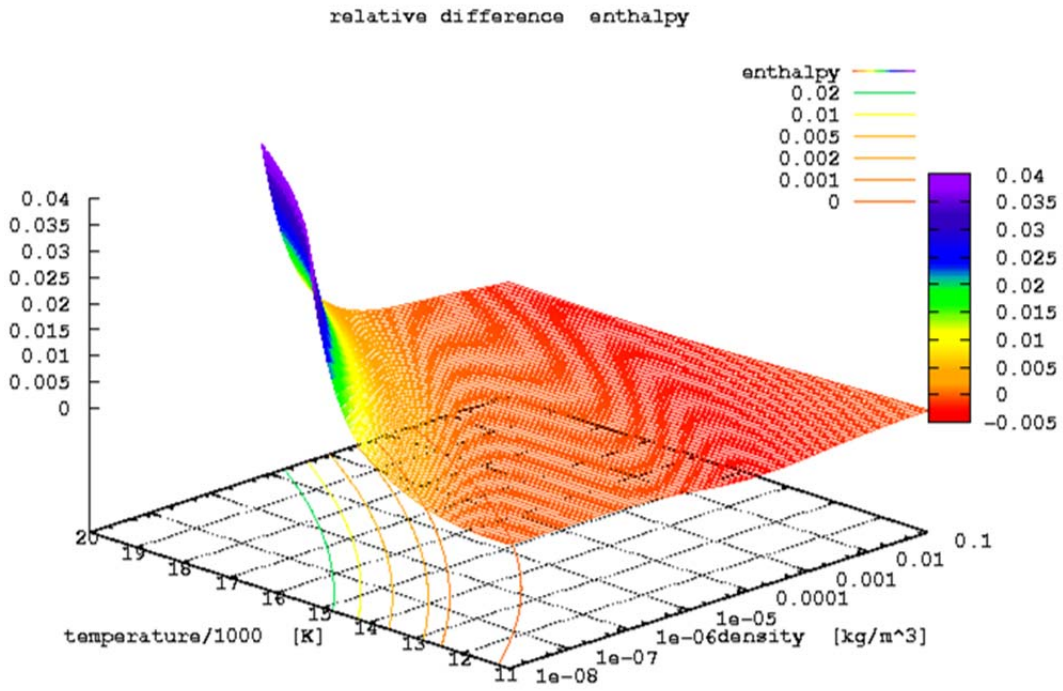

Figure 28. Relative Difference in Predicted Enthalpy as a Function of Temperature and Mass Density on an Expanded Scale

The plot is again terminated at 4% difference so that detail in the range of interest, ~1%, is observable. The various levels of disagreement occur at lower levels of temperature and density, compared to pressure. The shape of the surface and the shapes of the lines of constant disagreement are similar for the two properties. This similarity is suggested by Fig. 24.

The relative differences in the calculated entropy are shown in Fig. 29 as a function of temperature and density. Note the similarity to Figs. 27 and 28.

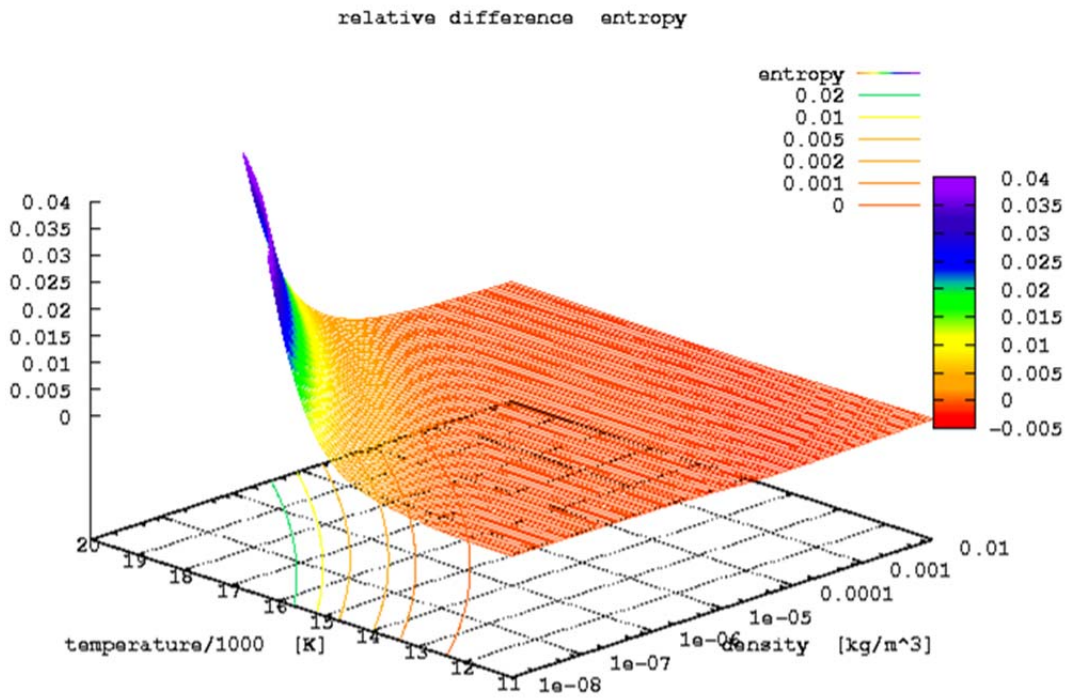

Figure 29. Relative Difference in Predicted Entropy as a Function of Temperature and Mass Density on an Expanded Scale

The various levels of disagreement in entropy occur at higher levels of temperature and density, compared to pressure and enthalpy. The shape of the surface and the shapes of the lines of constant disagreement are similar for all three properties. These similarities are suggested by Fig. 24.

3.2.2.7 Summary of Property Differences

The loci of points corresponding to two levels of disagreement for each of the three parameters is shown in Fig. 30 below in terms of the independent parameters of the EOS.

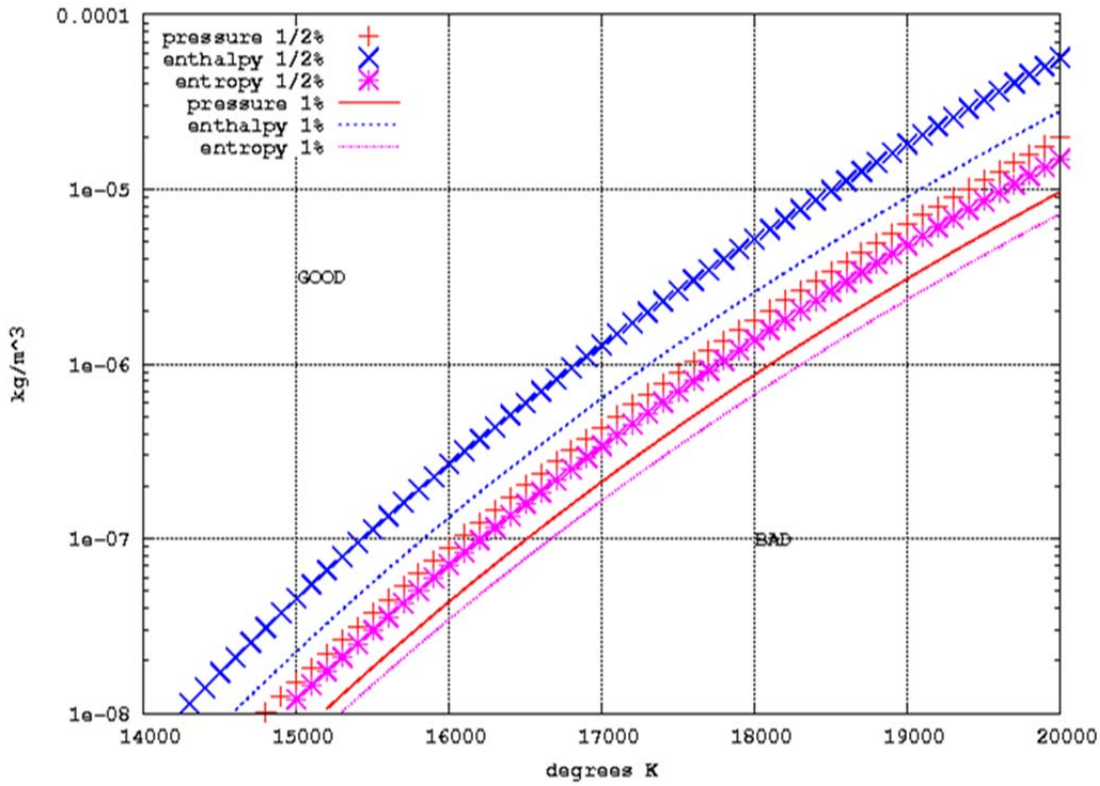

Figure 30. Temperature and Density Required to Produce 0.5% Relative Difference and 1.0% Relative Difference for Pressure, Enthalpy, and Entropy

The combinations of temperature and density which produce the specified level of disagreement between the AEDC Mollier 2008 EOS and cea2 are shown above. Enthalpy was the worst case for all nontrivial levels. The acceptable level of disagreement is problem dependent, but 0.5% seems to be a conservative but reasonable level in the absence of specific information.

A simple analytic equation that represents the worst-case line for the minimum density required to ensure less than 0.5% difference in all properties is

$$minimum\ density \;=\; 1.14 * 10^{-8} * e^{[(T-14300)/370]^{0.79}}\ kg/m^3\ .$$

This function is always greater than the worst-case line shown in Fig. 30. This limit will be incorporated into the AEDC Mollier 2008 EOS.

3.2.2.8 Impact on Mollier Chart

The Mollier chart as normally presented is shown in Fig. 7. The abscissa was truncated at s/R0 = 85 because the higher values corresponded to conditions not normally encountered in aerospace flight or ground testing. The conditions depicted in Fig. 30 correspond to s/R0 values of greater than 105. The 0.5% and 1.0% limit lines are shown in Mollier coordinates in Fig. 31.

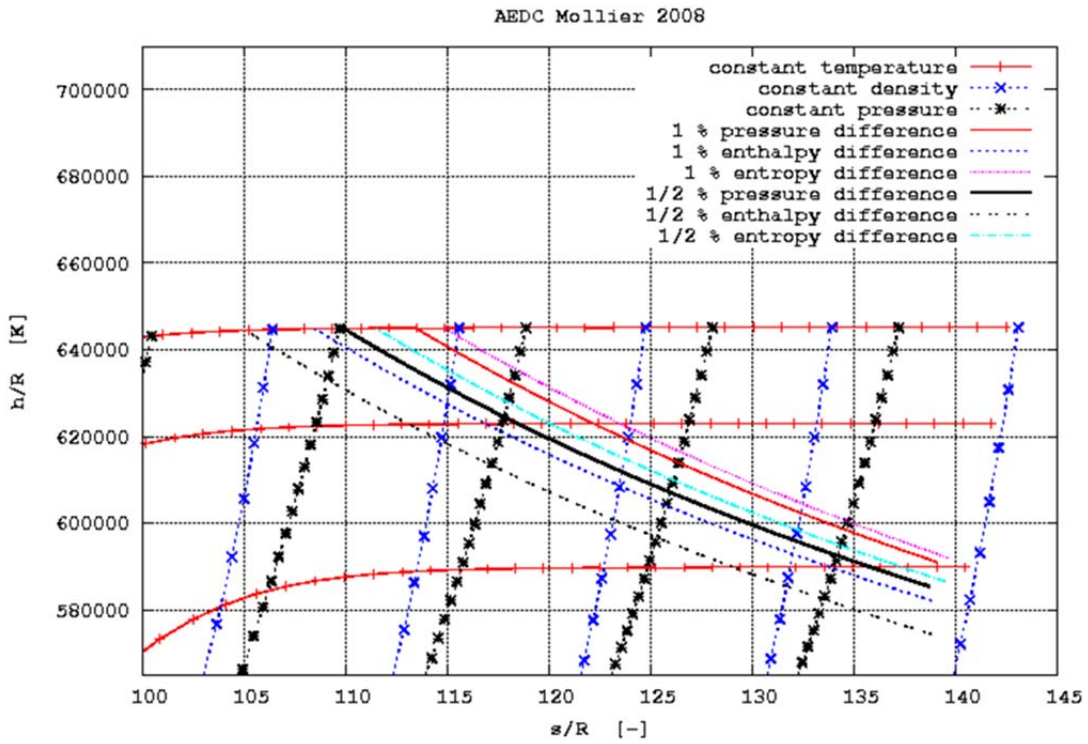

Figure 31. Limit to Produce 0.5% Relative Difference and 1.0% Relative Difference for Pressure, Enthalpy, and Entropy in Mollier Coordinates

The fact that the limits occur at such high values of s/R0 was initially a surprise, but it should not have been. Close examination of the figure shows that the limits correspond to the points where the constant temperature lines become essentially horizontal.

Along a constant temperature line, increase in entropy means decrease in density. Horizontal constant temperature lines in Mollier coordinates means that the partial derivative of enthalpy with respect to density is zero. Deviations from horizontal mean a nonzero derivative which is caused by high-density effects (low values of s/R0) or by changes in composition (high values of s/R0). Thus, at high values of s/R0, a horizontal constant temperature line means an unchanging composition. In this case, unchanging composition means that the limit of the equilibrium model has been reached. That limit is where the two models should begin to deviate.

The part of the Mollier chart to the right and above the limit lines shown in Fig. 31 is inaccurate due to the limitations of the thermodynamic model. This inaccuracy is of no practical consequence in this case because it occurs outside the range of interest.

3.2.2.9 Revised Mollier Chart

The portion of the Mollier chart shown in Fig. 31 is reproduced in Fig. 32 with the high-energy properties calculated by cea2 included. The constant temperatures used in the cea2 calculation are 12,000, 15,000, 18,000, and 20,000 K. The constant densities used in the cea2 calculation are 10^{-8} kg/m^3, 10^{-7} kg/m^3, 10^{-6} kg/m^3, 10^{-5} kg/m^3, and 10^{-4} kg/m^3. Note the log scale of the ordinate.

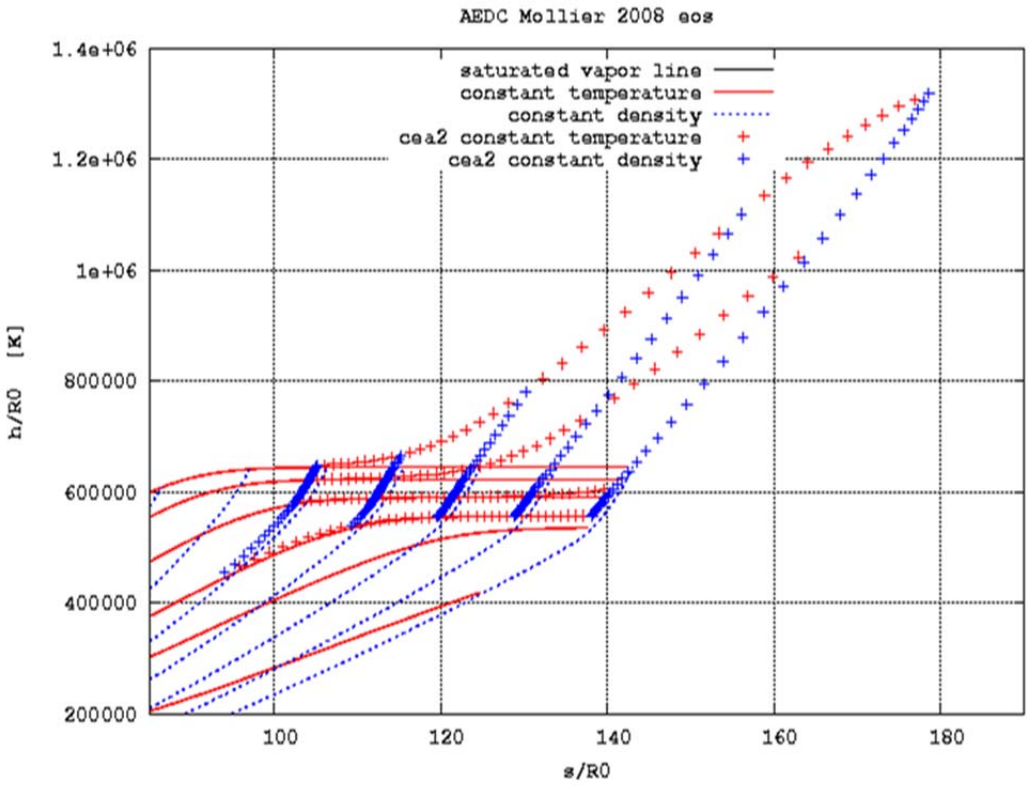

Figure 32. Highest Energy Region of Mollier Chart Including cea2 Calculations

The small offset in the abscissa is a result of the difference in entropy in that region and the small difference in assumed initial air composition. The entropy and enthalpy at 20,000 K and 10^{-8} kg/m^3 are about 1.26 times and 2.04 times the values calculated by the AEDC Mollier 2008 EOS, respectively. This figure demonstrates how rapidly the predictions of the two EOS diverge when the limit of the thermodynamic model of AEDC Mollier 2008 EOS is exceeded.

Note also that there is no horizontal region in the constant temperature lines for the cea2 calculations. This indicates that the thermodynamic model has not yet reached the limit of its applicability.

The full Mollier chart including the cea2 calculations is reproduced in Fig. 33.

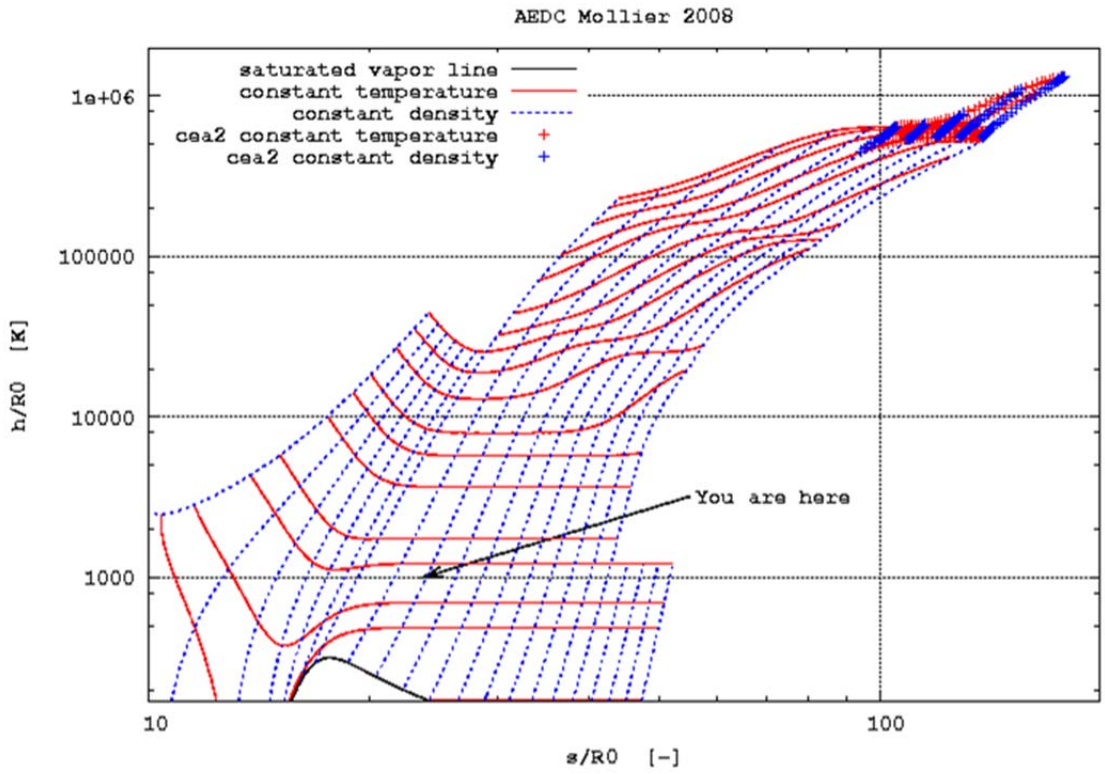

Figure 33. Mollier Chart Including CEA2 Calculations

Note that the abscissa scale is logarithmic in this case so that the details in the normal range can be seen. The divergence at high temperatures and low densities is dramatic even in the context of the entire Mollier chart.

3.2.2.10 Impact on Envelope of EOS

The final figure of the high-energy section is Fig. 34, the high-energy limits plotted on the envelope of the AEDC Mollier 2008 EOS.

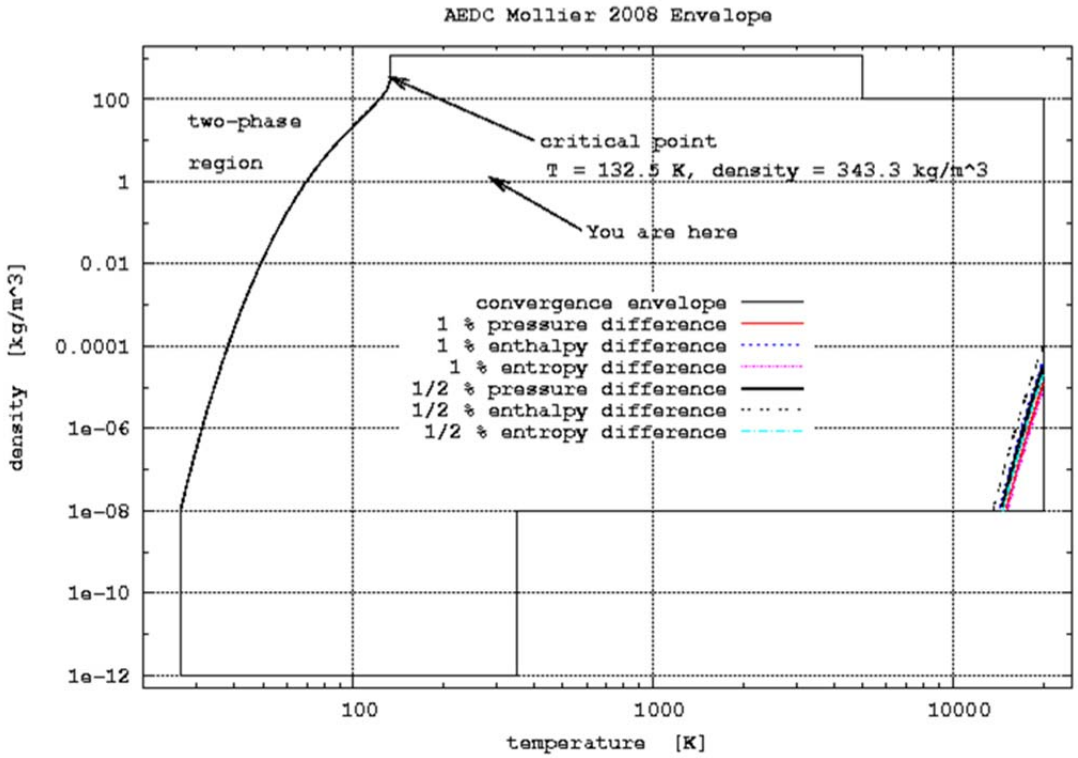

Figure 34. Envelope of the AEDC Mollier 2008 EOS with High-Energy Limits Indicated

The 0.5% difference limits and the 1.0% difference limits are shown on the envelope of the AEDC Mollier 2008 EOS. The minimal impact on the envelope is clearly shown.

3.3 CONSISTENCY

The limits of accuracy in the high-density limit and the limits of accuracy in the high-energy limit have been established as described above. The consistency of the AEDC Mollier 2008 EOS between those limits is the remaining task.

The fact that there is no standard for comparison of properties in the range where both high-density and high-energy effects are important is worth repeating.

3.3.1 Approach

The three properties of interest are pressure, enthalpy, and entropy. The independent parameters of the EOS are temperature and mass density. The consistency was checked by fixing the value of one input parameter and calculating the properties for a range of closely spaced values of the other input parameters. The resulting property values were then plotted as a series of lines. The lines were examined for any nonphysical behavior, slope discontinuities (kinks), discontinuities, line crossings, unexplained changes in slope, et al.

The property values are the parameters of interest but the plots of those values are not the most sensitive indicator of inconsistency. The 1st-order (point-to-point), finite-difference approximation to the first derivatives are more sensitive to some problems, notably function discontinuities or slope discontinuities. Those point-to-point divided differences, e.g., $\frac{(P_i - P_{i\text{-}1})}{(\rho_i - \rho_{i\text{-}1})}$, were plotted, and

again the plots were examined for nonphysical effects. Note that crossing of some of the point-to-point divided difference lines is expected in the cases of enthalpy and entropy.

3.3.2 Results

Individual lines were scrutinized. Only the summary plots are shown here, beginning with pressure as a function of density for a series of constant temperatures. This section by its nature is long and tedious. The tedium comes from the repeated demonstration of the absence of any problem.

3.3.2.1 Constant Temperature Results

The results for constant temperature, variable density will be presented first. The constant temperature lines span the envelope of the EOS. Temperatures which include the two-phase region are excluded. Results from the following temperatures are shown in Figs. 35 – 41. Constant temperatures (in degrees Kelvin) are 133; 140; 160; 180; 200; 220; 240; 260; 280; 300; 500, 1,000; 1,500; 2,000; 2,500; 3,000; 3,500; 4,000; 4,500; 5,000; 6,000; 8,000; 10,000; 12,000; 14,000; 16,000; 18,000; and 20,000.

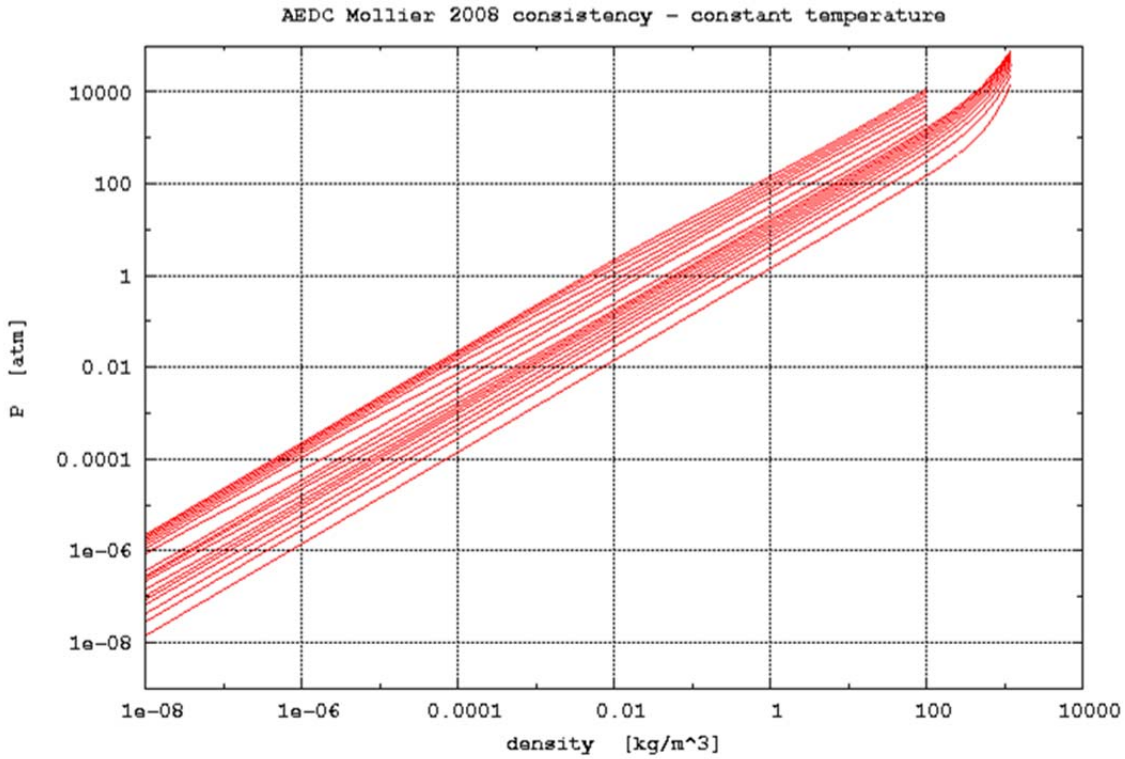

Figure 35. Pressure as a Function of Density for a Series of Constant Temperatures

The pressure as a function of density for a range of constant temperatures is shown in Fig. 35 above. The upturn in the lower lines at the right edge of the figure is the high-density effects. The “waves” in the upper lines at subatmospheric densities are the result of dissociation and ionization.

The “bunching” of the constant temperature lines for the upper temperature lines at the left (low-density) edge of the figure is consistent with the findings discussed in the preceding section. Succeeding figures show similar effects.

The point-to-point differences of the data in Fig. 35 are shown in Fig. 36.

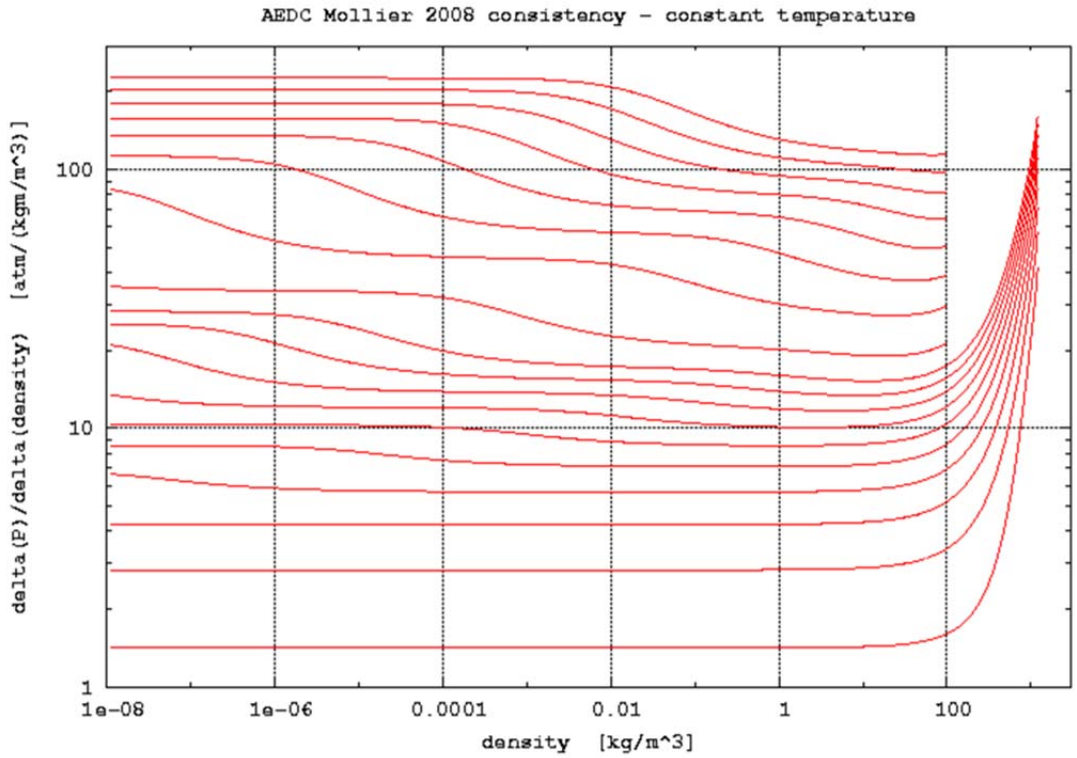

Figure 36. Point-to-Point Differences of Pressure as a Function of Density for a Series of Constant Temperatures

The point-to-point divided differences spread the constant temperature lines, making any anomalies easier to see. None were observed in this or the preceding figure.

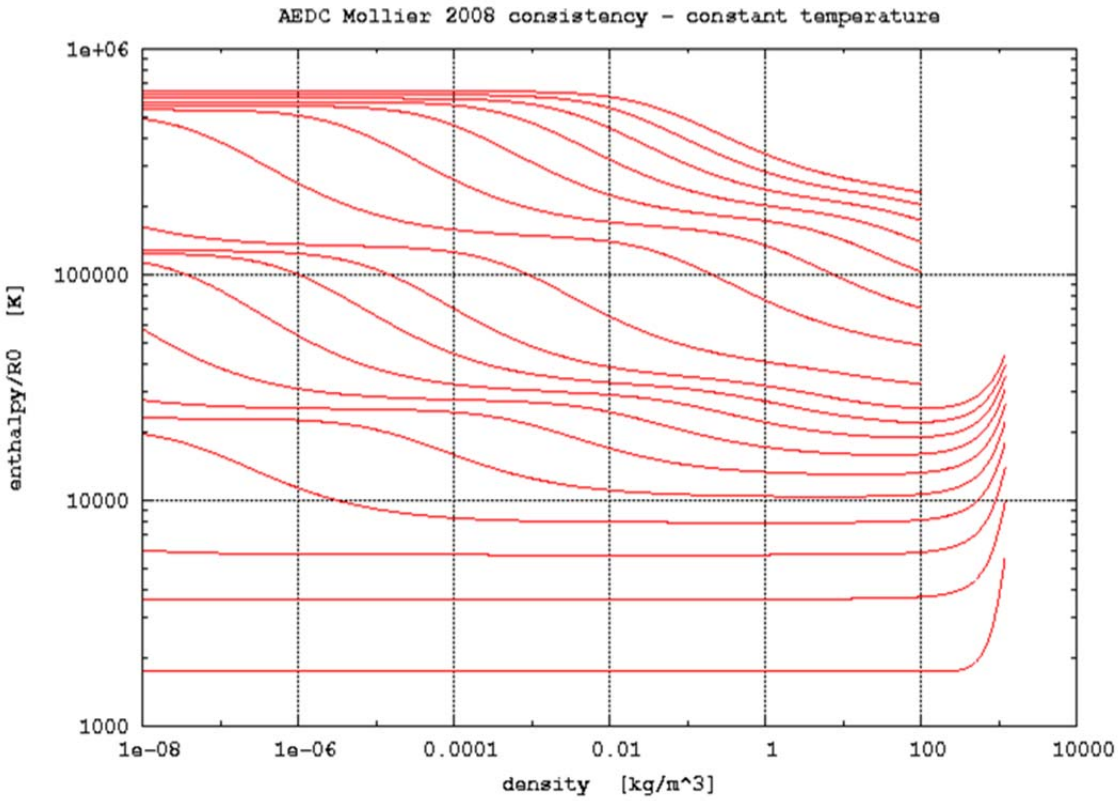

Figure 37. Enthalpy as a Function of Density for a Series of Constant Temperatures

The enthalpy as a function of density for a range of constant temperatures is shown in Fig. 37. Again, the upturn in the lower lines at the right edge of the figure is the high-density effects, and the “waves” in the lines at subatmospheric densities are the result of dissociation and ionization. In contrast to pressure, enthalpy is not a monotone function of density for constant temperatures. This makes the point-to-point divided difference plots much more interesting.

The point-to-point differences of the data in Fig. 37 are shown in Fig. 38.

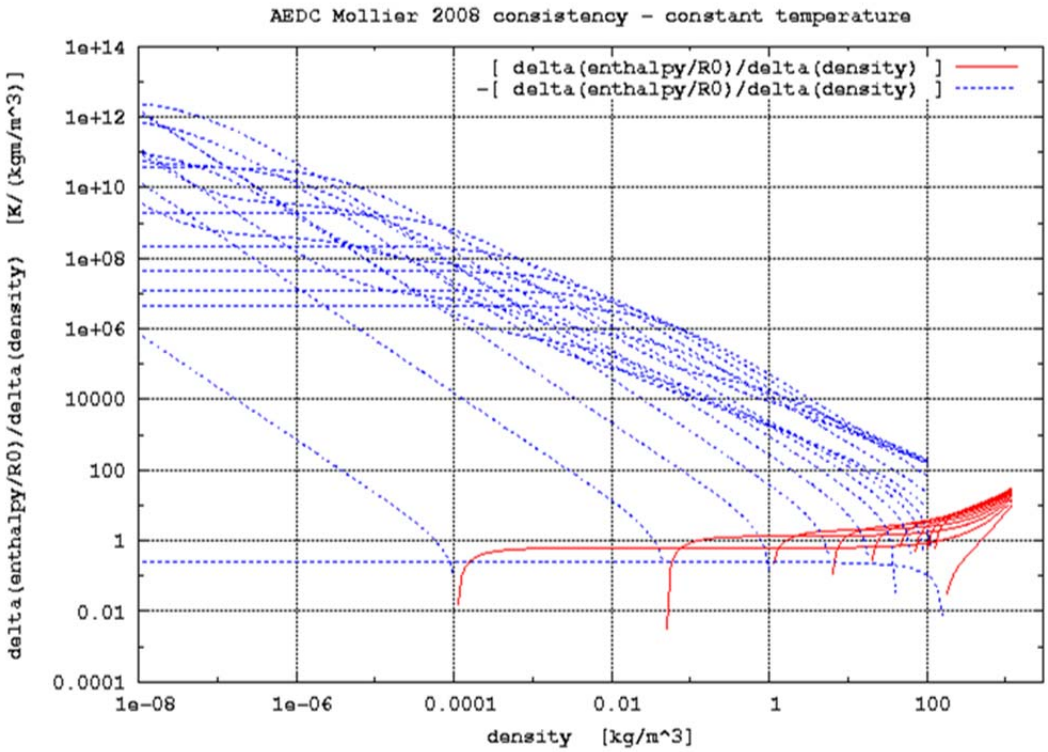

Figure 38. Point-to-Point Differences of Enthalpy as a Function of Density for a Series of Constant Temperatures

Figure 38 contains two plots, one of the function of interest and one of its negative. This is done because the magnitude of the function varies from zero to more than 10^{12}, requiring a logarithmic scale for resolution of the smaller values. Plotting functions which cross zero on a logarithmic scale creates some initially disquieting artifacts, to wit, the apparent cusps in the individual plots where one side of the cusp represents the function and the other side of the cusp represents the negative of the function. The cuspate behavior makes continuity in the region of the zero crossing impossible to verify.

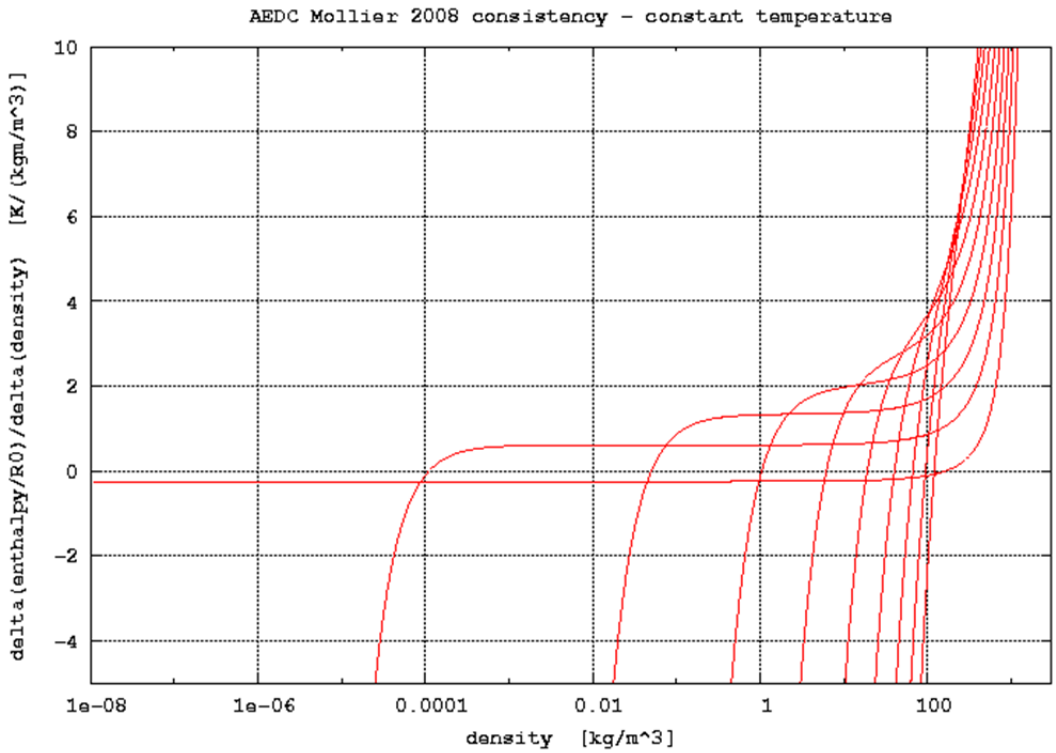

Figure 39. Point-to-Point Differences of Enthalpy as a Function of Density for the Temperatures which Produce a Zero Crossing

The 10 constant temperature lines from Fig. 38 which indicated zero crossings are replotted in Fig. 39 on a linear scale. The ordinate is restricted to the immediate vicinity of zero so that the continuity of the point-to-point differences can be verified.

No nonphysical behavior was observed in this or the preceding two figures.

The entropy as a function of density for a series of constant temperatures is shown in Fig. 40.

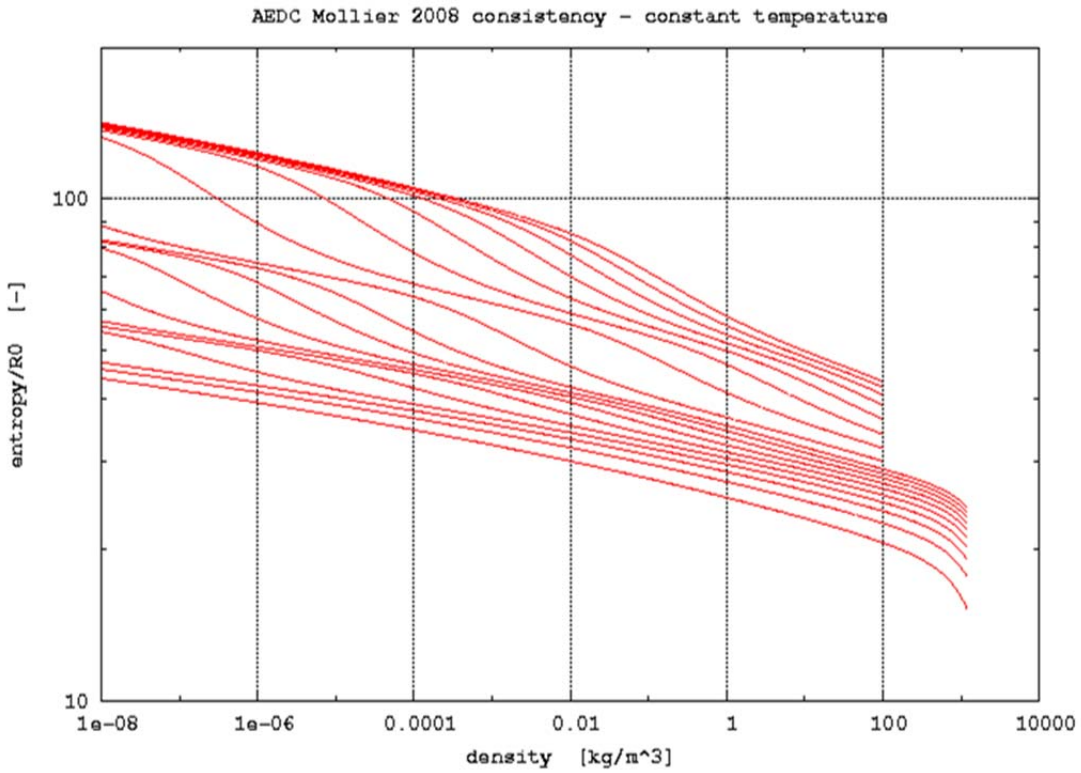

Figure 40. Entropy as a Function of Density for a Series of Constant Temperatures

The downturn in the lower constant temperature lines at the right side of the figure is a result of the high-density effects. The apparent waves in the higher constant temperature lines are the results of high-energy effects, first dissociation and then ionization. Both effects are anticipated.

The bunching of the six highest temperature lines in the upper left portion of the figure are a result of the limited ionization allowed in the thermodynamic model. This behavior is not physically realistic, but this limitation was addressed previously. Thus, this behavior is expected, given the constraints of the thermodynamic model, and is not indicative of a new or undocumented problem.

The point-to-point differences of entropy are shown in Fig. 41.

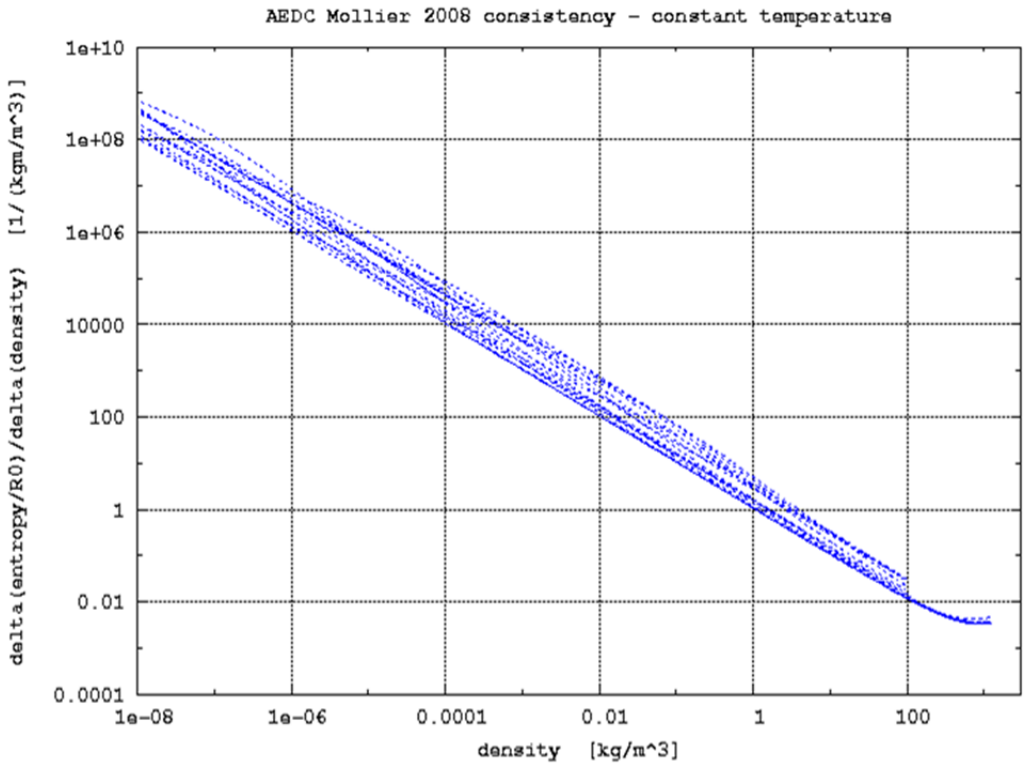

Figure 41. Point-to-Point Differences of Entropy as a Function of Density for a Series of Constant Temperatures

Note that unlike the enthalpy, the point-to-point divided differences for entropy are all negative. This is expected behavior. Note also that the crossing of the constant temperature lines in the point-to-point difference plot is expected behavior, again as a result of the different densities where dissociation and ionization occur at different temperatures.

To summarize of the consistency checks of properties as a function of density: no new anomalies were discovered as a result of examining the pressure, enthalpy, and entropy as a function of density for constant temperatures. The problems associated with the limits of the thermodynamic model (single ionization only) reappeared as they should.

3.3.2.2 Constant Density Results

The properties and their point-to-point variations as a function of temperature for a series of constant densities will be discussed next. The constant density lines span the envelope of the EOS, specifically from 10^{-8} kg/m^3 to 10^{+3} kg/m^3 in multiples of $10^{0.2}$ plus a final density of 1,220 kg/m^3.

The pressure as a function of temperature for a series of constant densities is shown in Fig. 42.

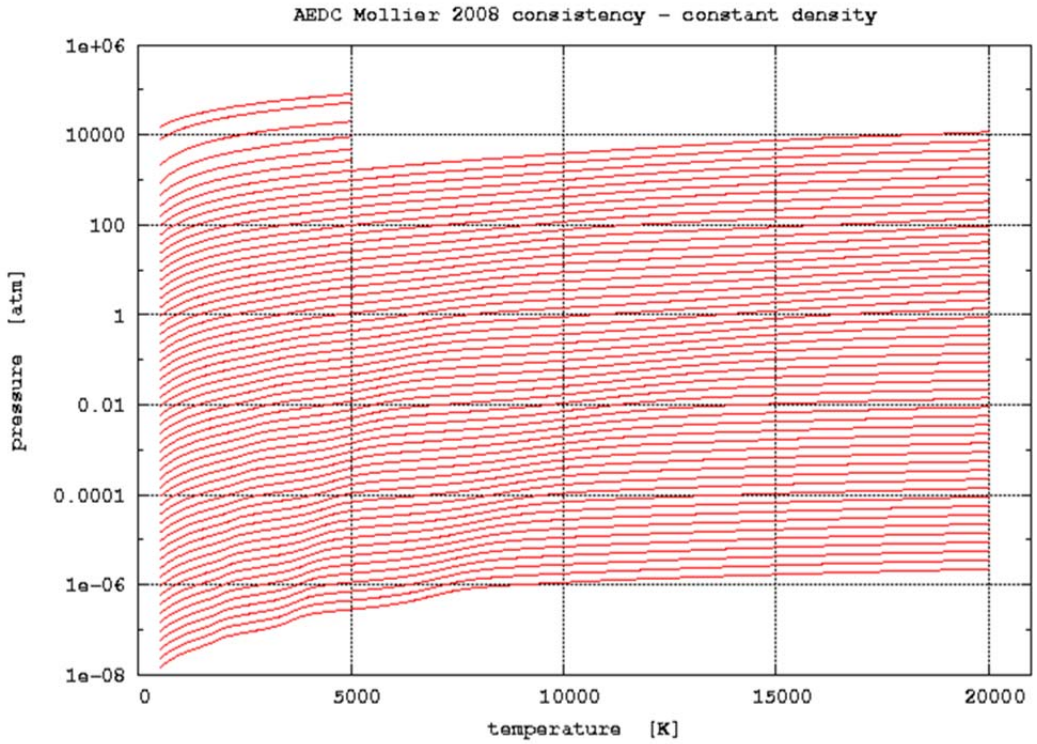

Figure 42. Pressure in Atmospheres as a Function of Temperature for a Series of Constant Densities

The pressure in atmospheres is shown as a function of temperature for a series of constant densities. All of the expected physical processes are shown in the individual and collective curves. The upper lines in the figure represent the higher densities, and the lower lines represent the lower densities in this and the next figure. The individual features will be discussed in terms of the point-to-point difference plots, shown in Fig. 43.

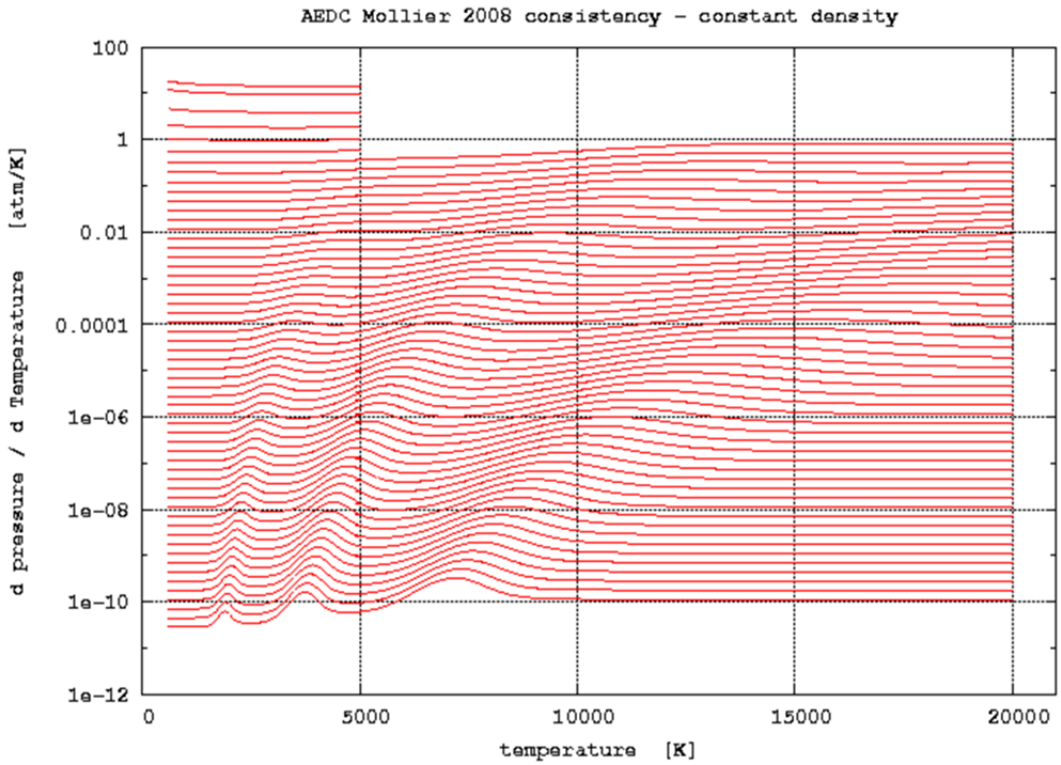

Figure 43. Point-to-Point Divided Differences in Pressure as a Function of Temperature for a Series of Constant Densities

Note the similarities between Figs. 42 and 43. This similarity is expected, with the oxygen dissociation, first of the maxima reading from left to right along each constant density line, the nitrogen dissociation, second of the maxima reading from left to right along each constant density line, and the ionization, last of the maxima reading from left to right along each constant density line. The variation along any one line and the variation from one line to another are as expected.

The enthalpy as a function of temperature for a series of constant densities is shown in Fig. 44.

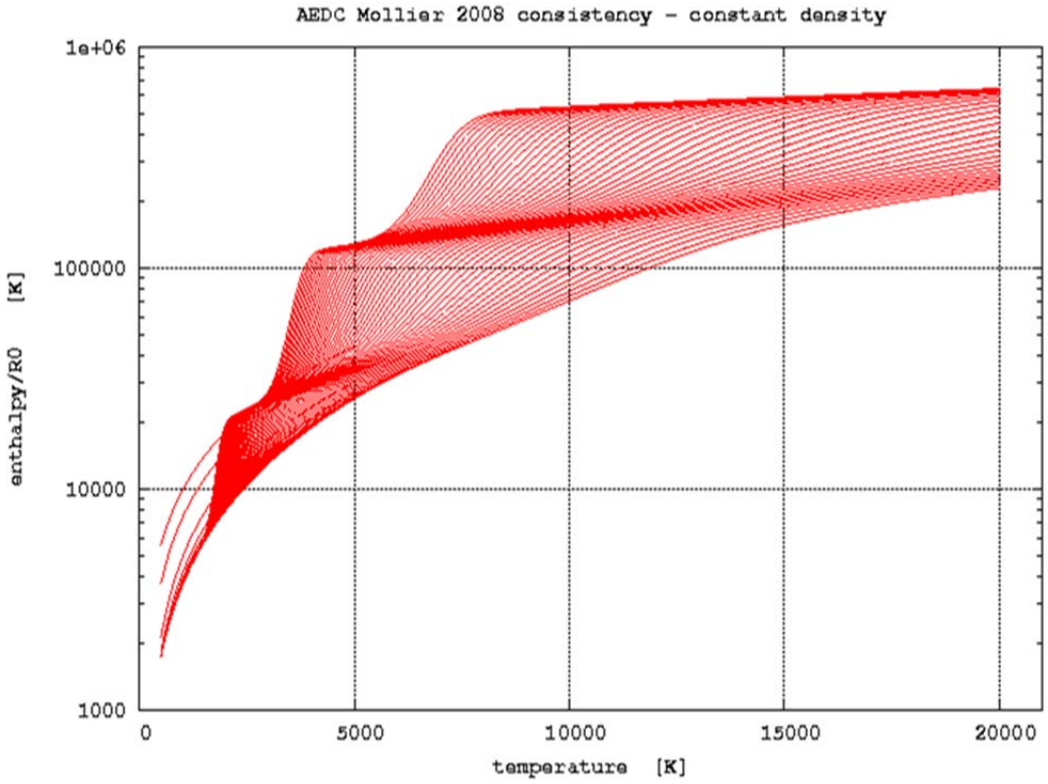

Figure 44. Enthalpy Divided by R0 as a Function of Temperature for a Series of Constant Densities

The enthalpy divided by R0 as a function of temperature for a series of constant densities is shown in Fig. 44. As above, the effects of all the expected physical processes appear in Fig. 44, and no unexpected effects appear. Also as above, the individual features will be discussed in terms of the point-to-point difference plots, shown in Fig. 45.

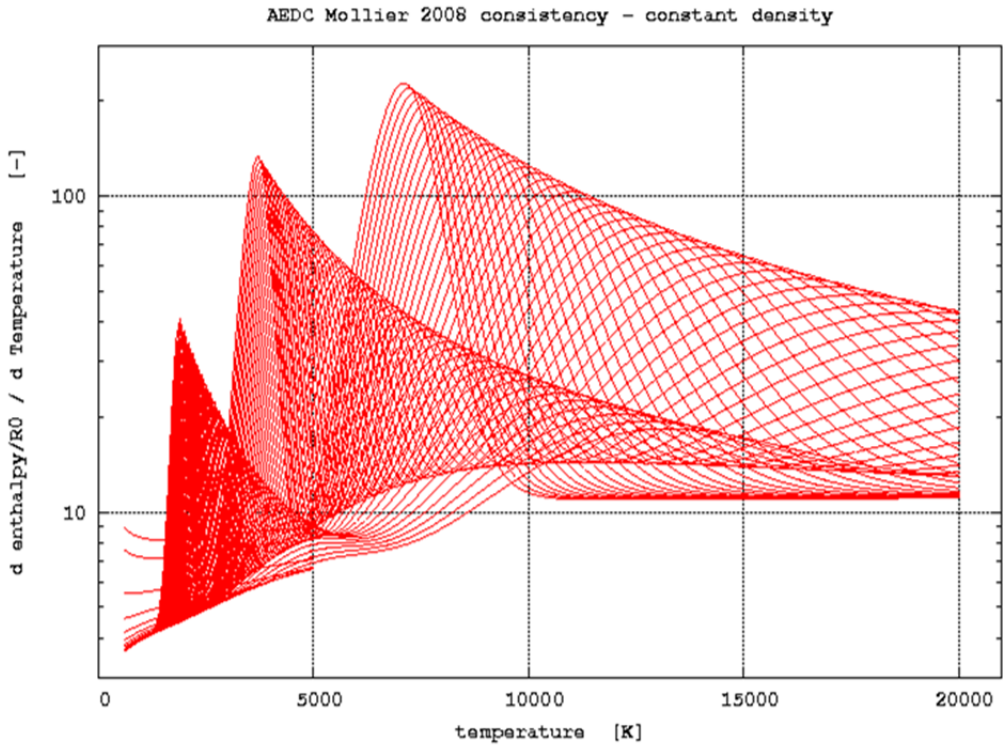

Figure 45. Point-to-Point Divided Differences in Enthalpy as a Function of Temperature for a Series of Constant Densities

The individual lines in Fig. 45 represent a 1st-order, forward, finite-difference approximation to the derivative $\left[\frac{\partial h}{\partial T}\right]_\rho$. Recall also that $c_p = \left[\frac{\partial h}{\partial T}\right]_\rho - \frac{\left[\frac{\partial h}{\partial \rho}\right]_T \left[\frac{\partial P}{\partial T}\right]_\rho}{\left[\frac{\partial P}{\partial \rho}\right]_T}$ thus the similarity of the plotted function to the isobaric specific heat is expected. The plotted function is functionally equal to the isobaric specific heat in the regions where $\left[\frac{\partial h}{\partial \rho}\right]_T = 0$, that is, no high-density effects and fixed composition.[12] The regions of O_2 dissociation, N_2 dissociation, and ionization are clearly shown in Fig. 45.

The apparent lack of smooth variation evident in the first two peaks is an artifact of the point-to-point plotting of the successive temperature points. Increasing the resolution, decreasing the increment in temperature, and expanding the plots to show only the local region (not shown here) made the variation in the individual curves smooth.

No inconsistencies in enthalpy were observed.

Entropy as a function temperature for a series of constant densities will be considered next.

[12] A similar argument could be made in terms of isochoric specific heat.

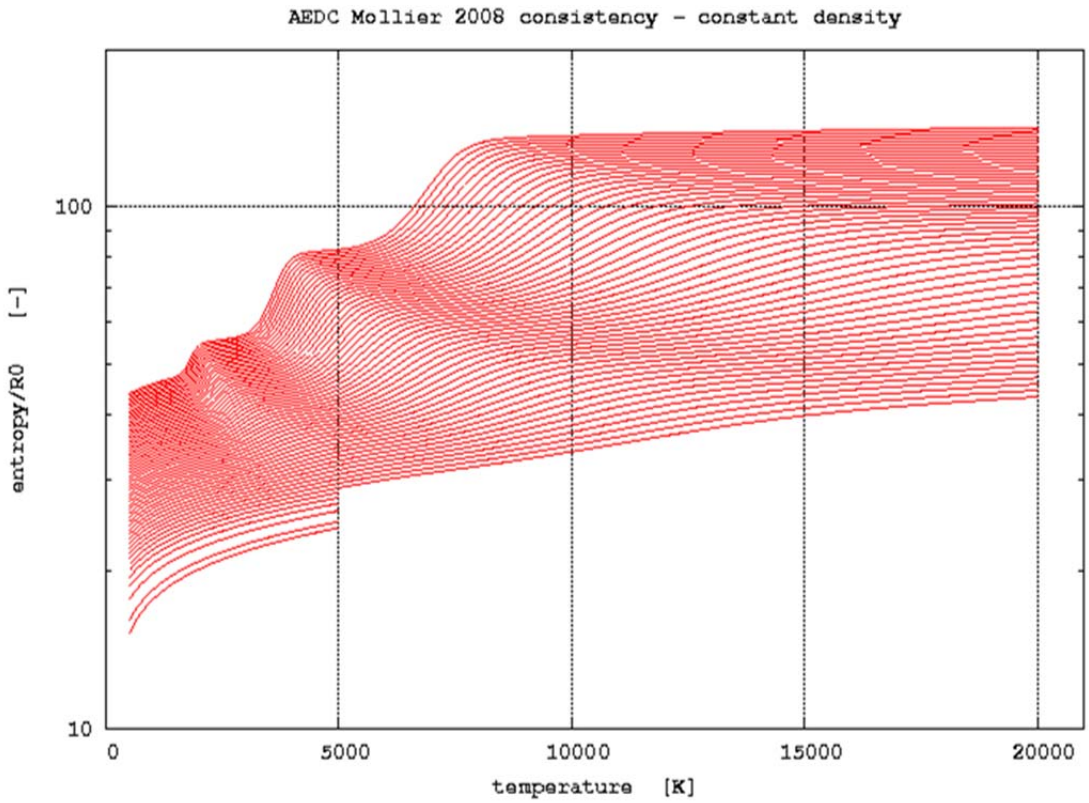

Figure 46. Entropy Divided by R0 as a Function of Temperature for a Series of Constant Densities

The entropy as a function of temperature for a series of constant densities is shown in Fig. 46. Nothing unexpected is shown in Fig. 46.

The point-to-point divided entropy differences are shown in Fig. 47.

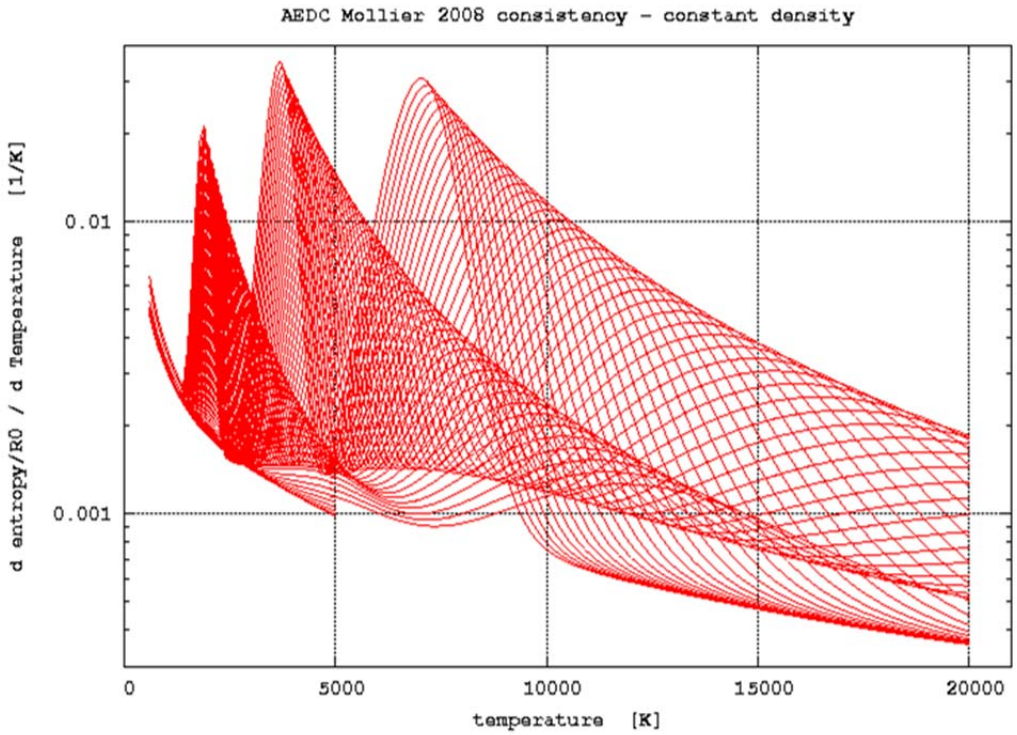

Figure 47. Point-to-Point Divided Differences in Entropy as a Function of Temperature for a Series of Constant Densities

The individual lines in Fig. 47 represent a 1st-order, forward, finite-difference approximation to the derivative $\left[\frac{\partial s/R0}{\partial T}\right]_{\rho}$. Recall that this derivative, in the region where high-density effects are negligible, is $\frac{c_v}{R0\ T}$. As above, the effects of the physical processes are clearly show. No unexpected features were observed.

3.3.2.3 Indirect Evidence of Consistency

The primary calculated thermodynamic properties are pressure, enthalpy, and entropy. The independent parameters were temperature and mass density. Temperature and mass density are not always the most convenient pair of properties. Auxiliary routines were written to calculate temperature and density (hence, all properties) given various pair combinations of temperature, mass density, pressure, internal energy, enthalpy, and entropy. A total of nine inverse combinations, (*T,P*), (*e,ρ*), (*h,s*), (*s,T*), (*s,P*), (*s,ρ*), (*h,P*), (*h,ρ*), and (*P,ρ*), were programmed.

Temperature-density pairs within the envelope of the AEDC Mollier 2008 EOS were selected at random. The remaining properties were calculated based on the temperature and density.

Each of the possible pairs were used to calculate temperature and density. The inverses, i.e., calculating temperature and density from another pair, are iterative and generally involve either a finite-difference Newton iteration or a secant iteration. Either of those iteration methods would fail to converge in the vicinity of a discontinuity in the property and may fail in the vicinity of a kink.

Several hundred million inverse calculations were made in the course of developing and checking the inverses. Some cases of nonconvergence were observed, but none could be attributed to discontinuous functional values. This suggests that the property values are smoothly varying and consistent.

3.3.3 Summary of Consistency Checks

The three properties, pressure, enthalpy, and entropy, were calculated and plotted as a function of a single parameter by fixing the value of the second parameters. The resulting plots showed no unexpected behavior.

The 1st-order, forward, finite-difference approximation to the derivative of the properties with respect to the varying parameter was calculated and plotted. The divided differences are more sensitive to small-scale irregularities. Again, nothing unexpected was observed in the plots.

No cases of a nonconvergent inverse calculation were observed which could be attributed to irregularities in the functional values.

Not every point was checked, nor could every point be checked. However, these three tests strongly suggest that the functional values calculated by the AEDC Mollier 2008 EOS are smoothly varying and consistent.

4.0 SUMMARY, CONCLUSIONS, AND RECOMMENDATIONS

4.1 SUMMARY

A computer-based EOS has been developed for air that provides reliable property values for all cases of interest in ground testing at AEDC and for flight conditions to conditions beyond lunar reentry speeds. The range of applicability is slightly greater than that of the venerable “AEDC Mollier Diagram for Equilibrium Air,” c. 1967.

The independent parameters of the EOS are temperature and mass density. The approach assumes that high-density and high-energy contributions to the basic thermodynamic properties can be added linearly to the thermally perfect, fixed-composition air properties.

The calculated property values have been compared to industry standard values for the limiting cases where only one effect, high-density or high-energy, is important. The comparisons indicate that the property values are accurate in the limits. The parameters in the limits of high-density and high-energy where the differences from the standards become significant have been determined.

The property values are continuous, consistent, and smoothly varying between the limits. The uncertainty in the numerical values is greatest in the elevated-density, high-energy portion of the range where the interaction is potentially the greatest. This region is of little immediate importance because these conditions are very difficult to achieve.

The transport property values are adequate but are the least well-developed part of the EOS.

The utility of the EOS is not the specific accuracy of the property values at any one point; rather, it is the overall accuracy and consistency over the entire range of the EOS.

4.2 CONCLUSIONS

The AEDC Mollier 2008 EOS has reached a state of development such that it should be used for calculations and predictions. There are no functionally important restrictions for its use at AEDC.

4.3 RECOMMENDATIONS

The EOS used to predict high-density effects should be replaced with the locally programmed version of the NIST EOS for air. This would remove all observed limitations on the high-density (low-entropy) end of the envelope. The only drawback would be that it would incorporate the industry standard for high-density property calculations into the EOS, thus eliminating any independent check.

The transport property calculation approach should be reviewed. Better alternatives may be available.

The possibility of developing density-dependent species property calculation procedures and appropriate equilibrium calculation procedures should be investigated. Successful development of such procedures would lead to a single approach for the entire envelope of the EOS. This would be a major effort, probably requiring several years. The potential gain is not known at present.

The most productive approach would to begin with a simplified system, perhaps N_2 or Ar, and develop the density-dependent properties and calculation procedures for the simplified system. Estimates for the effort and the effect for air could be made based on the simplified system. Absent this information, any recommendation would be highly speculative.

REFERENCES

1. Brahinsky, Herbert S. and Neel, Charles A., "Tables of Equilibrium Thermodynamic Properties of Air Volume I. Constant Temperature." AEDC-TR-69-89, April 1969. et seq.

2. Hilsenrath, J. and Klein, M. "Tables of Thermodynamic Properties of Air in Chemical Equilibrium Including Second Virial Corrections from 1500 K to 15,000 K." AEDC-TR-65-58, March 1965.

3. Hirshfelder, J. O., Curtiss, C. F., and Bird, R.B., *Molecular Theory of Gases and Liquids*, John Wiley & Sons, Inc., New York, 1954.

4. Span, Dr.-Ing. Roland, *Multiparameter Equations of State*, Springer, 2000, ISBN 3-540-67311-3.

5. Benedict, M., Webb, G. B., and Rubin, L. C. "An Empirical Equation for Thermodynamic Properties of Light Hydrocarbons and Their Mixtures: I. Methane, Ethane, Propane, and n-Butane." *J. Chem. Phys.*, Vol. 8, No. 4, pp 340-345 (1940).

6. Reynolds, W. C., *Thermodynamic Properties in SI, Graphs, Tables and Computational Equations for 40 Substances*. Department of Mechanical Engineering, Stanford University, 1979, ISBN 0-917606-05-1.

7. NIST Standard Reference Database 23, NIST Reference Fluid Thermodynamic and Transport Properties-REFPROP, ver. 7. et seq.

8. Mayer, J. E. and Mayer, M. G. *Statistical Mechanics*. John Wiley & Sons, Inc., 1940, QC 175.M3.

9. Powell, E. S. "Aerothermodynamic Properties of a Vitiated Air Test Medium." AEDC-TR-85-17, Arnold Engineering Development Center, Arnold Air Force Base, TN, 1985.

10. McBride, B. J., Zehe, M. J., and Gordon, S., NASA-TP-2002-211556, "NASA Glenn Coefficients for Calculating Thermodynamic Properties of Individual Species," September 2002.

11. Gordon, S. and McBride, B., "Computer Program for Calculation of Complex Chemical Equilibrium Composition and Applications, I. Analysis," NASA Reference Publication 1311, Part I, October 1994.

12. McBride, B. and Gordon, S., "Computer Program for Calculation of Complex Chemical Equilibrium Composition and Applications, I. Analysis," NASA Reference Publication 1311, Part II, June 1996.

13. Prabhu, Ramadas K. and Erickson, Wayne D., "A Rapid Method for the Computation of Equilibrium Chemical Composition of Air to 15,000 K," NASA Technical Paper 2792, March 1988.

14. Gupta, Roop N., Lee, Kam-Pui, Thompson, Richard A., and Yos, Jerrold M., "Calculations and Curve Fits of Thermodynamic and Transport Properties for Equilibrium Air to 30,000 K," NASA Reference Publication 1260, 1991.

15. Ueda, Masayoshi, et al., “Trajectory of HAYABUSA Reentry Determined from Multisite TV Observations.” *Astronomical Society of Japan*, 63(5): 947-953, October 2011.

16. Hansen, C. F., “Approximations for the Thermodynamic and Transport Properties of High-Temperature Air,” NASA Technical Report R-50, 1959.

17. Dean, D. E. and Stiel, L. I. “The Viscosity of Nonpolar Gas Mixtures at Moderate and High Pressure.” *A.I.Ch.E. Journal*, May, 1965, pp (526-531).

18. Kadoya, K, Matsunaga, N, and Nagashima, A. “Viscosity and Thermal Conductivity of Dry Air in the Gaseous Phase,” *J. Phys. Chem.* Ref. Data, Vol. 14, No. 4, 1985, pp (947-970).

19. Stephan, K., and Laesecke, A., “The Thermal Conductivity of Fluid Air,” *J. Phys. Chem. Ref. Data*, Vol. 14, No. 1, 1985, pp (227-234)

20. Lomax, Harvard, and Inouye, Mamoru, “Numerical Analysis of Flow Properties About Blunt Bodies Moving at Supersonic Speeds in an Equilibrium Gas,” NASA TR R-204, July 1964.

21. Tannehill, John C., and Mugge, P. H., “Improved Curve Fits for the Thermodynamic Properties of Equilibrium Air Suitable For Numerical Computation Using Time-Dependent or Shock-Capturing Methods,” NASA CR-2470, October 1974.

22. Lemmon, Eric W., Jacobsen, Richard. T., Penoncello, Steven G., and Friend, Daniel G., “Thermodynamic Properties of Air and Mixtures of Nitrogen, Argon, and Oxygen From 60 to 2000 K at Pressures to 2000 MPa,” *J. Phys. Chem. Ref. Data*, Vol. 29, No. 3, 2000, pp 331-385.

23. Laster, M. L., Limbaugh, C. C., and Jordan, J. L. “RDHWT/MARIAH II Hypersonic RDHWT/MARIAH II Hypersonic Wind Tunnel Research Program.” AEDC-TR-08-20, September 2008.

24. Kramida, A., Ralchenko, Yu., Reader, J. and NIST ASD Team (2012). *NIST Atomic Spectra Database* (version 5.0), [Online]. Available: http://physics.nist.gov/asd [Thursday, 20-Jun-2013 13:39:35 EDT]. National Institute of Standards and Technology, Gaithersburg, MD.

25. Downey J. R. Jr., “Calculation of Thermodynamic Properties of Ideal Gases at High Temperatures: Monatomic Gases,” AFOSR-TR-78-0960, March 1978, AD A054854.

26. Gordon, S. and McBride, Bonnie J., “Thermodynamic Data to 20,000 K for Monatomic Gases,” NASA/TP-1999-208523, June 1999.

27. McBride, B. J. and Gordon, S., “Computer Program for Calculating and Fitting Thermodynamic Functions,” NASA Reference Publication 1271, November 1992.

NOMENCLATURE

a	Speed of sound, m/sec
c_p	Specific heat at constant pressure, [J/(kg-K)] or $[(m/s)^2/K]$
c_{pe}	Equilibrium specific heat at constant pressure, [J/(kg-K)] or $[(m/s)^2/K]$
c_{pr}	Reaction specific heat at constant pressure, [J/(kg-K)] or $[(m/s)^2/K]$
c_v	Specific heat at constant volume, [J/(kg-K)] or $[(m/s)^2/K]$
δ	Relative difference between calculated parameters [-]
e	Internal energy, [J/kg] or $[(m/s)^2]$
mw	Molecular weight [kg/kg-mole]
γ	Ratio of specific heats, c_p/c_v, *[-]*
h	Enthalpy, [J/kg] or $[(m/s)^2]$
P	Pressure, [Pa]
R	Specific gas constant, R_u/mw, [J/(kg-K)] or $[(m/s)^2/K]$
R_u	Universal gas constant, 8314.4721 [J/(kg-mole K)]
R0	Specific gas constant at standard sea-level conditions, =287.1 J/(kg-K)
s	Entropy, [J/(kg-K)] or $[(m/s)^2/K]$
T	Temperature, [K]
ρ	Mass density, $[kg/m^3]$

Subscripts

c	Critical point
hd	High density
he	High enthalpy
0	Reference state
P	Constant pressure
ρ	Constant density
s	Constant entropy
T	Constant temperatures

Superscripts

0	Thermally perfect